Development of an *in vitro* model to assess wound-healing response and biocompatibility of intraocular biomaterials

by

Robert C. Pintwala

A thesis

presented to the University of Waterloo

in fulfillment of the

thesis requirement for the degree of

Masters of Applied Science

in

Systems Design Engineering

Waterloo, Ontario, Canada, 2014

Author’s Declaration

I hereby declare that I am the sole author of this thesis. This is a true copy of the thesis, including any required final revisions, as accepted by my examiners.

I understand that my thesis may be made electronically available to the public.

Abstract

Macrophages are master regulators of inflammation, fibrosis and wound-healing throughout the body. However, little work to date has examined their role in the inflammatory and fibrotic diseases of the eye. Mounting evidence for macrophage participation in the failure of intraocular implants (called posterior capsule opacification or PCO), and the well-established role of dysfunctional macrophage behaviour during diabetes motivated this investigation.

A novel *in vitro* model of macrophages and lens epithelial cells in co-culture was developed and first used to investigate the macrophage response to common intraocular lens materials, and the possible effect of this response on lens epithelial cells. We observed significant inflammatory macrophage activation and reduced macrophage adhesion by hydrophilic implant surfaces compared to hydrophobic ones. However, the macrophage response to both materials induced the same degree of inflammation in lens epithelial cells. In agreement with previous studies, we conclude that macrophage adhesion and activation are inversely related, and that net inflammatory effect is a function of the degree of macrophage activation and the number of activated cells.

The *in vitro* model was next used to explore the development of diabetic cataract. During hyperglycemic conditions a significant disruption of macrophage protein expression and delayed macrophage cell-death were observed, which may explain adverse inflammation in diabetes. Lens epithelial cell phenotype remained unchanged, though results from our *in vitro* model also suggest that lens epithelial cell death as a result of hyperglycemia occurs through a mechanism other than apoptosis, in agreement with the literature. We therefore provide additional evidence to the hypothesis that diabetic cataracts are a product of accumulated oxidative stress during hyperglycemia. Our findings provide a new method of inquiry into macrophage biocompatibility testing of intraocular materials, specifically through quantification of macrophage cell-surface markers and lens epithelial cell cytoskeletal elements.

Acknowledgements

First and foremost, I would like to thank Dr. Maud Gorbet for her never-ending support over the years, without which I would not be where I am today. Your faith and investment in me have helped me more than you know.

I was fortunate enough to work alongside a number of fantastic people in the Material Interaction with Biological Systems Lab, and am even more fortunate to call them my friends. Thank you to Sara Molladavoodi for her incredible patience, Saman Mohammadi for his infectious joyfulness, and Shahab Eslami for his ever-welcome laughter. A special thank you to the amazing Miriam Heynen for teaching me the importance of breakfast before giving blood.

I would like to gratefully acknowledge the Ontario Graduate Scholarship and the 20/20: NSERC Ophthalmic Materials Network for funding.

Incredible thanks are owed to my family and friends for putting up with me during my graduate studies. It did not go unnoticed and I am more than grateful for your patience and support.

Last but not least, I would like to thank Cameron Postnikoff for all of his help along the way. Were there a second author, it would be you.

Dedication

For Sara, Mom and Dad, of course.

Table of Contents

List of Figures

List of Tables

Chapter 1

Introduction

1.1 Motivation

Of all human senses, vision is perhaps most crucial to the maintenance of a high quality of life. The loss of vision, called blindness, is life-altering and world-wide is most often caused by the development of cataract,[1] or a clouding of the crystalline lens in the eye. The lens is the naturally clear structure of the eye responsible for accommodation, the ability of the eye to focus on objects at varying distances. An atypically visible cataract is shown below in Figure 1.1. Although our understanding of the etiology of cataract is incomplete, we now know that there is a strong genetic component to the disease.[2] As well, the onset of cataract is associated with the accumulation of damage to the lens over time from exposure to ultraviolent B (UVB) radiation, and oxidants from poor dietary and lifestyle choices or diabetes.[2] Globally, more than 20 million people are blind as a result of untreated cataract.[3] As global health care improves and life expectancy increases, so too will the number of people rendered blind by age-related cataract.

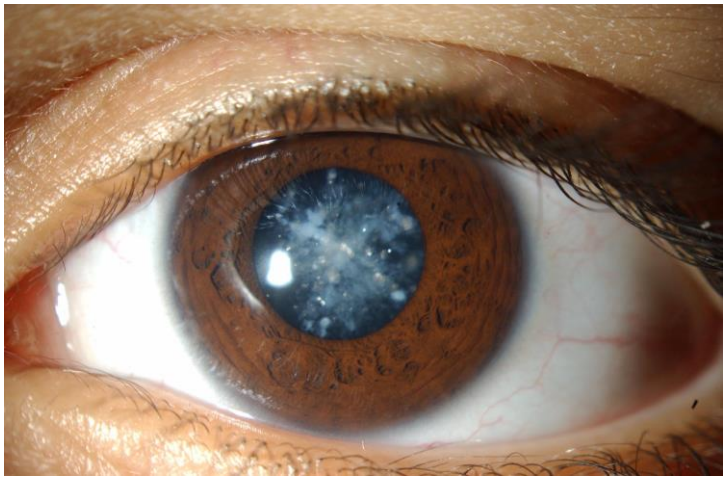

Figure 1.1: Photograph of female patient with cerulean cataract. Reprinted with permission from Dr. Arif O. Khan. Copyright Molecular Vision, 2009.[4]

At present, the only treatment for cataract is the surgical removal of the lens and its substitution with an artificial implant known as an intraocular lens (IOL), commonly made from foldable acrylic and silicone materials but originally made from rigid polymethylmethacrylate (PMMA). Modern cataract surgery, called phacoemulsification, involves perforation of the outer layers of the eye through a small incision and the emulsification and aspiration of the lens using an ultrasound device.[5] Patients recovering from cataract surgery generally enjoy much-improved visual acuity and a return to normalcy. However, in some cases, the trauma of surgery and subsequent implantation of an IOL induce the formation of a secondary cataract.[6] Posterior capsular opacification (PCO) is one form of secondary cataract and the most frequent complication of cataract surgery, occurring in 38.5% of patients after 3 years.[7] Despite decades of effort to improve surgical techniques and IOL design, PCO remains an important issue in ophthalmology.[1]

1.2 Anatomy of the Eye

The eye is a major sensory organ of the human body that enables vision. The eyeball, formally called the globe, is housed within the eye socket, a bony invagination of the skull known formally as the orbit. The gross anatomical structures of the globe are shown below in Figure 1.2. The walls of the globe comprise three layers of tissue with specific functions. The sclera is the protective, collagenous outermost layer of the globe. Although opaque and white, the anterior portion of the sclera – called the cornea – is transparent and enables passage of light to the interior of the globe. The uvea is the vascularized middle layer of the globe, and provides nutrients and gas exchange to the avascular tissues of the globe. The uvea also acts as a selective barrier between the blood and fluids of the eye called the aqueous humor. The anterior portion of the uvea – called the iris – is located behind the cornea and is responsible for dilating or constricting the aperture, or pupil, of the eye. The medial portion of the uvea – called the ciliary body – is a complex muscular structure responsible for

changing the shape of the lens (as part of the process of accommodation), as well as producing the aqueous humor. The lens, located behind the iris and surrounded by the ciliary body, focuses light onto the innermost layer of the globe, the retina. The retina is an epithelial layer of the globe that converts stimulation by photons into nerve impulses that are transmitted along the optic nerve into the visual centers of the brain. Typically, the anterior structures of the eye up to and including the lens are referred to as the anterior segment of the eye.

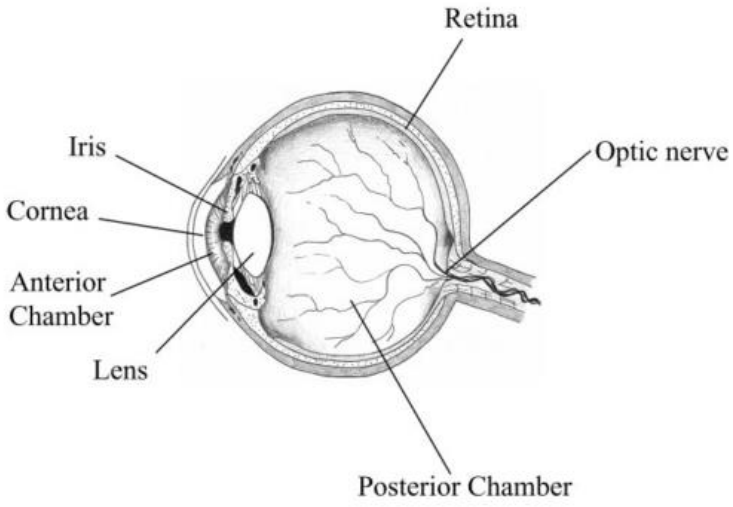

Figure 1.2: Gross anatomy of the human eye. Reprinted with permission from Elsevier. Source: A. W. Lloyd et. al, *Biomaterials*, 22, 2001.[8]

1.2.1 The Anterior Chamber

Within the anterior segment of the eye are two fluid-filled compartments: the Anterior Chamber, located between the corneal endothelium and the iris, and the comparatively smaller Posterior Chamber, located between the iris and the lens, and bounded along its equator by the ciliary body. Both compartments are filled with a clear fluid called the aqueous humor, which provides nutrients and removes metabolic by-products from the avascularised tissues of the cornea and lens. Aqueous

humor is produced primarily by active transport, diffusion and ultrafiltration of plasma proteins and nutrients across the ciliary epithelium into the posterior chamber.[9]

Although often compared to a blood plasma dilution, the aqueous humor has a unique chemical composition, as shown below in Table 1.1. By concentration, the aqueous humor is almost entirely water, with five-hundred times less protein than plasma (11 mg per 100 mL compared to 6 g per 100 mL in plasma).[10] The aqueous contains an elevated level of the antioxidant ascorbic acid,[11] but lower glutathione.[12,13] Although glucose and urea are roughly 80% of their plasma concentrations,[14] higher concentrations of pyruvate,[15] lactate and bicarbonate are found in the aqueous humor.[16] Amino acids appear in various concentrations relative to plasma due to active transport processes across the ciliary epithelium.[17] Immunoglobulins, or antibodies, are the attack and labeling proteins of the immune system, and are found at less than 1% of their serum concentration,[18] suggesting that other mediators may be responsible for the intraocular immunological response.

Table 1.1: Comparison of the mass compositions of blood plasma and aqueous humor

Component	Plasma Concentration (per 100 mL)	Aqueous Concentration (per 100 mL)
Protein	6 g	11 mg
Ascorbic Acid	0.35 mg	14.9 mg
Glutathione	0.11 mg	0.059 mg
Glucose	104 mg	58 mg
Urea	43.8 mg	37.8 mg
Pyruvate	1.94 mg	5.81 mg
Lactate	38.3 mg	65.9 mg
Bicarbonate	134.2 mg	155.6 mg
Amino Acids	Varies	Various Ratios to Plasma, 0.08 to 3.14
Immunoglobulins	1.3 g	7 mg

Information gathered on: protein,[10] ascorbic acid,[11] glutathione,[12,13] glucose and urea,[14] pyruvate,[15] lactate and bicarbonate,[16] amino acids,[17] immunoglobulins.[18]

The ciliary epithelium and the endothelium of capillaries within the ciliary body form a physical and immunological barrier called the blood-aqueous barrier (BAB). The BAB, along with other similar barriers throughout the eye, confer the properties of immune privilege to the intraocular environment.[19] Immune privilege is believed to be an evolutionarily conserved trait that protects critical tissues from inflammation due to injury or infection.[20] Immune privilege in the intraocular environment is discussed in Chapter 1.3.3.

1.2.2 The Lens

Located behind the iris, the lens is bathed in aqueous humor and connected along its equator to the ciliary body by suspensory ligaments known as the Zonule of Zinn. Physiologically, the lens is comprised of three parts: (1) the lens capsule, a type-IV collagen-rich basement membrane surrounding the lens, (2) the lens epithelium, a monolayer of lens epithelial cells on the inner surface of the anterior lens capsule, and (3) the lens fibres, transparent, enucleated cells filling the volume of the lens.[9] During cataract extraction, the surgeon pierces the lens capsule and attempts to remove the epithelium in its entirety. Oftentimes, however, islets of lens epithelial cells survive and experience rapid regrowth and migration on the anterior surface that may continue onto the previously cell-free posterior capsular surface, causing the scattering of light.[6,21].Some surviving lens epithelial cells undergo transdifferentiation into myofibroblast cells via a process called the epithelial-mesenchymal transition (EMT), leading to the pathological expression of the contractile protein α-smooth muscle actin (α-SMA), increased expression of the mobility protein vimentin, and a loss of expression of type-IV collagen and the intercellular cadherin E-cadherin.[22] These myofibroblasts induce fibrosis by overproducing proteins of the extracellular matrix (ECM) such as fibronectin, type-I and type-II collagen, and tenascin.[22] As a result, the lens capsule wrinkles, causing the substantial loss of vision experienced during PCO.[21] Proteins differentially regulated during PCO are listed below in Table 1.2.

Table 1.2: Changes in expression of lens epithelial cell proteins during PCO.

Protein	Nominally Expressed	Pathologically Expressed
α-SMA	No	Yes
Vimentin	Yes	↑
Fibronectin	Yes	↑
E-cadherin	Yes	No
Tenascin	Yes	↑
Type-I Collagen	Yes	↑
Type-III Collagen	Yes	↑
Type-IV Collagen	Yes	No

1.3 Cells and Components of the Immune System

The immune system is the collective defense of the human body to invasion by microorganisms that cause disease; called pathogens, these organisms include bacteria, fungi, parasites and viruses.[23] Without a functioning immune system, an infection cannot be halted, and human survival is all but impossible. The immune system is also involved in the host reaction to an implanted biomaterial called the foreign body response. The immune system begins with physical and chemical barriers to pathogens, namely the epithelium of the skin which consists of multiple layers of highly keratinized (tough and fibrous) cells.[23] Once through the epithelium, pathogens are quickly identified and attacked by elements of the innate immune system, the first subsystem of the overall immune system. The innate immune system is contrasted in function by the second subsystem, the adaptive immune system. All cells of both immune subsystems are called leukocytes (white blood cells) and are derived from the same progenitor cells in the bone marrow called hematopoietic stem cells.[23]

The innate immune system – so named because it is genetically inherited and does not change over the lifespan of an organism – is immediate in its identification of pathogens through one of two means: pattern recognition receptors, and complement. Pattern recognition receptors are cell-surface

proteins expressed on cells of the innate immune system that recognize pathogen-associated molecular patterns.[24] Complement is a complex system of proteins in blood that, once activated, bind to the surface of a pathogen, both marking the pathogen for attack and providing a means of adhesion, a process called opsonization.[25] The identifying cells then activate the innate immune response by the secretion of soluble proteins called cytokines. Cytokines are low molecular weight proteins (~30 kDa or less) produced and secreted by cells of the body to control cell growth and differentiation, remodel tissue, and to induce or suppress immunity and inflammation.[26] Inflammation is the symptom of an ongoing innate immune response and results from the recruitment of innate immune cells out of the circulatory system and into the site of infection where they can destroy pathogens and infected cells.

The cells of the innate immune system can be broadly separated into one of two categories: phagocytic cells that devour and destroy foreign pathogens, and cytotoxic cells that destroy pathogen-infected host cells.[27] All phagocytes are derived from the same myeloid progenitor stem cell in bone marrow. Neutrophil granulocytes are the most abundant cell of the innate immune system and are heavily involved in the early stages of inflammation,[28] often described as the "first responders" of the immune system and noted for their ability to rapidly secrete reactive oxygen species in a process called oxidative burst.[29] Reactive oxygen species (ROS) are highly oxidative molecules produced by leukocytes like the neutrophil and monocyte/macrophage to attack and destroy pathogens and foreign bodies.[30] Monocytes are longer-lived phagocytes of the innate immune system that circulate the body in the bloodstream. Once recruited out of the circulatory system by an inflammatory signal, monocytes differentiate into either macrophages, the tissue-resident phagocytic cells of the innate immune system,[31] or dendritic cells. Dendritic cells are responsible for the presentation of pathogenic material to cells of the adaptive immune system in a process called antigen presentation.[32] Antigens are molecules that induce an adaptive immune response.

Instead of targeting pathogenic microorganisms, cytotoxic cells target host cells that are infected with pathogenic material like viruses.[27] The cytotoxic cells of the innate immune system, called Natural Killer (NK) cells, are a class of cytotoxic lymphocytes responsible for the destruction of cancerous or infected host cells within the body.[33] NK cells induce apoptosis in their targets by secreting the membrane pore-forming protein perforin followed by caspase activating enzymes.[34] Caspases are essential enzymatic regulators of apoptosis, the process of programmed cell death.[35] The function of the NK cell in the innate immune system is mirrored by the cytotoxic T-cell in the adaptive immune system.

The adaptive immune system, also called the acquired immune system, produces a highly-specific and highly-severe immune response to a pathogen that can be recalled rapidly during subsequent invasions in a process called immunological memory.[23] Unlike the innate immune system, cells of the adaptive immune system recognize one specific antigen, but are able to mount a more substantial immune response.[36] Similar to the innate immune system, however, adaptive immunity has both a cell-mediated (action by cells) and humoral (action by circulating molecules) response.[23] T cells are responsible for cell-mediated adaptive immunity and have distinct subsets with distinct functions. Cytotoxic T cells detect antigens on infected host cells and, like cytotoxic NK cells, destroy them.[23] Helper T cells secrete cytokines to recruit and direct the innate and adaptive immune responses towards the destruction of their antigen.[23] Helper T cells also work to maintain immunity to a pathogen by promoting immunological memory of their antigen.[23] Regulatory T cells work opposite to their peers and suppress the immune response to an antigen instead of promoting it, often through the production of anti-inflammatory and immunosuppressive cytokines.[23] B cells are responsible for humoral adaptive immunity, and also have specific subsets and functions. Plasma B cells produce and secrete into the circulation proteins of the immune system called antibodies (or immunoglobulins).[23] Antibodies are highly specific to an antigen and may be used to identify, opsonize, or, neutralize a

pathogen by blocking the action of a vital protein on that pathogen's surface.[36] Lastly, memory B cells maintain humoral immunity to a pathogen by maintaining immunological memory of their antigen.[23] A summary of the various cells of the innate and adaptive immune systems are shown below in Table 1.3.

Table 1.3: Cells of the Immune System and their Function

Subsystem	Component	Immune Function
Innate	Neutrophils	Acute inflammation, phagocytosis, ROS production
	Monocytes	Replenishment of tissue phagocytes, phagocytosis, ROS
	Macrophages	Phagocytosis, sustained inflammation, antigen-presentation, ROS
	Dendritic cells	Antigen-presentation, phagocytosis
	NK cells	Destruction of infected host cells
	Complement	Opsonization, cell lysis
Adaptive	Cytotoxic T cell	Destroy infected host cells after detecting specific antigen
	Helper T cell	Secrete cytokines to direct immune response, maintain memory
	Regulatory T cell	Suppress immune response to a specific antigen
	Plasma B cell	Produce antibodies for specific antigen
	Memory B cell	Maintain immunological memory to specific antigen
	Antibody	Identify, opsonize, or, neutralize pathogens via blocking

Information gathered on the innate immune system,[23,27] and the adaptive immune system.[23,36]

1.3.1 The Macrophage

Macrophages are the resident phagocytic cells of the innate immune system, derived by the differentiation of monocytes in tissue.[31] Macrophages are highly responsive to their tissue environment and may exhibit a combination of host defence, wound healing and immunoregulatory phenotypes.[37] The exact nature of macrophage activation can be characterized by examining the expression of cell-surface proteins involved in the foreign-body response, like the cluster of differentiation (CD) proteins CD14, CD36 and CD54, as well as the production of reactive oxygen species (ROS) and reactive nitrogen species (RNS), which are used to chemically degrade targets of

macrophage attack.[38] Examination of cell-surface proteins associated with macrophage adhesion can also be used to characterize activation. The production of membrane-bound particles by activated macrophages via blebbing or shedding, called microparticles, provide a means of intercellular communication during inflammation and can also be examined. A summary of macrophage cell-surface markers relevant to macrophage function during inflammation is included below in Table 1.4.

Table 1.4: Macrophage cell-surface proteins and their function during inflammation

Protein	Receptor Class	Inflammatory Function
CD11b	Integrin	Adhesion, complement-mediated phagocytosis
CD11c	Integrin	Adhesion, complement-mediated phagocytosis
CD14	Pattern recognition	Detection and phagocytosis of bacteria
CD36	Scavenger	Phagocytosis of apoptotic cells
CD45	Integrin	Leukocyte common antigen
CD54	Integrin	Adhesion, complement-mediated phagocytosis
CD68	Scavenger	Phagocytosis of apoptotic cells
CD163	Scavenger	Phagocytosis of apoptotic cells
Fc	Immunoglobulin	Antibody-mediated (opsonized) phagocytosis
MRC1	Pattern recognition	Mannose residue recognition, pinocytosis
TLR2	Pattern recognition	Rapid detection and phagocytosis of bacteria
TLR4	Pattern recognition	Rapid detection and phagocytosis of bacteria

Information gathered on pattern recognition receptors[24,39,40]integrins,[39,41] scavenger receptors,[41–43] and the immunoglobulin superfamily of receptors (Fc).[39]

The cell-surface proteins CD11b, CD11c, CD14, CD36 and CD54 are of particular importance to this investigation. CD11b, also known as Integrin Alpha M, enables macrophage adhesion and migration and is upregulated on macrophages during systemic inflammatory conditions like obesity and diabetes.[44–48] CD11c, also known as Integrin Alpha X, is functionally cooperative with CD11b and regulated similarly.[49,50] Intercellular adhesion molecule-1 (ICAM-1), also known as CD54, is upregulated on macrophages in response to foreign-body stimuli *in vitro,*[51–53] and *in vivo,*[54,55] as well as during diabetes. CD36, a multi-ligand scavenger receptor, is down-regulated in

macrophages by the anti-inflammatory, wound-healing cytokine TGF-β and up-regulated by a select number of pro-inflammatory cytokines,[56,57] and is therefore useful for examining the wound-healing response of macrophages. CD14 is a pattern recognition receptor for bacterial and viral pathogens[58] and can be used to specifically examine the contribution of microbial contamination to the overall host-defence response.

Three secretory products of the macrophage have been identified as crucial chemical mediators of PCO. The primary mediator of PCO has been demonstrated both *in vitro* and *in vivo* to be the cytokine transforming growth factor beta (TGF-β).[59–66] Additionally, members of the matrix metalloproteinase (MMP) family – specifically MMP-2 and MMP-9 – have been shown to play a regulatory role in the formation of PCO.[22] Macrophages are well understood to play a crucial role in regulating inflammatory processes and the wound-healing response to biomaterials.[31,67,68] Macrophages are also important cellular mediators of fibrotic diseases elsewhere in the body,[69,70] suggesting they may play a role in PCO.

1.3.1.1 Measuring Macrophage Activation using Flow Cytometry

Expression of macrophage cell-surface proteins can be directly measured using flow cytometry. A flow cytometer is a measurement device that operates by passing cells in front of a laser one-by-one to gather information about their size, granularity, and fluorescence. Proteins of interest can be labelled on a cell using antibodies that are chemically conjugated with a fluorescent molecule called a fluorophore. By choosing fluorophores with different emission spectra, units of fluorescence measured from the flow cytometer can be used to determine the relative quantities of multiple proteins present on each cell of a culture. This is in contrast to other protein-quantification methods like Western Blotting, where a single measurement of expression is given for the entire culture. Flow cytometry also enables post-acquisition analysis like gating, which is the separation of flow

cytometry data into distinct subsets based on measured properties, like the separation of leukemia cells from healthy leukocytes based on fluorescently-labelled CD45.[71]

1.3.2 Macrophage Response to Biomaterials

Macrophages are often studied for their pivotal role in the foreign body reaction to biomaterials,[31,67,68] which are materials intended to interact with biological systems. Since the implantation of a biomaterial necessitates surgery, a central theme in biomaterials research is the design of materials and drug-delivery systems that can modulate the wound-healing response for the better.[72] The wound healing response is best described as four stages with varying degrees of overlap: hemostasis, inflammation, proliferation and remodeling.[73] Following trauma, blood enters the wound site and clots, resulting in hemostasis.[74] Inflammation at the wound-site begins as polymorphic neutrophils enter and phagocytize bacteria, foreign debris and damaged tissue before undergoing apoptosis.[73] Macrophages subsequently enter the wound-site and continue the inflammatory reaction, while stimulating angiogenesis, the growth of new capillaries and the beginning of the proliferation phase, by secreting platelet-derived growth factor (PDGF) and TGF-β.[31] The proliferation phase is named for the proliferation of fibroblasts and characterized by the rapid deposition of collagenous ECM throughout the wound bed, which is eventually reoriented and further modified in the remodelling phase.[74] Typically, the wound-healing response results in a resolved wound with no further activity. However, in the case of an implanted biomaterial, low levels of inflammation persist indefinitely in a process known as the foreign body reaction.[75] This unique reaction is driven primarily by the macrophage and their multi-nucleated successor, the foreign body giant cell (FBGC). The key to modulating the foreign body reaction, then, is to modulate the interaction between macrophages and material.

Upon contact with blood, a biomaterial is rapidly covered with blood plasma (serum) proteins, namely albumin, fibrinogen, fibronectin, vitronectin, gamma globulin, complement, and von Willebrand factor, in a non-binding and reversible process called adsorption.[31,76] Once adsorbed, serum proteins interact with the integrins of monocytes and macrophages and direct not only macrophage adhesion, but inflammatory activation, apoptosis, and fusion into FBGCs. The order of and rate at which these proteins adsorb to a material is largely determined by that material's surface chemistry.[77,78] The specific properties of a surface that affect protein adsorption are: (1) interfacial free energy, (2) hydrophobic (water repelling) or hydrophilic (water attracting) behaviour, (3) functional groups present, (4) type and quantity of ionic charge, and (5) topography and roughness.[77] Extensive work in the literature has determined that of central concern to macrophage-biomaterial interaction is the degree of hydrophobicity or hydrophilicity of a surface.[79] Hydrophilic surfaces in particular have been shown to strongly increase inflammatory activation of macrophages compared to hydrophobic surfaces.[80] This increase in inflammatory activation is paradoxically accompanied by a strong resistance to macrophage adhesion onto hydrophilic surfaces.[79]

1.3.2.1 Macrophage Response to IOLs

Although damage to the BAB during phacoemulsification may permit blood interaction with IOLs, blood components entering the anterior and posterior chambers will likely be diluted by aqueous humor. Correspondingly, few studies have examined the interaction of IOL materials with blood.[81,82] Despite mounting evidence of macrophage presence in PCO, the leukocyte biocompatibility of IOL materials (often referred to as uveal biocompatibility) and its potential contribution to the development of PCO have rarely been investigated. One important finding regarding uveal biocompatibility is the effect of implant surface chemistry on the leukocyte response to intraocular materials;[83–85] an observation reinforced by our current understanding of macrophage

biocompatibility elsewhere in the body.[80] In the eye, macrophages have been observed on the surface of IOLs explanted from human patients.[86–89] In an animal model of PCO, depletion of macrophages reduced the number of lens epithelial cells in the center of the posterior capsule,[90] suggesting that macrophages may play a role in lens epithelial cell mobility during PCO. Despite this evidence, few studies have investigated the leukocyte biocompatibility of IOL materials (often referred to as uveal biocompatibility) and its potential contribution to PCO development. To date, uveal biocompatibility has been measured by counting the number of adherent leukocytes on the surface of an IOL,[83–85] the hypothesis being that a higher number of adherent cells indicates a less biocompatible material. Meta-studies of IOL biocompatibility *in vivo* have noted a lower incidence rate of PCO in patients using IOLs with hydrophobic surfaces compared to hydrophilic surfaces of the same haptic design.[83,91–93] However, a causative link between leukocyte biocompatibility in the post-operative lens and PCO development remains unclear. Additionally, there is limited information on the potential for IOL materials to induce an inflammatory response in leukocytes, how this response is related to adhesion, and how the release of macrophage inflammatory mediators may affect lens epithelial cells.

1.3.3 Immune Privilege

Classically, immune privilege has been thought of as immunological ignorance, where a tissue graft could survive in a region of the body without immune rejection.[94–96] This definition, however, has since been broadened as the cells and molecular environments that facilitate prolonged allograft survival have become increasingly well understood. Modern thinking about immune privilege is perhaps confounded with the notion that immune privileged sites are able to resolve inflammation without provoking typical white blood cell (or leukocyte) mediated immune responses. An assumption is often made that immune privileged environments are therefore absent of leukocytes,

but in many cases this is incorrect, and certain leukocytes may be present and active in immune privileged sites.[i]

Several organs in the body are immune privileged, including the brain, the eye, and the testes.[97] The eye is of particular interest to studies of immune privilege since the ocular surface has to contend with pathogens on a daily basis. Additionally, the eye is the target of many biomedical devices, including contact lenses, intraocular lenses, and glaucoma drainage devices. Indeed, there are many cases where biomaterial interactions may exacerbate inflammation or are implicated in adverse events like PCO.[98] We now understand that ocular immune privilege is a complex and active system of immunosuppressive mediators coupled with the selective recruitment of innate and adaptive immune cells across the BAB into the aqueous humor during normal and pathological states.[95] It follows then that studies of material biocompatibility in the eye should expand to include leukocyte biocompatibility.[i]

1.3.3.1 The Aqueous Humor and Immune Privilege

The aqueous humor, under normal circumstances, contains a high concentration of immunosuppressive and anti-inflammatory molecules that reinforce the immune privileged tissue microenvironments of the inner eye. These molecules fall into the broad categories of signaling molecules called cytokines. The aqueous humor appears to contain a careful mixture of cytokines to modulate a number of cellular properties. Specifically, extracted aqueous humor has been demonstrated to suppress reactive oxygen species generation in macrophages *in vitro* by calcitonin gene-related peptide (CGRP).[99] Aqueous humor also inhibits NK cell target lysing via macrophage migration inhibitory factor (MIF), and suppresses CD95-induced neutrophil activation via soluble

[i] These paragraphs were co-authored with Cameron Postnikoff as part of an as-yet unsubmitted review paper on immune privilege in the anterior eye and its role in material biocompatibility.

CD95 ligand.[100] CD95 is also known as Fas ligand or apoptosis antigen-1, and apoptosis is induced by CD95 receptor-ligand activity.[101]

A large portion of the aqueous humor's anti-inflammatory properties can be attributed to the neuropeptide alpha-melanocyte stimulating hormone (αMSH). αMSH prevents cytotoxic T-cells from secreting inflammatory cytokines like interferon-gamma (IFN-γ) and interleukin-10 (IL-10),[102] while promoting the induction of immunosuppressive regulatory T-cells.[103] αMSH also inhibits neutrophil-mediated lysing of corneal endothelial cells,[101] and Toll-like receptor 4 (TLR4) signaling in macrophages.[104] Secondary to αMSH in maintaining the immunosuppressive environment of the aqueous humor is the anti-inflammatory cytokine transforming growth factor-β_2 (TGF-β_2). TGF-β_2 has been identified as a potent immunosuppressive molecule of the aqueous humor,[105] and thoroughly investigated for its regulation of T-cell proliferation, differentiation and survival in immune privileged microenvironments like the aqueous humor, as well as its suppression of NK activity[106].

Under normal conditions, these immunosuppressive cytokines and peptides ensure that leukocytes and lymphocytes entering the intraocular environment express their regulatory, anti-inflammatory phenotypes. The trauma of surgery and introduction of a biomaterial, however, can disrupt the complex homeostatic processes that reinforce ocular immune privilege, leading to adverse biocompatibility outcomes like PCO. Diabetes mellitus can also cause a similar breakdown of the BAB that precedes the development of pathological diabetic conditions in the eye like diabetic retinopathy.[107] Studies examining the cytokine composition of the aqueous humor in healthy and diabetic patients have demonstrated a number of key differences specifically involving pro-inflammatory mediators. A comparison of the cytokine composition of the aqueous humor in healthy and a number of pathological states, including diabetes, post-cataract surgery and uveitis, is included below in Table 1.5. Uveitis is a state of inflammation of the uveal layer of the eye, caused by a failure of ocular immune privilege in response to infection or injury.[108]

Table 1.5: Summary of cytokine effect on inflammation and aqueous humor composition in healthy patients, in the post-phacoemulsification environment, during diabetic ocularpathy and during uveitis.

Cytokine	Inflammation	In Health	Post-Surgery	Diabetes	Uveitis
αMSH	Anti	High			
IL-1β	Pro	Very Low	↑	↑	
IL-1rα	Anti	Low			
IL-2	Pro	Very Low			↑
IL-4	Pro	Very Low			
IL-5	Pro	Very Low			
IL-6	Pro	Low	↑	↑	↑
IL-7	Anti	Very Low			
IL-8	Pro	Low	↑	↑	↑
IL-9	Pro	Very Low			
IL-10	Anti	Very Low		↓	
IL-12	Pro	Low		↓	
IL-13	Pro	Very Low			↑
IL-15	Pro	Very Low			
IL-17	Pro	None			
b-FGF	Anti	Low			
Eotaxin	Pro	Very Low			
G-CSF	Pro	None			↑
GM-CSF	Pro	Low			↑
IFN-γ	Pro	None			↑
IP-10	Pro	Very Low		↑	
MCP-1	Pro	High	↑	↑	↑
MIF	Anti	None			
MIP-1α	Pro	None			↑
MIP-1β	Pro	High			
PDGF-BB	Anti	Very Low			
RANTES	Pro	Very Low			↑
TGF-β_2	Anti	High			
TNF-α	Pro	None	↑		↑
VEGF	Anti	High		↑	

Information gathered on cytokines: in healthy populations,[109] after phacoemulsification,[110,111] in diabetics,[109,112] and in uveitis.[113,114]

1.3.3.2 Posterior Capsule Opacification and Immune Privilege

Following cataract surgery a disturbance of the BAB has been observed,[115] either owing to mechanical injury sustained during the procedure or a selective lens epithelial cell response to trauma.[110,116] Elevated levels of the pro-inflammatory cytokines monocyte chemoattractant protein-1 (MCP-1), IL-8 and tumor necrosis factor-alpha (TNF-α) were observed in the post-operative aqueous humor for up to one year after surgery.[110] As well, expression of MCP-1 was localized to proliferating lens epithelial cells in the capsular bag,[110] providing evidence of a lens epithelial (or perhaps myofibroblast) recruitment of innate immune cells across a disturbed BAB. Given its name, MCP-1 recruits monocytes and macrophages into active sites of trauma and inflammation; however, it also strongly influences T-cell activation and differentiation,[117] providing a possible means for the induction of an adaptive and innate immune response to the trauma of cataract surgery. The question of what effect this selective deviation from immune privilege has on the development of PCO remains unanswered. Despite the well-established capability for selective recruitment of inflammatory cells across the BAB,[97] leukocyte and lymphocyte ingress into the lens from the aqueous humor under healthy conditions appears to be unreported. This impenetrability by patrolling cells may be a result of the anti-proteolytic properties of the aqueous humor preventing a breakdown of the collagenous lens capsule combined with the tight-junction organization of the lens epithelium.[118] However, since the barrier function of the lens capsule and epithelium are disturbed during surgical intervention, an avenue of entry for cells of the innate immune system does exist.

1.4 Diabetes and Macrophage Biocompatibility

Diabetic complications are increasingly believed to be caused by the pathological activation or inactivation of inflammatory processes in the human body.[46] In the diabetic disease state, pathological changes to macrovascular and microvascular endothelial tissues induce further pathological changes

to the tissues being vascularized.[46,119] The adverse behaviour of diabetic macrophages are increasingly well understood in the contexts of diabetic complications like impaired wound healing,[120,121] atherosclerosis,[47,122–125] diabetic nephropathy,[126–130] and diabetic retinopathy.[131–133] Although avascularised, the lens can be compromised by what is called diabetic cataract,[134] the pathogenesis of which is not well understood but believed to be a result of metabolic and oxidative damage in a high glucose environment.[134–136] Similar to studies of IOL biocompatibility, little work has examined the possible role of macrophages in diabetic complications of the lens.

Extensive work has demonstrated that impaired diabetic wound healing leads to worse biocompatibility outcomes in patients. The change in macrophage phenotype observed during diabetes mellitus prevents the resolution of the inflammatory phase in the diabetic wound healing response,[50,121,137,138] causing a prolonged and more severe foreign body response. Meta-studies of dental implant survival have demonstrated higher rejection rates in diabetic subjects compared to non-diabetic patients,[139] and similar survival rates in those diabetic patients with excellent glycemic control.[140,141] Similar observations were made for coronary stent implantation, with diabetic patients displaying a higher need for follow-up surgical intervention than non-diabetic patients.[142] Differences in IOL biocompatibility have long been observed in diabetic patients. Interestingly, diabetic patients undergoing phacoemulsification experience a lower rate of PCO than non-diabetic patients after 3 years.[143] However, diabetics with PCO experience a more severe loss of vision,[144] and experience higher rates of PCO with hydrophilic IOLs than non-diabetics with PCO.[145] Additionally, the rate of calcification of hydrophilic IOLs appears to be higher in diabetic patients.[146] Since the role of macrophages in impaired wound-healing and the foreign body response to implanted biomaterials are well understood, their unclear role in the lens warrants further investigation.

1.5 Thesis Objective and Outline

The objective of this investigation was to further our understanding of the role of macrophages in the immune privileged environment of the inner eye. The evidence of macrophage participation in the development of PCO provides a good starting point for examining the interplay between lens epithelial cells and macrophages. If PCO is a fibrotic disease, macrophages likely play a role in its onset and development. Likewise, if diabetic lens pathology is similar to diabetic retinopathy, then macrophages likely play a role in the lens as well. As the first step, a novel *in vitro* co-culture system incorporating macrophages and lens epithelial cells in the same fluid environment was developed and detailed herein. In Chapter 2, the co-culture model was used to quantify – for the first time – macrophage activation to common IOL biomaterials, and the effect of this activation on lens epithelial cell phenotype.[ii] In Chapter 3, the effect of acute hyperglycemia on the co-culture model was investigated. In Chapter 4, the use of the co-culture model in biocompatibility testing and the next steps in development of the model are discussed.

[ii] A modified version of Chapter 2 has been accepted for publication by the Journal of Biomaterials Applications

Chapter 2

Leukocyte Biocompatibility of IOL Materials and the Effect of Macrophage Activation on Lens Epithelial Cell Phenotype *in vitro*

2.1 Introduction

The widespread use of foldable IOLs in cataract surgery have reduced the size of incision necessary during phacoemulsification, reducing the extent of damage done to the corneal and uveal layers of the eye. Foldable IOLs are made from materials called hydrogels, defined as highly water-absorbent polymer networks. Although all hydrogels are internally hydrophilic, their surfaces may exhibit either hydrophilic or hydrophobic properties depending on their polymeric structure, as well as any chemical modifications made to the surface. The hydrogels and surface chemistries commonly used in IOL manufacturing include: (i) hydrophilic acrylic made of poly(2-hydroxyethyl methacrylate) (or pHEMA), (ii) hydrophobic acrylic based on poly(methyl methacrylate) (or PMMA), and (iii) hydrophobic silicone hydrogels. Older IOLs were made from a rigid composition of hydrophobic PMMA (acrylic glass) and still see regular use in many areas of the world.[5]

Macrophages have been observed on the surface of IOLs explanted from human patients,[86–89] and animal models of PCO have suggested a role for macrophages in lens epithelial cell mobility,[90] during PCO, and therefore the severity of the disease. Studies examining the PCO incidence rate *in vivo* have noted a significantly lower rate of PCO in patients using IOLs with hydrophobic surfaces compared to hydrophilic surfaces of the same haptic design.[83,91–93] Despite this, limited work has quantified the macrophage response to IOL materials and a possible effect on lens epithelial cell phenotype. Macrophages are well known to respond to hydrophobic and hydrophilic surfaces differently, with hydrophilic surfaces causing more pro-inflammatory activation than hydrophobic

ones.[147–149] Uveal biocompatibility should therefore differ for hydrophilic and hydrophobic IOL materials.

In this study, we hypothesized that IOL material-activated macrophages may secrete pro-inflammatory cytokines and other mediators to induce a PCO-like phenotype in lens epithelial cells. Two biocompatibility outcomes were investigated: whether common IOL biomaterials could activate macrophages, and whether this activation could induce an inflammatory phenotype in lens epithelial cells. To examine the interplay between both cell populations, a tissue model of the post-operative lens system must therefore be developed. Systems biology is a modern approach to biological research that stands in contrast to reductionism: the traditional assumption that a system behaves as the sum of its parts. A system-level understanding requires knowledge of three properties: (1) the structure of the system, (2) the dynamics of the system, and (3) the control method of the system.[150] Any suitable design methodology should address all three aspects, or the aspects most in need of further examination. As the one-way effect of macrophage activation on lens epithelial cell phenotype is of interest, an *in vitro* model that incorporates both cell types (called a co-culture model) can be used to mechanistically supplement high-level animal studies of macrophage involvement in PCO. A better understanding of the role of macrophage activation in the post-operative lens will enable the development of more biocompatible IOL materials and further reduce the incidence rate of PCO.

2.2 Materials and Methods

2.2.1 Cell Culture

A novel *in vitro* co-culture model of the post-operative lens environment was developed. The human acute monocytic leukemia cell line THP-1 (ATCC, Manassas, VA) was selected as the macrophage surrogate for its confirmed ability to produce macrophage secretory products.[151] The SV-40 virus

immortalized human lens epithelial cell line HLE B-3 (ATCC) was used as the lens epithelial surrogate due to its widespread use in *in vitro* PCO studies.[152–154]

2.2.1.1 Macrophage Culture

THP-1 monocytes were cultured in RPMI 1640 cell culture medium (Invitrogen, Oakville, ON) supplemented with 10% fetal bovine serum (FBS; VWR, Mississauga, ON) and 0.9% penicillin/streptomycin (Invitrogen, Oakville, ON) and maintained in suspension at 5 x 10^5 cells/mL at 37°C and 5% CO_2. THP-1 monocytes were differentiated into macrophages using the protein kinase C (PKC) activator phorbol 12-myristate 13-acetate (PMA; Sigma-Aldrich, Oakville, ON), following an optimized protocol combining that of Park *et al.* and Daigneault *et al*.[155,156]. THP-1 monocytes were seeded in 6-well tissue-culture polystyrene (TCPS) plates at a concentration of 5x10^5 cells/well and treated with 5 nM PMA for 72 hours. THP-1 cells were inspected after 24 and 48 hours for adherence and viability. At 72 hours, media was replaced without PMA, and the adherent THP-1 cells were allowed to rest for 48 hours. Media was replaced once again and the THP-1 macrophages were allowed to rest for a further 48 hours. Figure 2.1 shows macrophage-like cell phenotype throughout the differentiation process.

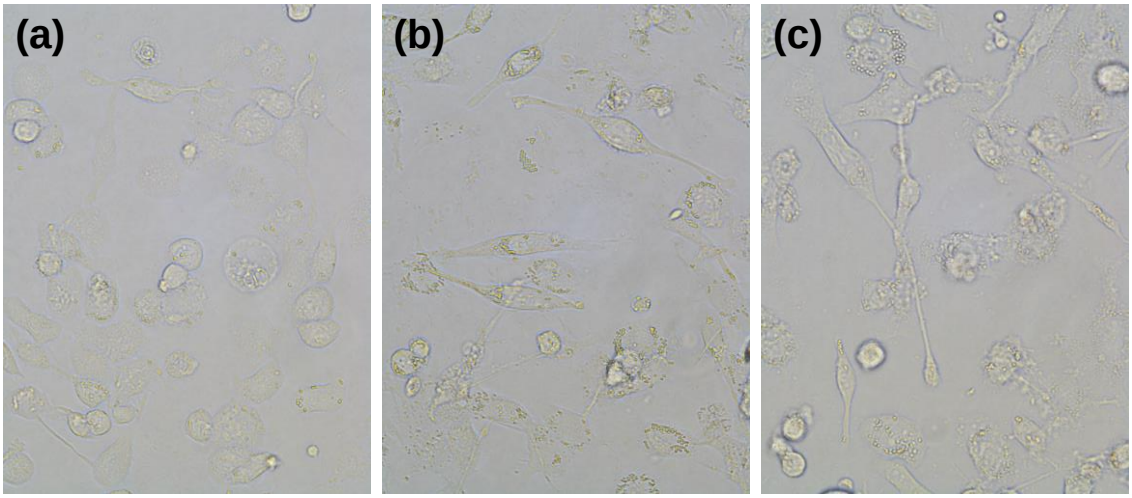

Figure 2.1: Macrophage differentiation progress. Images taken at 40x with visual field microscope after: (a) 72 hour treatment with PMA, (b) 48 hour rest in PMA-free media, (c) additional 48 hour rest.

To prepare for co-culture, mature differentiated macrophages were washed twice with room temperature phosphate-buffered saline (PBS) for 5 minutes and disassociated by incubation with TrypLE^{TM} Express (Invitrogen, Oakville, ON) for 20 minutes at 37°C. Cells were centrifuged in RPMI 1640 media with 10% FBS, re-suspended in fresh media and transferred to the co-culture plate.

2.2.1.2 Lens Epithelial Cell Culture

HLE B-3 were cultured in Dulbecco's Modified Eagle Medium (DMEM; Invitrogen, Oakville, ON) supplemented with 10% FBS and 0.9% penicillin/streptomycin and maintained at 37.0°C in 5% CO_2. To prepare for co-culture, cells were serum starved for 24 hours[60]. Serum starvation allows cells to recover signalling pathways to baseline levels of activity, where cytokines and signalling molecules in serum may have induced an effect.[130,157,158] Cells were dissociated from a flask with TrypLE Express and then centrifuged in serum-free DMEM.

To begin co-culture, 24-well polyethylene terephthalate 1-µm membrane hanging cell-culture inserts (EMD Millipore, Billerica, MA) were inverted in a 6 well plate, and 5 x 10^4 HLE B-3 cells were seeded onto the superior surface. Inserts were incubated overnight to allow for strong cellular adherence, and then returned to their normal orientation in serum-free media in a 24-well plate (EMD Millipore) until the start of the co-culture.

2.2.2 IOL Preparation

Commercially available, surgical-grade PMMA and pHEMA IOLs were purchased from Freedom Ophthalmic (Mississauga, ON) in both square and round-edged designs. To prepare for culture, the IOLs were incubated in RPMI 1640 with 10% FBS for 2 hours to allow for protein adsorption, specifically albumin and fibronectin.[82] Manufacturer information pertaining to the IOLs used in the co-culture system are included below in Table 2.1.

Table 2.1: IOL designs used in co-culture system

Model	PCC 503	PMC 533SQ	HFC 603	AFC 603SQ
Material	PMMA	PMMA	poly-HEMA	poly-HEMA
Optic Design	Equiconvex	Equiconvex	Equiconvex	Equiconvex
Optic Size	5.00 mm	5.50 mm	6.00 mm	6.00 mm
Overall Length	12.50 mm	12.50 mm	12.50 mm	12.50 mm
Haptic Angle	Cap.C step vault	Mod.C step vault	0’	0’
Dialing Holes	-	-	-	-
A.Constant	118.4	118.4	118.0	118.0
AC Depth	5.00 mm	5.00 mm	5.00 mm	5.00 mm

2.2.3 Co-culture

The co-culture system diagram is shown in Figure 2.2. Prepared IOLs were transferred into fresh wells of a 24-well Millipore plate in RPMI containing 10% FBS. Disassociated mature THP-1

macrophages were then seeded at 1 x 10^5 cells/well. Plates were incubated for 2 hours to allow for macrophage adherence. Hanging inserts with adherent HLE cells were then introduced to the wells containing one of the following: macrophages and an IOL (treatment), macrophages and no IOL (control), no macrophages and an IOL, or no macrophages and no IOL. Co-culture plates were incubated for either 1, 2, 4 or 6 days before analysis. Media was replaced every 2 days.

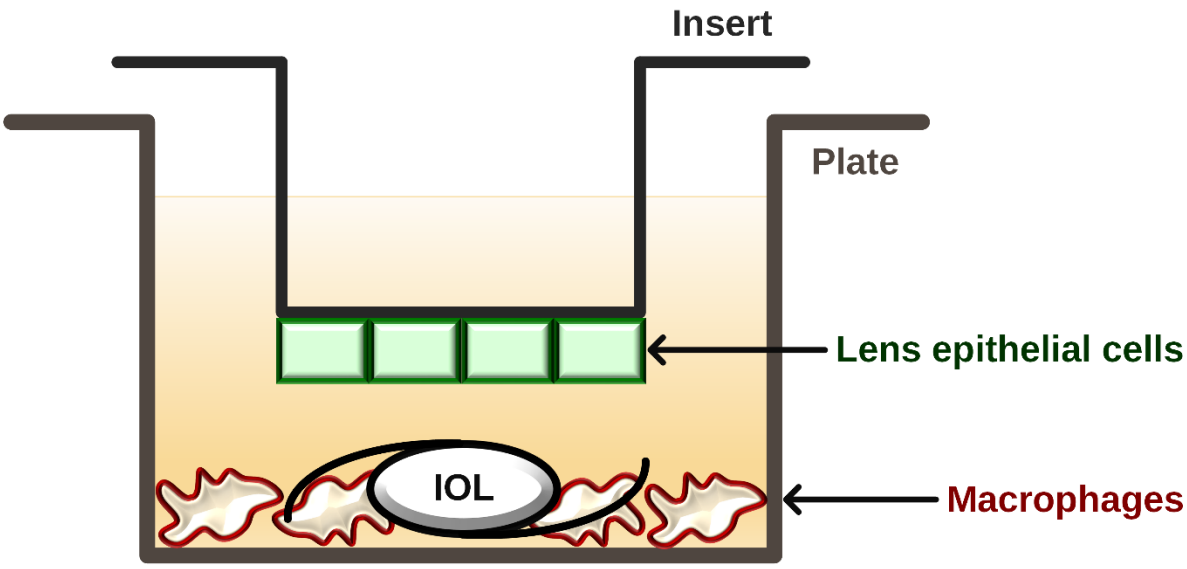

Figure 2.2: Co-culture system diagram. Inserts are inverted and lens cells are seeded on the superior surface before being returned to their normal orientation in a well containing adherent macrophages and an IOL.

2.2.4 Immunolabelling Reagents

Fluorescein isothiocyanate (FITC) conjugated mouse monoclonal antibody against CD36 (multi-ligand scavenger receptor), R-phycoerythrin-cytochrome 5 (PE-Cy5) conjugated monoclonal antibody against CD45 (human leukocyte common antigen), R-phycoerythrin (PE) conjugated monoclonal antibody against CD54 (intercellular adhesion molecule 1 or ICAM1), PE conjugated

mouse monoclonal antibody against CD14 (pattern recognition receptor), Alexa Fluor® 647 (AF647) conjugated mouse monoclonal antibody against E-cadherin, and PE conjugated polyclonal antibody against rabbit IgG produced in donkey were purchased from Becton Dickinson Pharmingen (San Diego, CA, USA). Monoclonal rabbit antibody against fibronectin, and FITC conjugated mouse monoclonal antibody against α-smooth muscle actin (α-SMA) were purchased from Sigma-Aldrich. All other chemicals were of analytical reagent grade.

2.2.5 Flow Cytometry

Upon completion of the co-culture, inserts with adherent HLE cells were removed from the co-culture system. Wells containing macrophages were incubated at 37°C with TrypLE Express for 45 minutes. THP-1 cells were then centrifuged in media containing 10% FBS and re-suspended in 100 µL fresh media with serum. Aliquots of 50 µL were incubated in saturating concentrations of conjugated fluorescent monoclonal antibodies for 1 hour at room temperature in the dark. Leukocyte populations were identified by adding anti-CD45 antibody to all samples. To assess macrophage activation, samples were incubated with anti-CD54 or anti-CD14 antibody, as well as anti-CD36 antibody. After incubation, samples were diluted with HEPES-Tyrode's buffer (HTB: 137 mM NaCl, 2.7 mM KCl, 5 mM MgCl2, 3.5 mM HEPES, 1 g/L Glucose, and 2 g/L BSA, PH 7.4) and fixed with paraformaldehyde (final concentration of 1% w/v). Samples were read on a three-color FACSCalibur flow cytometer (Becton Dickinson).

To assess intracellular ROS/RNS production, macrophages were cultured with or without an IOL for 24 hours. Macrophages on the IOL surface were dissociated separately from those on the TCPS surface. After centrifugation, samples were incubated in serum-free media containing 100 µM of 2′,7′-dichlorodihydrofluorescein diacetate (DCFH-DA) (Invitrogen) for 30 minutes at 37°C in the dark. Cells were read immediately on a three-color FACSCalibur flow cytometer. Samples were

analysed to completion. Cell counts for adherent macrophage on each IOL were performed in CellQuest Pro (BD) by distinguishing single cells from subcellular debris on the basis of size and granularity, estimated by forward scatter and side scatter respectively.

Inserts with adherent HLE cells were submerged in 0.25% Trypsin-EDTA (Invitrogen) and incubated at 37°C for 2 hours on a shaker at 250 RPM. Once detached, cells were re-suspended in DMEM with 10% FBS before centrifugation. Excess media was removed. Cells were re-suspended and then fixed in paraformaldehyde at a final concentration of 4% w/v for 15 minutes, at room temperature in the dark. Samples were washed, and cells were re-suspended and permeabalized with 0.5% Triton-X (Sigma-Aldrich) for 5 minutes, at room temperature in the dark. Samples were then centrifuged and re-suspended in PBS containing 1% w/v fatty-acid free bovine serum albumin (BSA; EMD Millipore). Samples were separated into three aliquots and stained with antibodies against either α-SMA (FITC conjugated), E-cadherin (AF647 conjugated) or fibronectin overnight, at 4°C in the dark. The following morning, samples containing anti-fibronectin were labelled with PE anti-rabbit IgG secondary antibody for 1 hour, at room temperature in the dark. Samples were read immediately on a three-color FACSCalibur flow cytometer (Becton Dickinson).

2.2.6 Confocal Microscopy

Confocal microscopy was used to confirm the phenotype of the lens epithelial cells, as well as to determine macrophage adherence to each IOL material. To serve as a positive control, some HLE cells were cultured without macrophages and treated with 5 ng/mL of TGF-β2 (Sigma-Aldrich) for 2 days prior to imaging. To serve as a negative control, HLE cells were cultured without macrophages for 6 days and not exposed to any other treatment.

Adherent HLE cells on the insert were washed twice with room-temperature PBS for 5 minutes. Cells were fixed in paraformaldehyde at a final concentration of 4% w/v for 15 minutes,

washed once with PBS, and then permeabalized with 0.5% Triton-X in PBS for 5 minutes in the dark[152]. Cells were washed with PBS, and then stained overnight in 1% BSA in PBS with antibodies for α-SMA, fibronectin or E-cadherin at 4°C in the dark. For the samples labelled with anti-fibronectin, secondary antibody was added after washing with PBS and the samples were incubated for one hour at room temperature in the dark. Samples were washed with PBS at room temperature and then imaged by an inverted laser scanning confocal microscope (LSM 510 Meta, Carl Zeiss, Germany) using an argon laser (488 nm excitation) and HeNe laser (543 nm and 633 nm excitation). IOLs were removed from the co-culture model and fixed in 4% paraformaldehyde for one hour. To confirm the presence of adherent macrophages on the IOLs, samples were blocked with 1% BSA in PBS and then incubated with saturating concentrations of fluorescently labelled antibodies against CD36, CD54 or CD14, and CD45 overnight at 4°C in the dark. The following morning, samples were rinsed in PBS and imaged by an inverted laser scanning confocal microscope (LSM 510 Meta, Carl Zeiss, Germany) using an argon laser (488 nm excitation) and HeNe laser (543 nm and 633 nm excitation).

2.2.7 Statistical Analysis

Flow cytometry fluorescence values are presented as the mean ± the standard error of the mean (SEM). Fluorescence values and fluorescence-ratios were subjected to a multivariate analysis of variance (ANOVA) using a general linear model, including terms for length of incubation, lens material, and when applicable, the presence or lack of macrophages in the co-culture. Pairwise comparisons between materials, incubation times, and material-time combinations were performed using the Bonferoni criterion in Minitab 16.2.3 (State College, PA, USA). A p value of less than 0.05 was required for significance. The number of experiments was always equal to or greater than three.

2.3 Results

2.3.1 Macrophages increase α-SMA expression in lens epithelial cells

The novel co-culture model was employed to examine the possible effect of macrophages on lens epithelial cells. As illustrated in Figure 2.3, after a 6-day incubation, both the presence of macrophages and an IOL material were required to significantly ($p < 0.03$) affect the expression of the myofibroblast protein α-SMA in lens epithelial cells. In the lens cell mono-culture, the presence of an IOL alone had no effect on α-SMA expression ($p > 0.59$); note that in our *in vitro* model, the lens cells are not in physical contact with the lenses. In the absence of an IOL, the presence of macrophages in the co-culture model induced a small but significant increase in α-SMA expression ($p < 0.031$). Co-culture with pHEMA IOLs induced a significant upregulation of α-SMA in lens epithelial cells when compared to both lens cell mono-culture with pHEMA IOLs ($p < 0.033$) and co-culture with no IOL ($p < 0.007$). Similarly, co-culture with PMMA IOLs induced a significant upregulation of α-SMA when compared to the lens cell mono-culture with PMMA IOLs ($p < 0.02$), but this upregulation was not statistically significant when compared to co-culture with no IOL ($p < 0.08$). Neither 2 nor 4 days of co-culture provided the required length of time to detect differences in the expression of α-SMA in lens cells.

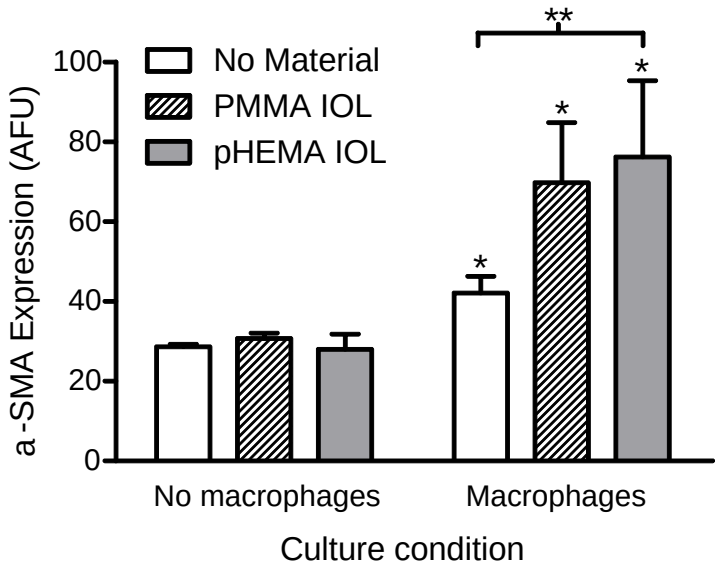

Figure 2.3: Co-culture with macrophages increases expression of α-SMA in HLE B-3 cells versus cells in a mono-culture. All cells were cultured for 6 days. α-SMA expression was measured by flow cytometry and is reported as the mean of arbitrary fluorescence units (AFU). * indicates significant difference from respective α-SMA expression observed in lens cells in monoculture (no macrophages) ($p < 0.031$); ** significant difference ($p < 0.01$). n = 4 for all treatments and controls.

As shown in Table 2.2, no significant difference in fibronectin expression in co-cultured lens cells was induced by the presence of an IOL material. However, fibronectin expression significantly decreased between 2 and 4 days of co-culture ($p < 0.0008$) with a PMMA IOL, and between 4 and 6 days of co-culture with no IOL ($p < 0.003$). Similarly, no significant difference in E-cadherin expression was induced by the presence of an IOL material. However, E-cadherin expression was significantly upregulated ($p < 0.03$) after 6 days of co-culture with a pHEMA IOL compared to E-cadherin expression at both 2 days and 4 days.

Table 2.2: Fibronectin and E-cadherin expression on lens epithelial cells cultured for 2, 4, or 6 days with a PMMA lens, pHEMA lens or no lens. Protein expression was measured by flow cytometry and is reported as the geometric mean of arbitrary fluorescence units (AFU) ± the standard error of measurement (SEM).

IOL Material	Incubation Time	Fibronectin	E-cadherin
No material	2 days	34 ± 8	13 ± 1
	4 days	22 ± 5	12 ± 3
	6 days	18 ± 6[*]	14 ± 1
PMMA	2 days	35 ± 5	13 ± 1
	4 days	22 ± 4[+]	13 ± 2
	6 days	21 ± 7[+]	14 ± 1
pHEMA	2 days	29 ± 4	12 ± 1
	4 days	23 ± 4	13 ± 2
	6 days	21 ± 7	15 ± 1[‡]

n = 7 at 2 days, and n = 4 at both 4 days and 6 days.
[*] Significantly different from corresponding value at 2 days ($p < 0.003$).
[+] Significantly different from corresponding value at 2 days ($p < 0.0008$).
[‡] Significantly different from corresponding value at 2 days ($p < 0.00001$) and 4 days ($p < 0.03$).

Differences in α-SMA expression observed in flow cytometry were confirmed by confocal microscopy. For comparison purposes, treatment with 5 ng/mL of TGF-β_2 for 2 days was included as a positive control, and lens cell mono-culture included as a negative control. As illustrated in Figure 2.4, high levels of α-SMA expression (shown in green) were observed for the TGF-β_2, co-culture with pHEMA IOLs and co-culture with PMMA IOLs groups (Figure 2.4a, 3b and 3c respectively). Co-culture in the absence of an IOL resulted in a reduced expression of α-SMA (Figure 2.4d) and lens cell mono-culture (Figure 2.4e) showed the weakest staining for α-SMA. Regardless of incubation conditions expression of E-cadherin (shown in red) was similar, with significant background staining on all PET substrates.

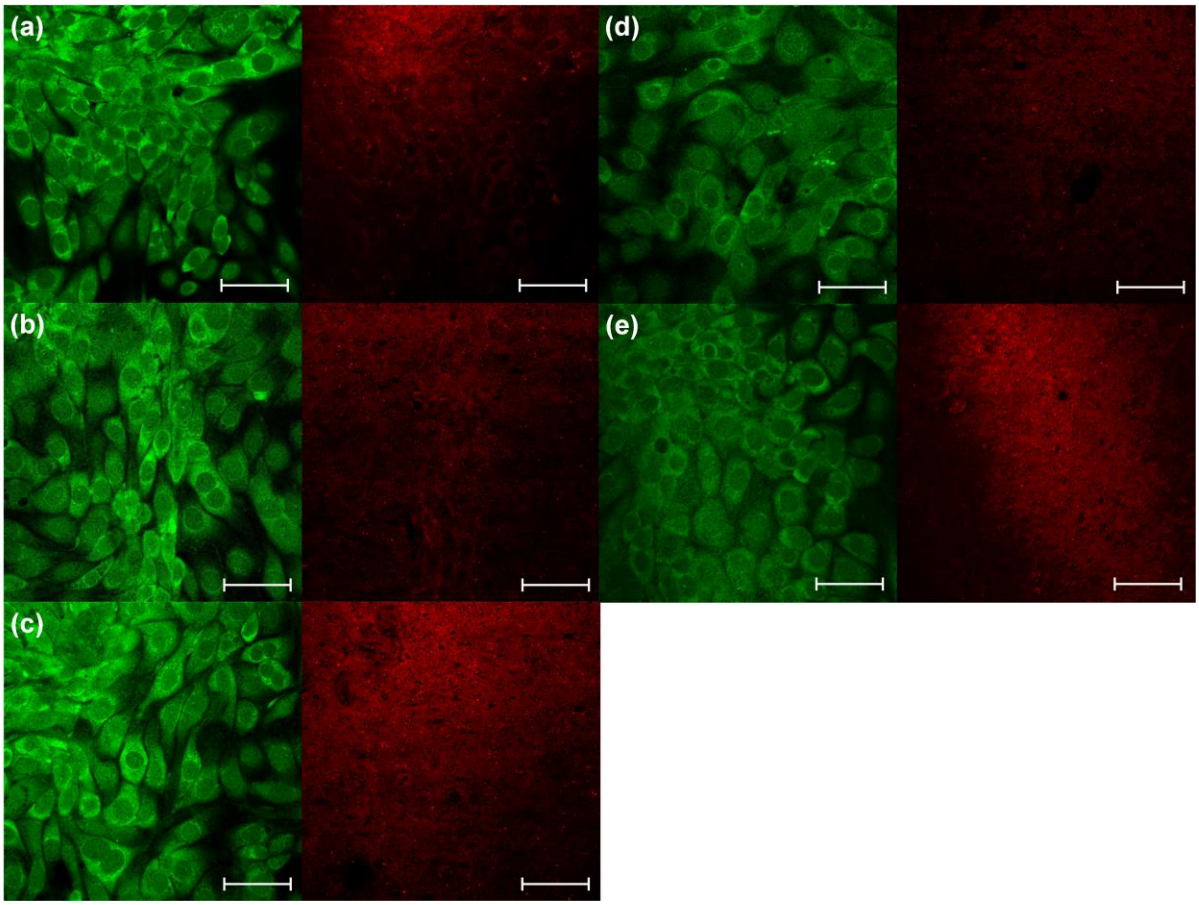

Figure 2.4: HLE B-3 cells imaged at 40x zoom using a confocal laser scanning microscope. Scale bar represents 50 μm. Left (green): stained for α-SMA. Right (red): stained for E-cadherin. (a) Mono-culture with 5 ng/mL of TGF-β_2 for 2 days; positive control. (b) Co-culture with pHEMA IOL for 6 days. (c) Co-culture with PMMA IOL for 6 days. (d) Co-culture with no IOL for 6 days. (e) Mono-culture with no IOL for 6 days; negative control. Images are representative of triplicate of each treatment category.

2.3.2 Macrophages upregulate CD54 expression in response to pHEMA lenses

Macrophage activation induced by the presence of IOL materials was characterized over 6 days. Upregulated cell-surface CD54 receptor expression was observed at 2 days, 4 days and 6 days of incubation. As shown in Figure 2.5, after 2 days of incubation, macrophages cultured with a pHEMA lens significantly upregulated CD54 expression relative to cells cultured with no lens ($p < 0.03$), but not compared to the expression on cells cultured with PMMA lens ($p < 0.117$). CD54 expression decreased significantly after 2 days ($p < 0.0001$) and remained approximately constant between 4 and 6 days incubation (Figure 2.5). The presence of a PMMA lens did not result in a significant upregulation of CD54 when compared to control (macrophages with no IOL, $p = 1.0$).

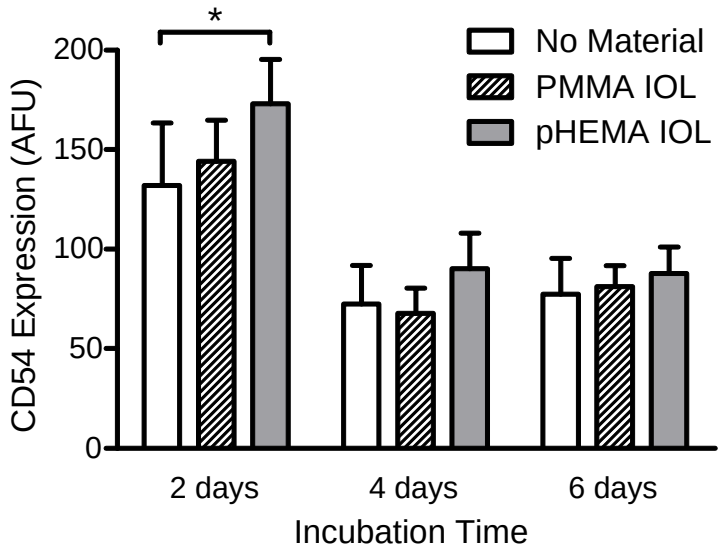

Figure 2.5: CD54 cell-surface receptor expression on macrophages cultured for 2, 4 or 6 days with a PMMA lens, pHEMA lens, or no lens. CD54 expression was measured by flow cytometry and is reported as the mean of arbitrary fluorescence units (AFU). * indicates a significant difference of $p < 0.03$. $n = 7$ at 2 days and $n = 4$ at both 4 and 6 days.

Cell-surface expression of CD45, the human leukocyte common antigen, and CD36, the thrombospondin receptor, were not affected by the presence of an IOL material (Table 2.3). However, for all samples, expression of both receptors on macrophages appeared to decrease over time: CD45 expression was significantly decreased at 6 days when compared to both 2 and 4 days ($p < 0.01$), while significantly decreased expression of CD36 was observed at 4 and 6 days when compared to 2 days ($p < 0.0001$). As for the expression of the lipopolysaccharide receptor CD14, the presence of an IOL material induced no changes in expression. However, CD14 expression was down-regulated at 6 days relative to both 2 days and 4 days ($p < 0.02$).

Table 2.3: CD45, CD36 and CD14 cell-surface receptor expression on macrophages cultured for 2, 4, or 6 days with a PMMA lens, pHEMA lens or no lens. Receptor expression was measured by flow cytometry and is reported as the geometric mean of arbitrary fluorescence units (AFU) ± the standard error of measurement.

IOL material	Incubation time	CD45	CD36	CD14
No material	2 days	57 ± 13	26 ± 6	17 ± 5
	4 days	57 ± 12	16 ± 8[*]	24 ± 6
	6 days	38 ± 9[*+]	17 ± 7[*]	15 ± 4[+]
PMMA	2 days	58 ± 6	26 ± 4	22 ± 5
	4 days	54 ± 9	16 ± 5[*]	21 ± 2
	6 days	38 ± 6[*+]	14 ± 8[*]	15 ± 2[+]
pHEMA	2 days	54 ± 6	23 ± 4	19 ± 4
	4 days	64 ± 8	19 ± 6[*]	26 ± 4
	6 days	40 ± 6[*+]	15 ± 6[*]	17 ± 3[+]

n = 7 at 2 days, and n = 4 at both 4 days and 6 days.

[*] Significantly different from corresponding value at 2 days ($p < 0.01$).

[+] Significantly different from corresponding value at 4 days ($p < 0.02$).

2.3.3 pHEMA surfaces prevent strong macrophage adhesion

The relationship between CD54 upregulation and macrophage adhesion to IOL materials was investigated using confocal microscopy. After 2 days of incubation the surface of the pHEMA IOL was devoid of macrophages, as determined by immunostaining for CD45. Instead, the surface was covered in CD45+/CD54+ microparticles of two forms: a sharp, jagged appearance that stained strongly for CD54 (* in Figure 2.6a), and a granular appearance that stained less strongly for CD54 (‡ in Figure 2.6b). Also found infrequently on the surface were larger, cell-sized impressions staining positively for CD54 and CD45 (+ in Figure 2.6a). These impressions lacked the three-dimensional geometry of macrophages and instead appeared as a thin film on the IOL surface. A pHEMA lens cultured without macrophages and treated with the same staining protocol served as a negative control for the binding of CD45 and CD54 (Figure 2.6c), confirming specific binding of the fluorescent antibodies.

In contrast, many hundreds of CD45+ macrophages but very few microparticles were found on the hydrophobic surface of the PMMA IOL after 2 days of incubation time. These cells stained very strongly for CD54, and took one of three appearances. First observed were giant, circular cells of diameter greater than 100 μm, as shown in Figure 2.7a. These cells were multinucleated and resembled foreign body giant cells (FBGCs). Also observed were macrophages with pseudopodia extended, often times joining the body of other macrophages, as shown in Figure 2.7d. These cells were typically around 250 μm in length, varying in width along their length. Lastly were globular macrophages with sharp cytoplasmic projections that extended in all directions, as shown in Figure 2.7c and Figure 2.7d. These cells varied in size between 30 μm and 60 μm in diameter, and were the most common adherent cells observed on the hydrophobic PMMA IOL surface.

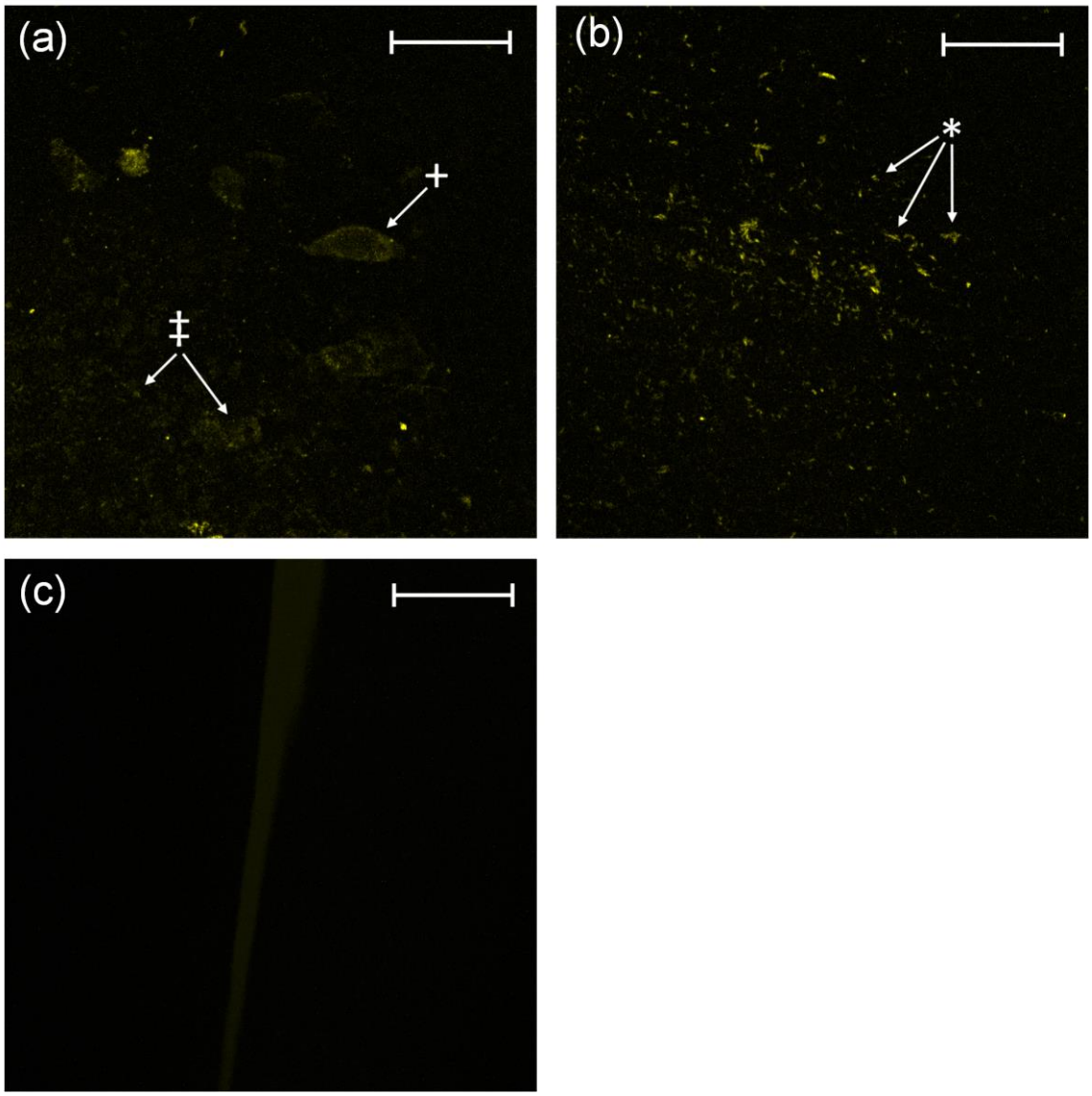

Figure 2.6: The surface of a pHEMA IOL observed on a confocal laser scanning microscope with a 40x objective. Scale bar represents 50 µm. Images (a) and (b) show a lens cultured with macrophages for 2 days and then stained with anti-CD54 (shown in yellow) prior to imaging. Both images depict different sections of the same IOL, and are representative of three samples. Image (c) depicts a lens cultured without macrophages, stained for CD54 and CD45, included as a negative control. + indicates a large, cell-sized impression staining positive for CD54 and CD45. ‡ indicates granular microparticles staining weakly for CD54 and CD45. * indicates jagged microparticles staining strongly for CD54 and CD45.

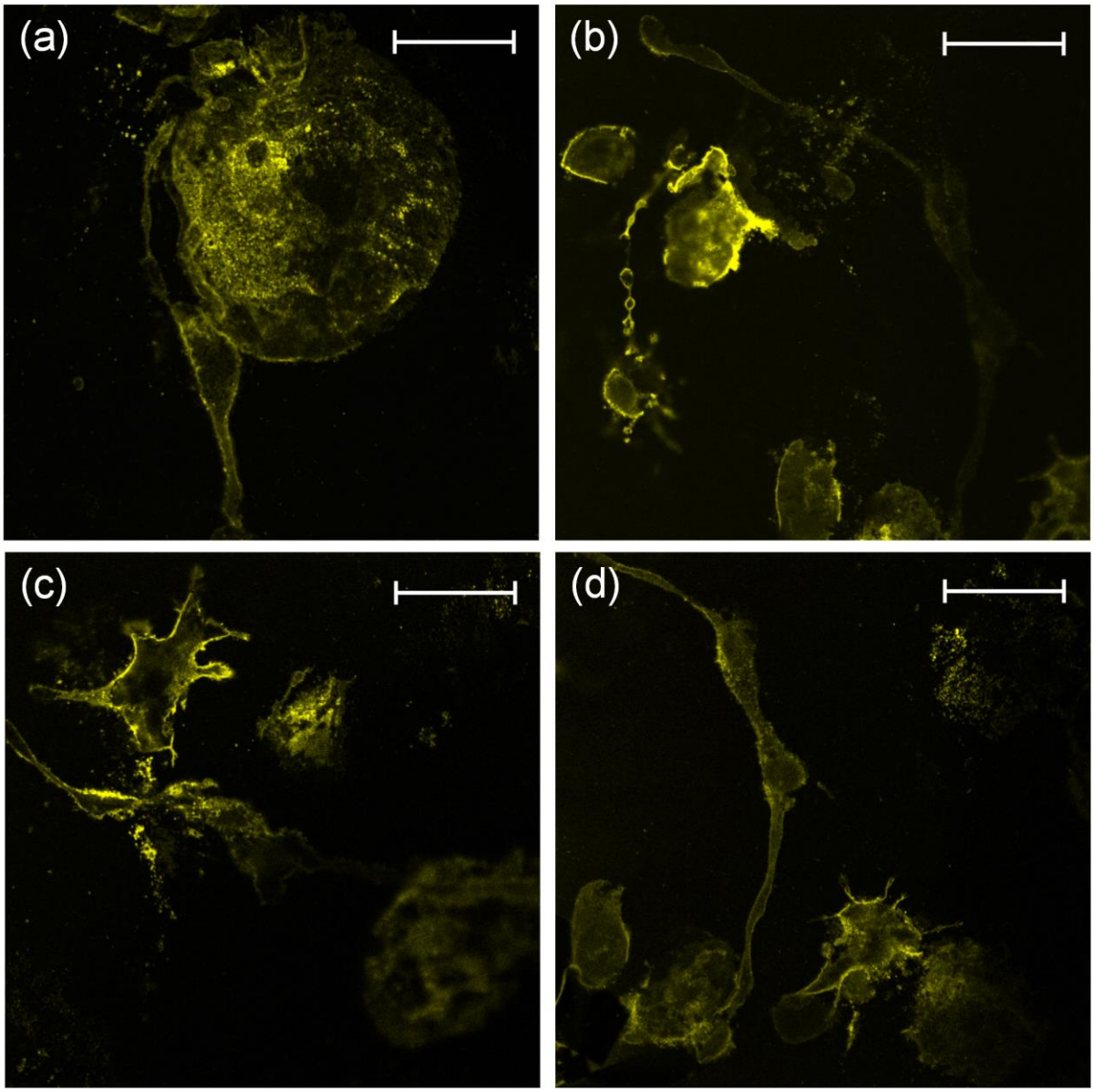

Figure 2.7: The surface of two PMMA IOLs imaged with a confocal laser scanning microscope on a 40x objective. Scale bar represents 50 µm. Lenses were cultured with macrophages for 48 hours and then stained with anti-CD54 (shown in yellow) prior to imaging. (a) depicts a multinucleated FBGC. (c) and (d) depict smaller macrophages with sharp cytoplasmic projections. (b) and (d) depict macrophages with elongated pseudopodia. Images are a representative area of at least 3 different IOLs studied.

2.3.4 Oxidative species are generated in response to PMMA and pHEMA lenses

ROS and RNS generation have been implicated in the development of a number of inflammatory disorders[30]. ROS/RNS production and overall oxidative stress, assessed by DCF fluorescence, was measured in macrophages adhered to the IOL as well as those adhered to the tissue-culture plate after one day of incubation. This incubation length was chosen as a result of the confocal study, where the absence of strongly-adherent macrophages on pHEMA IOLs at 2 days of incubation was observed. As shown in Figure 2.8, incubation in the presence of either a PMMA or pHEMA IOL caused a significant increase in production of ROS/RNS in macrophages adherent to the TCPS surface ($p < 0.03$) compared to control macrophages (no IOL). Furthermore, macrophages on the PMMA or pHEMA IOL surface exhibited significantly lower DCF fluorescence when compared to both control macrophages (no IOL) ($p < 0.004$) and macrophages that remained on TCPS ($p < 0.0001$).

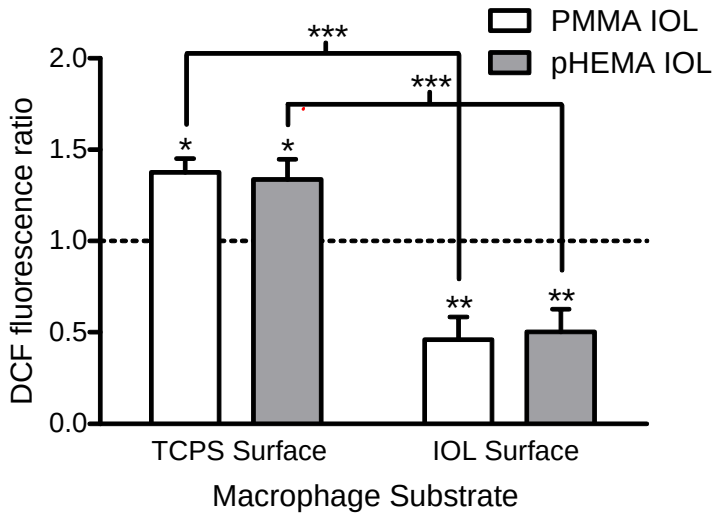

Figure 2.8: ROS/RNS production in macrophages cultured for 24 hours with a PMMA or pHEMA IOL. Macrophage adhered to the IOL were treated separately from those on the tissue culture plate (TCPS) surrounding the IOL. Values presented are DCF fluorescence measured by flow cytometry and normalized to control DCF fluorescence (no IOL). * indicates ($p < 0.03$); ** indicates ($p < 0.004$); * indicates ($p < 0.0001$). n = 6 for all treatments.**

To examine the capability of macrophages to adhere to each IOL material after one day of incubation, adherent macrophage were dissociated and counted using a flow cytometer. The hydrophilic surface of the pHEMA IOL had fewer adherent cells at 1 day (1773 ± 844) than the hydrophobic surface of the PMMA IOL (3376 ± 1367), however this difference did not reach statistical significance ($p < 0.07$, $n = 6$).

2.4 Discussion

Upon exposure to the protein kinase C activator PMA, the human monocytic leukemia cell line THP-1 differentiate into macrophage-like cells that resemble native monocyte-derived-macrophages in morphology,[159] phagocytic ability, cell-surface receptor expression and cytokine/chemokine production.[151,156,160,161] Owing to this, THP-1 macrophages have been used extensively to investigate material biocompatibility *in vitro*.[162–165] Further work has optimized THP-1 differentiation protocols to ensure sensitivity to weak stimuli,[155] and a high phenotypic similarity to native macrophages,[156] combined for the first time in the present study. The SV-40 virus immortalized human lens epithelial cell line HLE B-3 was selected for use in the co-culture model. Although differences between the proteomes of native lens epithelial cells and HLE B-3 have been investigated, namely the absence of crystallin protein expression in HLE B-3,[166] the cell line continues to be used extensively to study signalling pathways and mechanisms in PCO,[60,63,64,152,153,167] and capsular biocompatibility with IOL materials.[168,169]

Our objective was to examine the uveal biocompatibility of PMMA and pHEMA IOL materials by quantifying cellular activation. To measure activation, we chose to examine expression of the cell-surface adhesion protein CD54 (or ICAM-1) on macrophages *in vitro*. CD54 has been shown extensively in the literature to be upregulated on macrophages in response to inflammatory stimuli (see Roebuck *et. al*,[51] Sheikh *et. al* [52]). Specifically, Imanaka *et. al* observed a strong

correlation *in vivo* between CD54 upregulation and increased production of TGF-β1,[54] and Koyama *et. al* reported that CD54 activity functioned as a signal transducer for IL-1β gene transcription *in vitro*.[53] Following 2 days exposure to an IOL, we observed significant increases in expression of CD54 on macrophages cultured with a hydrophilic acrylic (pHEMA) IOL compared to cells cultured on TCPS, as well as cells cultured with a hydrophilic acrylic (PMMA) IOL, suggesting that hydrophilic acrylic materials may cause significant macrophage activation compared to hydrophobic acrylic materials. This observation is in agreement with previous work by Anderson and Jones who reported significant levels of macrophage activation to hydrophilic polyacrylamide (PAAm) surfaces compared to hydrophobic poly(styrene-co-benzyl N,N-dimethyldithio-carbamate) (BDETDC) surfaces, resulting in significantly increased production of IL-10, IL-1β, IL-6 and MIP-1β.[79] They concluded that a strong inverse relationship exists between macrophage adhesion and macrophage activation. A similar inverse relationship was observed in the present study; macrophages exposed to a pHEMA IOL showed signs of significant activation but an inability to strongly adhere to the IOL surface. Differences in CD54 expression between the hydrophobic PMMA IOL and TCPS were insignificant, corroborating work by Bernatchez *et. al* wherein no CD54 upregulation was observed with peritoneal macrophages cultured on hydrophobic polylactic acid surfaces versus TCPS.[170] Our results appear to agree with previous work investigating hydrophobic and hydrophilic materials, further suggesting that differentiated THP-1 macrophages represent a good model of macrophage biocompatibility.

The scavenger receptor CD36 plays a crucial role in the phagocytosis of apoptotic cells,[171–173] although little evidence supports inducible expression by biomaterials. We observed no effect on the expression of CD36 by the inclusion of an IOL, but detected a reduction in CD36 expression after 2 days of culture. Draude and Lorenz reported that exposure to the wound-healing cytokine TGF-β_1 supressed CD36 expression on macrophages,[174] indicating a possible macrophage phenotypic shift in

the present study. The pattern recognition receptor CD14 plays a role in the phagocytosis of both apoptotic cells,[175] and bacterial and viral pathogens,[58] but is typically used as a marker of monocyte differentiation into macrophages.[176,177] We observed no effect on the expression of CD14 by the inclusion of an IOL, but identified a decrease in CD14 expression by 6 days of macrophage culture. Bosshart *et. al* observed a spontaneous decrease in CD14 expression in blood-isolated monocytes *ex vivo*, indicating a quiescent state capable of rapid reactivation upon lipopolysaccharide stimulation.[178] Kindlund *et. al* concluded that CD14 down-regulation occurred during the differentiation process from monocyte to osteoclast.[179] Also observed in the present study was a reduction in CD45 expression after 4 days of culture, perhaps indicating a change in macrophage activity to a more quiescent state.[180] In their work examining the macrophage response to biomaterial surface chemistry, Anderson and Jones noted a phenotypic change after 3 days of macrophage culture that resembled a shift from a host-defence phenotype to a wound-healing phenotype.[79] This shift to a less inflammatory state may have been echoed in the present study by the decrease in expression of CD36, CD14 and CD45 observed after 4 days of macrophage culture.

ROS and RNS are important signalling molecules in a number of inflammatory processes and disorders.[30] To analyze the acute inflammatory response of macrophages to hydrophobic and hydrophilic IOL materials, ROS/RNS production and overall oxidative stress were measured using the probe DCFH-DA. Due to the fact that very few cells were found adherent to the pHEMA IOLs at 2 days of incubation, ROS/RNS generation was quantified after one day of culture. After exposure to either the hydrophobic PMMA or hydrophilic pHEMA IOL we observed an increase of ROS/RNS production in macrophages on the TCPS substrate compared to macrophages not exposed to an IOL. This finding coincides with but cannot be correlated with the increased expression of CD54 after 2 days of culture with either IOL material. Iribarren *et. al* noted a similar correlation *in vivo* between increased ROS generation and CD54 upregulation.[55] However, we observed significantly less

ROS/RNS production in macrophages on the surface of either IOL compared to macrophages on the TCPS substrate surrounding the IOL, as well as macrophages not exposed to an IOL. The DCFH-DA probe is a membrane-permeable fluorogenic compound that is de-acetylated by cytosolic esterases into the membrane-impermeable 2'-7'-dichlorodihydrofluorescein ($DCFH_2$).[181] Once trapped inside the cell, $DCFH_2$ is oxidized by peroxidases, cytochrome *c* and Fe^{2+} in the presence of intracellular hydrogen peroxide, producing the fluorescent compound 2'-7'-dichlorofluorescein (DCF).[182] Brubacher and Bols showed that the DCFH-DA probe underestimated ROS production in macrophages due to either low esterase expression or a sequestering of esterase into inaccessible cellular compartments,[183] a conclusion made previously by Robinson *et. al*.[184] Labow *et. al* showed previously that monocyte-derived macrophages secrete a number of esterases to degrade biomaterial surfaces,[185] a process known as frustrated phagocytosis.[186] In the present study, it is likely that the compartmentalization and secretion of cellular esterases led to an underestimation of oxidative stress in macrophages adherent to the IOL surfaces.

Using confocal microscopy, the number and phenotypic appearance of adherent macrophages on each biomaterial surface was investigated *in vitro*. Ziegelaar *et. al* previously reported that THP-1 cells showed decreased adherence to pHEMA surfaces compared to TCPS and noted a relationship between adhesion and collagenase production,[162] but did not normalize for the number of adherent cells. In the present study, fewer cells were found adhered to the pHEMA IOLs than the PMMA IOLs despite what appears to be significant macrophage activation. After one day of incubation, approximately half as many macrophages were counted via flow cytometry on the pHEMA surface compared to the PMMA surface. After 2 days of incubation, the PMMA surface showed signs of FBGC fusion while the pHEMA IOL was devoid of cells. Macrophages were instead found on the TCPS substrate surrounding the pHEMA IOL for up to 6 days of culture. Macrophages were found loosely adherent to the pHEMA IOL surface after 1 day exposure but were no longer present at 2

days incubation. Rice *et. al* observed the migration of primary osteoblasts from titanium oxide surfaces to exposed TCPS surfaces *in vitro* during a 7 day period,[187] and thus a similar migration may have occurred. Furthermore, CD45+/CD54+ impressions of detached cells and microparticles were found on the surface of the pHEMA lens at 2 days incubation. Macrophage microparticles were observed by Cerri *et. al* to upregulate inflammatory processes in human airway endothelial cells.[188] Gauley *et. al* observed that Toll-like-receptor stimulation of macrophages lead to microparticle release; a process influenced by ROS production.[189] These findings suggest that the microparticles observed on the pHEMA surface, as well as the changes in ROS/RNS production, may mediate the response of lens epithelial cells in the co-culture. While many studies have characterized macrophage adhesion on biomaterials, there is limited work reporting on the adherence of macrophage microparticles on biomaterial surfaces, perhaps owing to the limited use of confocal microscopy for macrophage markers on implant surfaces. Although the pHEMA lens surface prevented adherence, in the post-operative *in vivo* environment, the newly-exposed collagen-IV rich anterior lens capsule may serve as a substrate for macrophage adherence in patients with pHEMA IOLs. On the other hand, the PMMA lens allowed for strong adherence of macrophages and enabled fusion into what appeared to be multi-nucleated FBGCs. Similar to our *in vitro* results, Ravalico *et. al* observed significant inflammatory cell adhesion and fusion on PMMA lenses in human patients between 7 and 180 days after corrective surgery for cataracts, with a corresponding lack of cellular adhesion and fusion on pHEMA lenses.[190]

During the development of PCO, myofibroblasts in the lens capsule overexpress the extracellular matrix protein fibronectin and halt expression of the epithelial adhesion protein E-cadherin.[22] Chung *et. al* showed that treatment with TGF-β_1 induced fibronectin expression in HLE B-3 cells,[152] while Hosler *et. al* showed that treatment with TGF-β_2 induced fibronectin gene activation in HLE B-3 and primary cells.[64] Choi *et. al* observed that TGF-β_1 treatment repressed E-

cadherin expression in HLE B-3 cells,[60] while a similar study by Yao *et. al* observed the same finding but in alveolar epithelial cells.[191] In the present study, no difference in fibronectin or E-cadherin expression was induced by lens cell and macrophage co-culture with an IOL material. These findings may indicate that the TGF-β family of cytokines may not participate in the interaction between co-cultured macrophages and lens epithelial cells. Indeed, an enzyme-linked immunosorbent assay (ELISA) for TGF-β_1 was performed on co-culture and activated-macrophage supernatants to examine a possible effect, but TGF-β_1 was observed at background levels. In light of these findings, it seems probable that another soluble mediator is responsible for the observed interaction.

The novel *in vitro* co-culture model presented herein incorporated lens epithelial cells and macrophages on separate substrates in the same media environment. Similar co-culture models have demonstrated the ability of macrophages to promote inflammation in hepatocytes and adipocytes,[151,192,193] stimulate bone resorption,[194] direct apoptosis and suppress cell division in mesangial cells.[195] More relevant to this investigation, Glim *et. al* demonstrated that M2 (wound-healing) macrophages induced the expression of the myofibroblast protein and secondary-cataract marker α-SMA in dermal and gingival fibroblasts via the secretion of platelet derived growth factor.[196] After 6 days of co-culture with macrophages activated by a pHEMA IOL, lens epithelial cells significantly increased expression of α-SMA relative to co-culture with no IOL, as demonstrated both by flow cytometry and confocal microscopy. α-SMA expression has been shown to increase contractile force in fibroblasts[197], and Lois *et. al* observed a reduction in the number of lens epithelial cells in the center of the posterior capsule after systemic macrophage depletion,[90] indicating a possible role for macrophage activation to IOL biomaterials in the severity of posterior capsule wrinkling during PCO. Anderson and Jones noted that macrophages cultured on hydrophilic PAAm surfaces produced greater quantities of inflammatory cytokines than macrophages cultured on hydrophobic BDETDC despite being substantially fewer in number,[79] concluding that total volume of

cytokine production was a function of the number of activated cells and the degree to which they were activated. In the present study, macrophages cultured on a hydrophilic pHEMA surface were significantly more activated and fewer in number than macrophages cultured on a hydrophobic PMMA surface. However, both groups induced approximately the same upregulation of α-SMA in co-cultured lens cells, lending further evidence to the hypothesis that the gross foreign body reaction to a biomaterial is a function of both the numbers and degree of macrophage activation.

2.5 Conclusions

Our findings provide a novel insight into uveal biocompatibility. Previous work exploring IOL biocompatibility with inflammatory cells have based their conclusions on the number of leukocytes adherent to a given material, concluding that hydrophilic surfaces that prevent cellular adhesion are more biocompatible with leukocytes as they prevent fusion into FBGCs.[83–85] Our results have shown *in vitro* that FBGC formation, and indeed macrophage adherence in general, are not necessary for a strong inflammatory response to an IOL. Rather, the inflammatory response to an IOL appears to be a function of both the amount of stimulation and the number of inflammatory cells stimulated, with a hydrophilic acrylic surface providing a stronger stimulus for macrophage activation than a hydrophobic acrylic one. These findings provide a new method of inquiry into uveal biocompatibility, specifically through the quantification of cell-surface markers of leukocyte activation.

Chapter 3

The Effect of Elevated Glucose Levels on the Co-culture System

3.1 Introduction

Diabetes mellitus is a family of diseases characterized by an inability to regulate blood glucose levels, resulting in prolonged periods of high blood sugar called hyperglycemia that cause damage to vital tissues of the human body.[46,119,123,125,198–204] Diabetes typically manifests as one of two chronic illnesses: Type 1 Diabetes Mellitus, formerly known as juvenile diabetes, and Type 2 Diabetes Mellitus, formerly known as adult-onset diabetes.[205] Type 1 diabetes is caused by the autoimmune destruction of pancreatic β-cells, the insulin producing cells of the body. Insulin is a vital hormone responsible for regulating carbohydrate and fatty acid metabolism in the human body, and without functioning β-cells type 1 diabetics are dependent on injections of synthetic insulin to survive.[205] Type 2 diabetes, on the other hand, is a state of dysfunctional blood glucose regulation as result of increased tolerance to insulin in the human body, called insulin resistance.[200] Type 2 diabetes is highly associated with obesity and is treated foremost with diet and exercise, although drug therapies can also be used.[205]

Despite different underlying pathologies, both Type 1 and Type 2 diabetes cause the same complications in patients as a result of prolonged periods of hyperglycemia.[205] Diabetic hyperglycemia is defined by the American Diabetes Association as any blood glucose concentration higher than 11.1 millimolar (mM),[205] which is twice the healthy upper limit of fasting blood glucose at 5.5 mM. However, pathological issues associated with diabetes and hyperglycemia are typically not observed until acute hyperglycemic concentrations exceed 20 mM.[138,199,206–209] Diabetic complications are increasingly believed to be caused by the dysfunction of inflammatory processes

involving the macrophage,[46,50] and include impaired wound healing,[120,121] narrowing of arterial walls (atherosclerosis),[47,122–125] kidney damage (diabetic nephropathy),[126–130] and retinal damage (diabetic retinopathy).[131–133] The lens can also be compromised by what is called diabetic cataract,[134] the pathogenesis of which is not well understood but believed to be a result of metabolic and oxidative damage in a high glucose environment.[134–136] Little work to date has examined the possible role of macrophages in diabetic complications of the lens. In the present study, we propose the use of a co-culture model of macrophages and lens epithelial cells in hyperglycemic and isoglycemic conditions to further investigate the tissue environment of the lens in diabetes.

3.1.1 Cell Culture

The *in vitro* co-culture model developed in Chapter 2 was modified to isolate the effect of glucose concentration on the model. Changes to the macrophage, lens cell and co-culture protocols are detailed below. Unless otherwise noted, culture procedures were identical to those previously established in Section 2.2.1.

3.1.1.1 Macrophage Culture

THP-1 monocytes were maintained in suspension in RPMI 1640 media with 10% FBS and differentiated using PMA as described in Section 2.2.1.1. However, upon plating for differentiation THP-1 monocytes were incubated in a media mixture comprised of 67% v/v RPMI 1640 and 33% v/v DMEM. After 72 hours, media was replaced with a new mixture comprised of 33% v/v RPMI 1640 and 67% v/v DMEM. After 48 hours, media was replaced with 100% DMEM for a final 48 hours until co-culture began. This process allowed THP-1 macrophages to be slowly transitioned from the higher glucose concentration found in RPMI 1640 (11 mM) to the lower glucose concentration of

DMEM (5.5 mM) through two intermediary concentrations of 9.185 mM (67% RPMI + 33% DMEM) and 7.315 mM (33% RPMI + 67% DMEM), as shown below in Table 3.1.

Table 3.1: Cell-culture media combinations used to transition macrophages to low glucose

Glucose Concentration	Media Combination
11 mM	100% RPMI + 0% DMEM
9.185 mM	67% RPMI + 33% DMEM
7.315 mM	33% RPMI + 67% DMEM
5.5 mM	0% RPMI + 100% DMEM

3.1.1.2 Lens Epithelial Cell Culture

Prior to co-culture, HLE B-3 were cultured according to the protocol described in Section 2.2.1.2. To begin co-culture, 24-well polyethylene terephthalate 1-µm membrane hanging cell-culture inserts were inverted in a 6 well plate. To provide a more compliant surface for lens epithelial cell adhesion and therefore reduce background expression of intracellular stress fibres like αSMA[210], inserts were coated with 0.05 mg/mL of collagen type I for 30 min at 37°C. After two washes with PBS, inserts were seeded with either 1×10^4, 2.5×10^4, 5×10^4 or 1×10^5 lens cells per insert, based on the intended length of co-culture: 6 and 12 hour co-cultures were seeded with 1×10^5 cells, 1 day co-cultures were seeded with 5×10^4 cells, 2 day co-cultures with 2.5×10^4 cells and 6 day co-cultures with 1×10^4 cells. These seeding concentrations ensured a final cell density of approximately 1×10^5 cells per insert while preventing overconfluence. Inserts were incubated overnight, and then returned to their normal orientation in serum-free media in a 24-well plate until the start of the co-culture.

3.1.2 Co-culture

To examine the effect of glucose concentration on the post-operative lens, HLE B-3 cells and THP-1 macrophages were co-cultured or monocultured in DMEM with 10% FBS containing either 5.5 mM

D-glucose, representing non-diabetic physiologic blood glucose levels and referred to hereafter as "low glucose", or 25 mM D-glucose, representing diabetic pathological blood glucose levels and referred to hereafter as "high glucose". 1 x 10^5 disassociated mature THP-1 macrophages were added to two wells of a 24-well plate containing 1 mL of low glucose DMEM and two wells containing 1 mL high glucose DMEM. Plates were incubated for 2 hours to allow for macrophage adherence. Hanging inserts with adherent HLE cells were then introduced to the co-culture plate. Two inserts were added to wells containing macrophages (one high glucose and one low glucose) and two inserts were introduced to blank wells with 1 mL of either high or low glucose DMEM. Co-culture plates were incubated for 6 hours, 12 hours, 1 day, 2 days or 6 days and then assayed for changes in cellular phenotype. Media was refreshed every 2 days. Upon the completion of co-culture, supernatant was collected and frozen at -20°C for assay at a later time.

3.1.3 Immunolabelling and fluorescent reagents

FITC conjugated mouse monoclonal antibody against CD36 (multi-ligand scavenger receptor), FITC conjugated mouse monoclonal antibody against CD11c (alpha chain subunit of complement receptor 4), PE-Cy5 conjugated monoclonal antibody against CD45 (human leukocyte common antigen), PE-Cy5 conjugated monoclonal antibody against CD11b (alpha chain subunit of macrophage antigen-1 or complement receptor 3), PE conjugated monoclonal antibody against CD54 (intercellular adhesion molecule 1 or ICAM1), PE conjugated mouse monoclonal antibody against CD14 (pattern recognition receptor), Alexa Fluor® 647 (AF647) conjugated mouse monoclonal antibody against E-cadherin were purchased from Becton Dickinson Pharmingen (San Diego, CA, USA). PE conjugated monoclonal mouse antibody against vimentin, and FITC conjugated mouse monoclonal antibody against α-smooth muscle actin (α-SMA) were purchased from R&D Systems (Minneapolis, MN). As

a new α-SMA antibody was used, fluorescence values of α-SMA are not comparable to those presented in Chapter 2. All other chemicals were of analytical reagent grade.

Both propidium iodide (PI) and a FLICA caspase kit were purchased from ImmunoChemistry Technologies (Bloomington, MN, USA). The FLICA kit uses the membrane-permeable, fluorescent – pan caspase inhibitor FAM-VAD-FMK for caspase detection.

3.1.4 Flow Cytometry

Tissue digestion was performed as described in Section 2.2.5. Briefly, inserts containing adherent HLE cells were removed from the co-culture system, and wells containing macrophages were incubated at 37°C with TrypLE Express for 30 minutes. THP-1 cells were then centrifuged in media containing 10% FBS and re-suspended in 100 µL fresh media with serum. Aliquots of 50 µL were incubated in saturating concentrations of conjugated fluorescent monoclonal antibodies for 1 hour at room temperature in the dark. Leukocyte populations were identified by expression of CD45 or CD14. To assess macrophage behaviour, samples were split into two aliquots and incubated with one of two antibody combinations: FITC anti-CD36, PE anti-CD54 and PE-Cy5 CD45, or, FITC anti-CD11c, PE anti-CD14 and PE-Cy5 anti-CD11b. After incubation, samples were diluted with HEPES-Tyrode's buffer and fixed with paraformaldehyde. Samples were read on a three-color FACSCalibur flow cytometer.

Inserts with adherent HLE cells were submerged in 0.25% Trypsin-EDTA and incubated at 37°C for 2 hours on a shaker at 250 RPM. Once detached, cells were re-suspended in DMEM with 10% FBS before centrifugation. Excess media was removed. Cells were re-suspended and then fixed in paraformaldehyde at a final concentration of 4% w/v for 15 minutes, at room temperature in the dark. Samples were washed, and cells were re-suspended and permeabalized with 0.5% Triton-X for 5 minutes, at room temperature in the dark. Samples were then centrifuged and re-suspended in PBS

containing 1% w/v fatty-acid free BSA. Samples were separated into three aliquots and stained with antibodies against either α-SMA (FITC conjugated), E-cadherin (AF647 conjugated) or vimentin (PE conjugated) overnight, at 4°C in the dark. Samples were read the following morning on a three-color FACSCalibur flow cytometer.

3.1.4.1 Caspase Activity

To assess the effect of different culture conditions on apoptosis and necrosis in macrophages and lens cells, caspase activity was measured by flow cytometry using the fluorogenic pan caspase inhibitor FAM-VAD-FMK, which fluoresces most intensely in cells with active caspases. Dead cells were identified by PI staining. As per the FLICA Kit instructions, cell suspensions were incubated with saturating concentrations of FAM-VAD-FMK for 60 minutes at 37°C. Samples were washed in caspase wash buffer three times before 0.5µL of PI was added. Caspase/PI samples were read immediately on a three-color FACSCalibur flow cytometer.

For each sample, cells were separated into four quadrants using post-acquisition gating on a plot of caspase fluorescence versus PI fluorescence. A typical plot of lens epithelial cells is shown below in Figure 3.1. Each quadrant delineates a subset of the population experiencing either apoptosis, cell death from apoptosis (secondary necrosis), necrosis, and live cells. Division into quadrants is performed by isolating the PI-positive and Caspase-positive population (cells experiencing secondary necrosis) into the upper-right Quadrant 2 (Q2). The same gating strategy was applied to all samples on the same cell-culture plate. The percentage of the total population within each quadrant was then analyzed for changes due to treatment or other factors. Additional examples of the gating strategy employed are included in Appendix A.

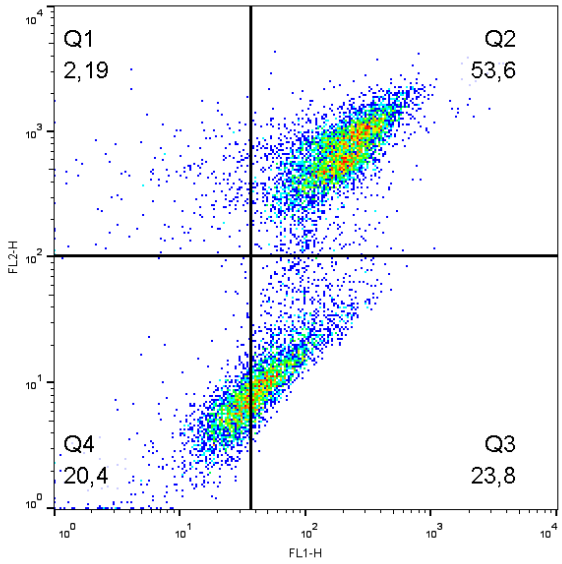

Figure 3.1: Representation of the gating strategy employed in live/dead analysis of lens epithelial cells and macrophages. Caspase fluorescence is plotted on the X-axis and PI fluorescence on the Y-axis. Shown here is a sample of lens epithelial cells that are mostly experiencing secondary necrosis. Quadrant 1 (Q1) depicts 3.03% of cells experiencing primary necrosis, Quadrant 2 (Q2) depicts 54.1% of cells experiencing secondary necrosis, Quadrant 3 (Q3) depicts 15.0% of cells undergoing apoptosis and Quadrant 4 depicts 27.8% of cells as alive.

3.1.5 Statistical Analysis

Flow cytometry fluorescence values and percentage values are presented as the mean ± the standard error of the mean (SEM). Fluorescence and percentage values were subjected to a multivariate analysis of variance (ANOVA) using a general linear model, including terms for length of incubation, glucose concentration (high glucose vs. low glucose), and the culture condition (monoculture vs. co-culture). Pairwise comparisons between glucose concentration, culture condition, incubation time, and glucose-culture-time combinations were performed using the Bonferoni comparison in Minitab 16.2.3. A *p* value of less than 0.05 was required for significance. The number of experiments was always equal to or greater than three.

3.2 Results

3.2.1 Culture with high glucose media down-regulates integrin expression

The co-culture model was employed to determine the effect of glucose concentration on macrophage phenotype by examining cell-surface integrin expression. Overall, the co-culture model showed no difference on macrophage integrin expression when compared to a monoculture model. Integrin expression declined significantly over time ($p < 0.05$) for both high and low glucose culture media, with the decline occurring sooner (at 1 day of culture versus 6 days of culture) and more sharply with high glucose media. Glucose concentration in both models therefore had a prevailing, significant effect on all macrophage integrins beginning at 1 day of culture ($p < 0.05$). Significant differences between high and low glucose were observed at 2 days ($p < 0.05$) but not 6 days due to the decline in expression over time.

The intercellular adhesion molecule-1, otherwise known as CD54, was analyzed for changes in expression due to glucose concentration. As shown in Figure 3.2, macrophage monoculture and co-culture in high glucose media significantly down-regulated CD54 expression at 1 day (monoculture: $p = 0.0092$, co-culture: $p = 0.001$) and 2 days (monoculture: $p = 0.0025$, co-culture: $p = 0.0007$) of incubation. In high glucose, CD54 expression peaked at 12 hours of incubation before decreasing very significantly by 1 day of incubation (monoculture: $p = 0.0004$, co-culture: $p = 0.0001$), where it remained nominally low through 2 and 6 days of incubation. In low glucose, CD54 expression peaked at 12 hours of incubation before decreasing significantly by 1 day of incubation (monoculture: $p = 0.0025$), and decreasing yet again between 2 days and 6 days of incubation (monoculture: $p = 0.0284$, co-culture: $p = 0.0025$).

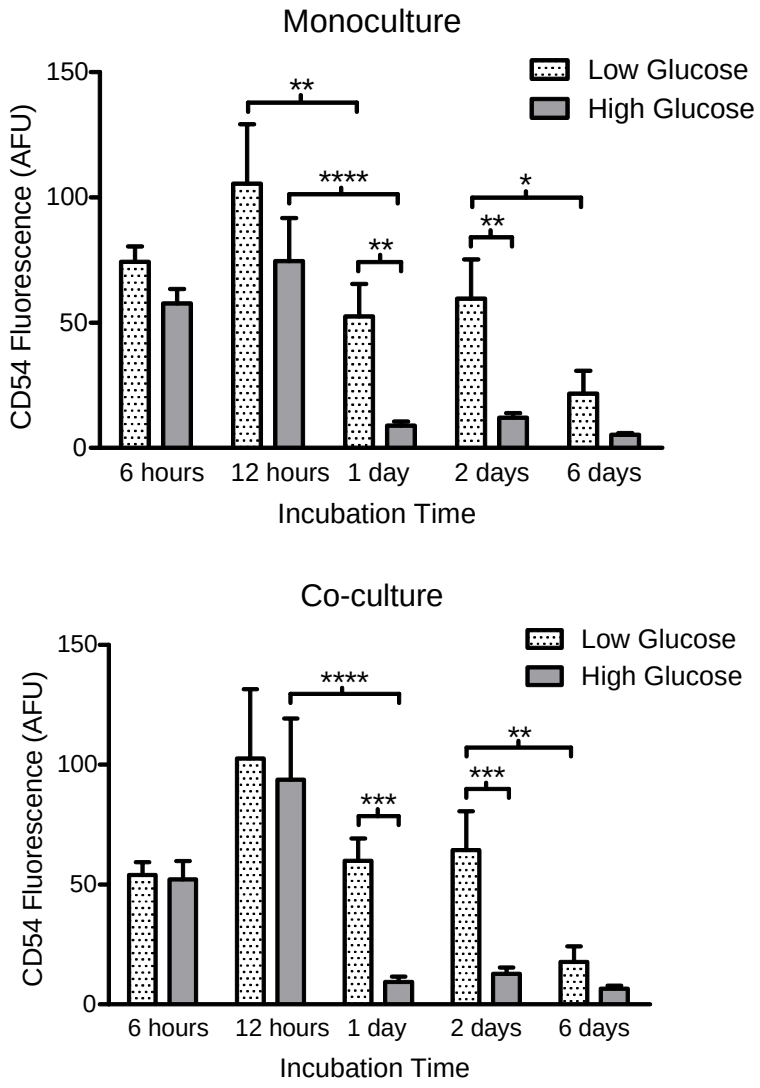

Figure 3.2: High glucose culture media down-regulates expression of CD54 in macrophages. Cells were cultured for 6 hours, 12 hours, 1 day, 2 days or 6 days in a monoculture (top) or in a lens co-culture system (bottom). CD54 expression was measured by flow cytometry and is reported as the mean ± the standard error of measurement (SE) of arbitrary fluorescence units (AFU). * indicates significant difference ($p < 0.05$); ** significant difference ($p < 0.01$), * significant difference ($p < 0.001$), **** significant difference ($p < 0.0001$). n = 4 for all treatments and controls.**

CD11c, an adhesion integrin, was also analyzed for changes in expression. As shown in Figure 3.3, macrophage monoculture and co-culture in high glucose media significantly down-regulated CD11c expression at 1 day (monoculture: $p = 0.0001$, co-culture: $p = 0.0001$) and 2 days (monoculture: $p = 0.0001$, co-culture: $p = 0.0001$) of incubation. In high glucose, CD11c expression peaked at 12 hours of incubation before decreasing very significantly by 1 day of incubation (monoculture: $p = 0.0003$, co-culture: $p = 0.0001$), where it remained nominally low through 6 days. In low glucose, CD11c expression peaked at 12 hours of incubation but did not decline significantly until 6 days of culture (monoculture: $p = 0.0001$, co-culture: $p = 0.0001$).

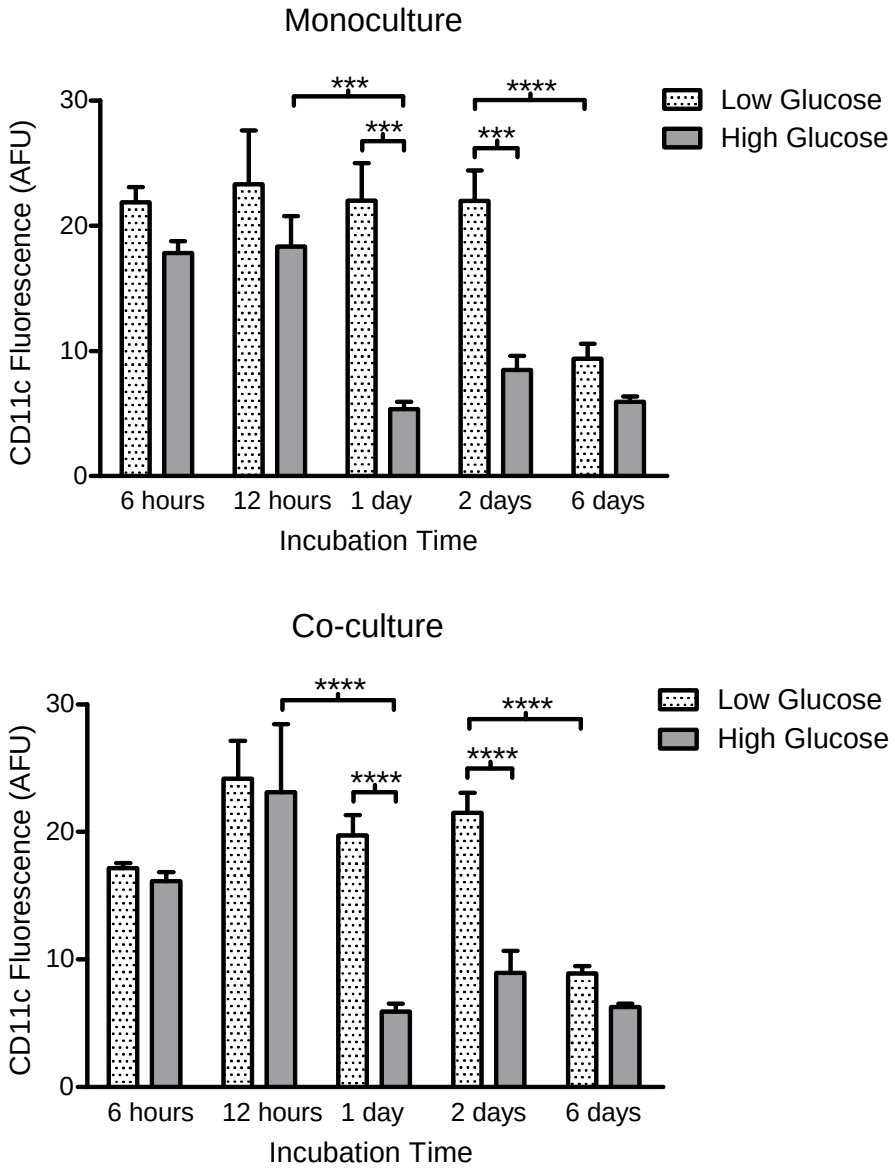

Figure 3.3: High glucose culture media down-regulates expression of CD11c in macrophages. Cells were cultured for 6 hours, 12 hours, 1 day, 2 days or 6 days in a monoculture (top) or in a lens co-culture system (bottom). CD11c expression was measured by flow cytometry and is reported as the mean ± the standard error of measurement (SE) of arbitrary fluorescence units (AFU). * indicates significant difference ($p < 0.05$); ** significant difference ($p < 0.01$), * significant difference ($p < 0.001$), **** significant difference ($p < 0.0001$). n = 4 for all treatments and controls.**

The pattern recognition receptor CD14 exhibited similar patterns of expression to CD11c. As shown in Figure 3.4, macrophage monoculture and co-culture in high glucose media significantly down-regulated CD14 expression at 1 day (monoculture: $p = 0.0007$, co-culture: $p = 0.0019$) and 2 days (monoculture: $p = 0.0008$, co-culture: $p = 0.015$) of incubation. In high glucose, CD14 expression peaked at 12 hours of incubation before decreasing very significantly by 1 day of incubation (monoculture: $p = 0.0029$, co-culture: $p = 0.0001$), where it remained nominally low through 6 days. In low glucose, CD14 expression peaked at 12 hours of incubation but did not decline significantly until 6 days of culture (monoculture: $p = 0.0242$, co-culture: $p = 0.0153$).

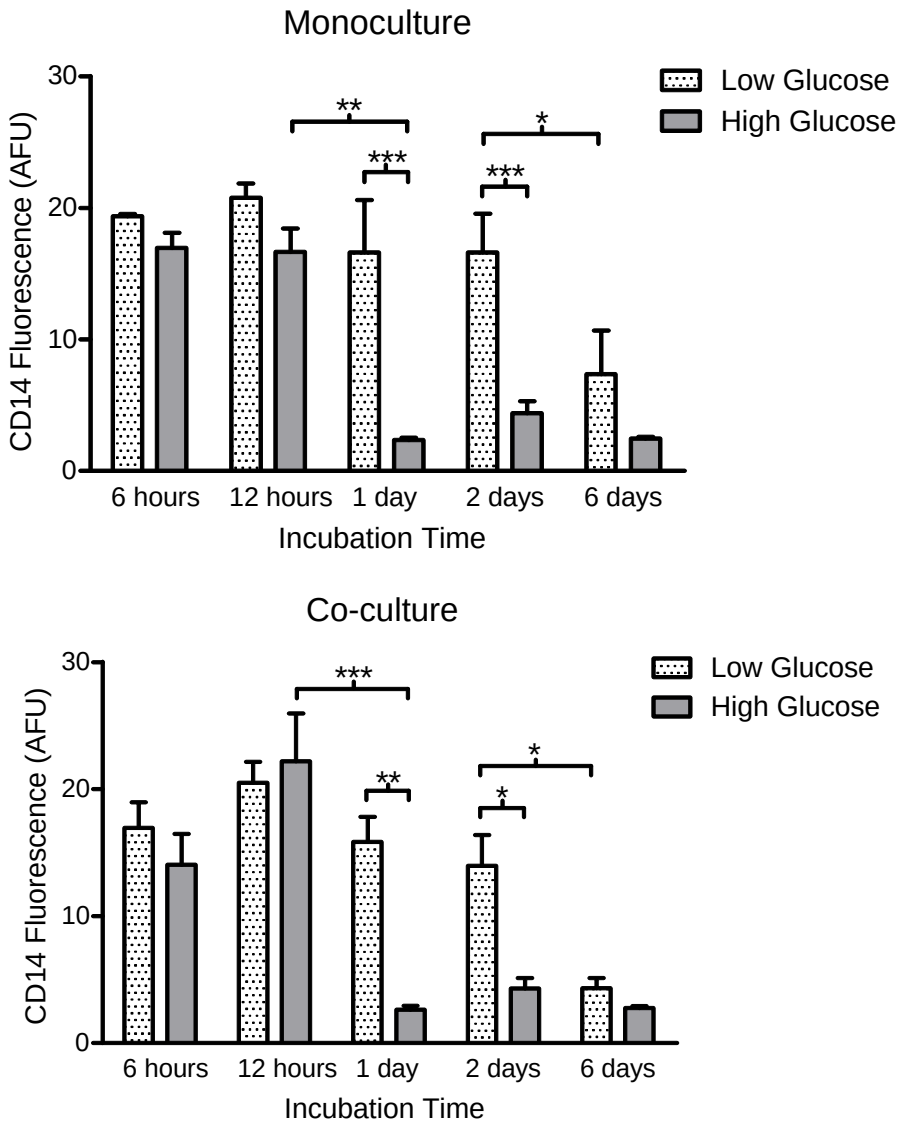

Figure 3.4: High glucose culture media down-regulates expression of CD14 in macrophages. Cells were cultured for 6 hours, 12 hours, 1 day, 2 days or 6 days in a monoculture (top) or in a lens co-culture system (bottom). CD14 expression was measured by flow cytometry and is reported as the mean± the standard error of measurement (SE) of arbitrary fluorescence units (AFU). * indicates significant difference ($p < 0.05$); ** significant difference ($p < 0.01$), * significant difference ($p < 0.001$), **** significant difference ($p < 0.0001$). n = 4 for all treatments and controls.**

Unlike CD11c, the adhesion integrin CD11b exhibited no discernible peaks in expression and minimal time variance. As shown in Figure 3.5, high glucose media significantly down-regulated CD11b expression at 1 day (monoculture: $p = 0.0001$, co-culture: $p = 0.0002$) and 2 days (monoculture: $p = 0.0001$, co-culture: $p = 0.0011$) of incubation. In high glucose, CD11b expression declined significantly between 12 hours and 1 day of incubation (monoculture: $p = 0.015$, co-culture: $p = 0.0006$), where it remained through 6 days of incubation. In low glucose, CD11b expression declined significantly between 2 days and 6 days of incubation (monoculture: $p = 0.0001$, co-culture: $p = 0.0001$).

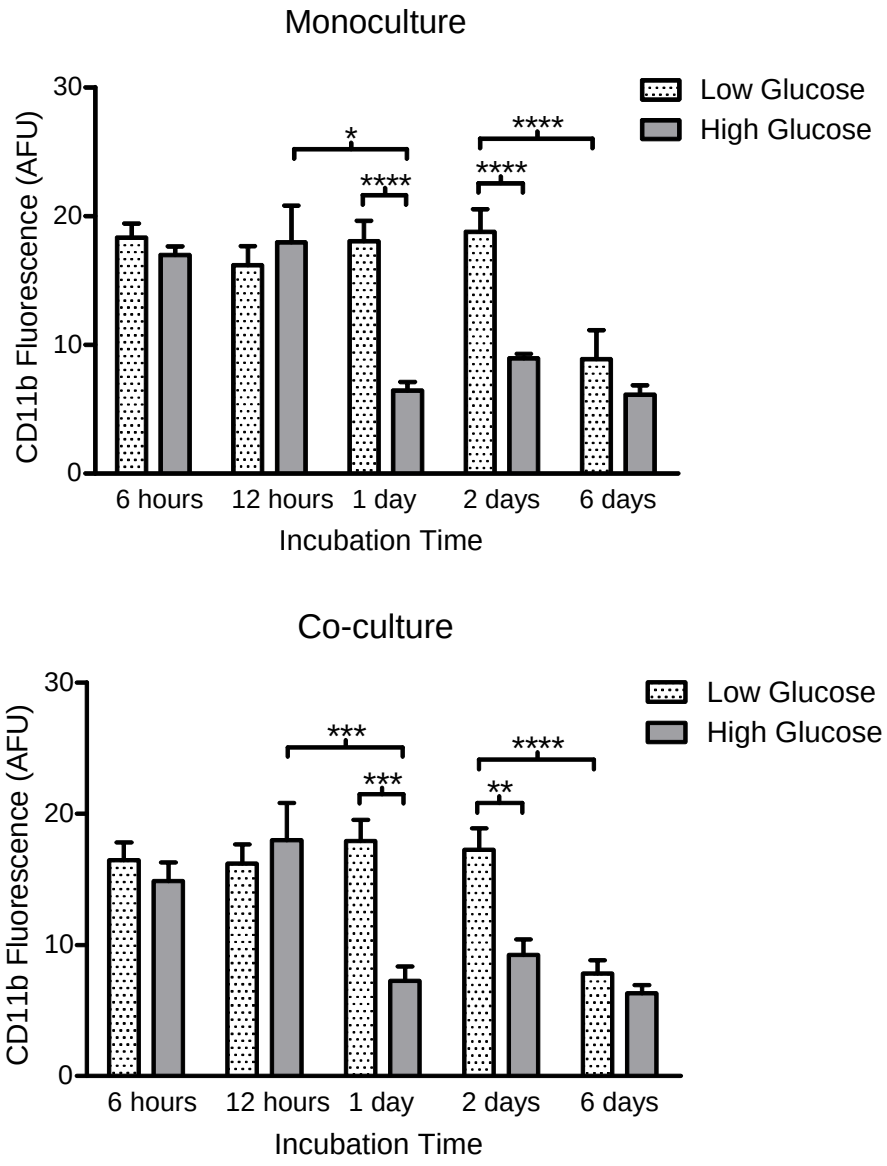

Figure 3.5: High glucose culture media down-regulates expression of CD11b in macrophages. Cells were cultured for 6 hours, 12 hours, 1 day, 2 days or 6 days in a monoculture (top) or in a lens co-culture system (bottom). CD11b expression was measured by flow cytometry and is reported as the mean ± the standard error of measurement (SE) of arbitrary fluorescence units (AFU). * indicates significant difference ($p < 0.05$); ** significant difference ($p < 0.01$), * significant difference ($p < 0.001$), **** significant difference ($p < 0.0001$). n = 4 for all treatments and controls.**

Due to limited quantities of antibodies for the scavenger receptor CD36, changes in expression were measured only at 1 day, 2 days and 6 days of incubation. As shown in Figure 3.6, culture in high glucose media significantly down-regulated CD36 expression at 1 day (monoculture: $p = 0.0001$, co-culture: $p = 0.0001$) and 2 days (monoculture: $p = 0.0001$, co-culture: $p = 0.0153$) of incubation. In high glucose, CD36 expression levels remained consistently low over time. In low glucose, CD36 expression declined significantly between 1 day and 2 days of co-culture (co-culture: $p = 0.0258$) and between 2 days and 6 days of mono-culture (monoculture: $p = 0.0001$).

The flow cytometry results of CD45 are included in Appendix B.

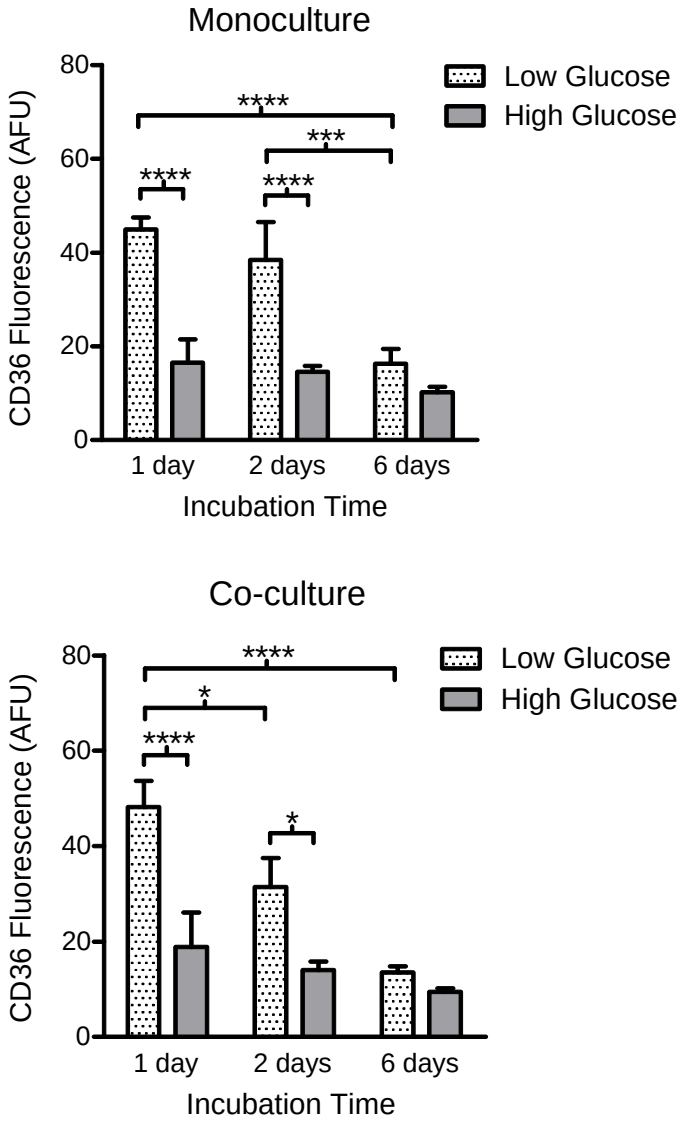

Figure 3.6: High glucose culture media down-regulates expression of CD36 in macrophages. Cells were cultured for 6 hours, 12 hours, 1 day, 2 days or 6 days in a monoculture (top) or in a lens co-culture system (bottom). CD36 expression was measured by flow cytometry and is reported as the mean ± the standard error of measurement (SE) of arbitrary fluorescence units (AFU). * indicates significant difference ($p < 0.05$); ** significant difference ($p < 0.01$), * significant difference ($p < 0.001$), **** significant difference ($p < 0.0001$). n = 4 for all treatments and controls.**

3.2.2 High glucose media delays macrophage apoptosis and decreases necrosis

A FLICA kit from ImmunoChemistry Technologies was used to examine the possible effect of elevated glucose concentration on macrophage apoptosis. As shown in Figure 3.7, the number of apoptotic macrophages in both monoculture and co-culture increased significantly over time to a maximum of 69% of cells undergoing apoptosis. In high glucose, the proportion of apoptotic cells remained low between 6 hours and 1 day of incubation (around 35% of all cells) before significantly increasing to 69% at 2 days of culture (monoculture: $p = 0.0072$, co-culture: $p = 0.0028$). In low glucose, a significant increase in the proportion of apoptotic cells was observed earlier, at 1 day of culture (monoculture: $p = 0.0297$, co-culture: $p = 0.0083$). No significant difference in the proportion of apoptotic cells was observed between high and low glucose media.

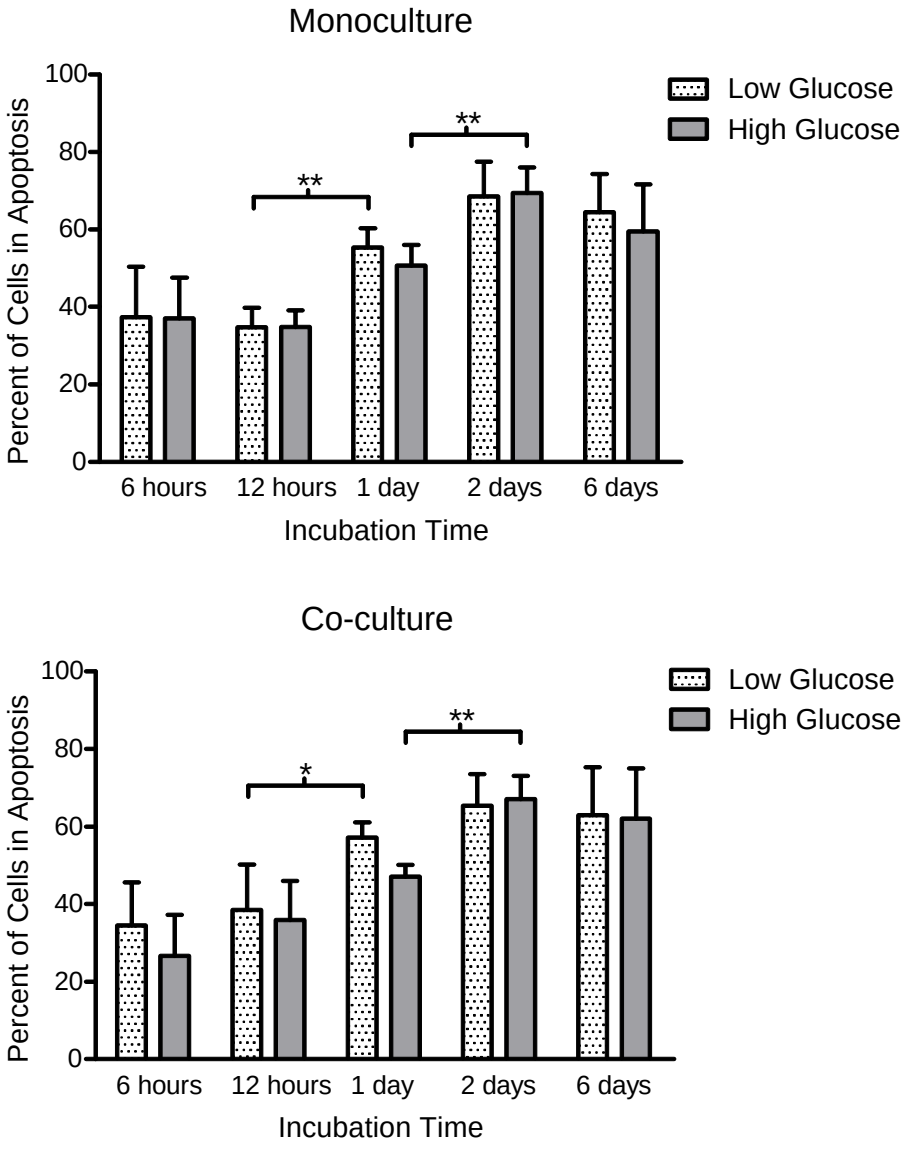

Figure 3.7: High glucose culture media delays macrophage apoptosis. Cells were cultured for 6 hours, 12 hours, 1 day, 2 days or 6 days in a monoculture (top) or in a lens co-culture system (bottom). Caspase activity was measured by flow cytometry and is reported as the percentage of cells staining positively for caspase and negatively for PI ± the standard error of measurement (SE). * indicates a significant difference ($p < 0.05$), ** indicates ($p < 0.01$). n = 4 for all treatments and controls.

Likewise, the nucleic stain PI was used to examine the effect of elevated glucose concentration on macrophage necrosis. As shown in Figure 3.8, monoculture with high glucose media significantly reduced the proportion of necrotic cells at 1 day of monoculture ($p = 0.0424$) compared to monoculture in low glucose media. In high glucose media, the proportion of necrotic cells peaked at 12% of cells at 12 hours of monoculture before significantly decreasing to 5% by 1 day of monoculture ($p = 0.0162$), compared to around 10% of cells in low glucose at 1 day. These trends were not observed in the co-culture model, though no significant difference was observed between the monoculture and co-culture models.

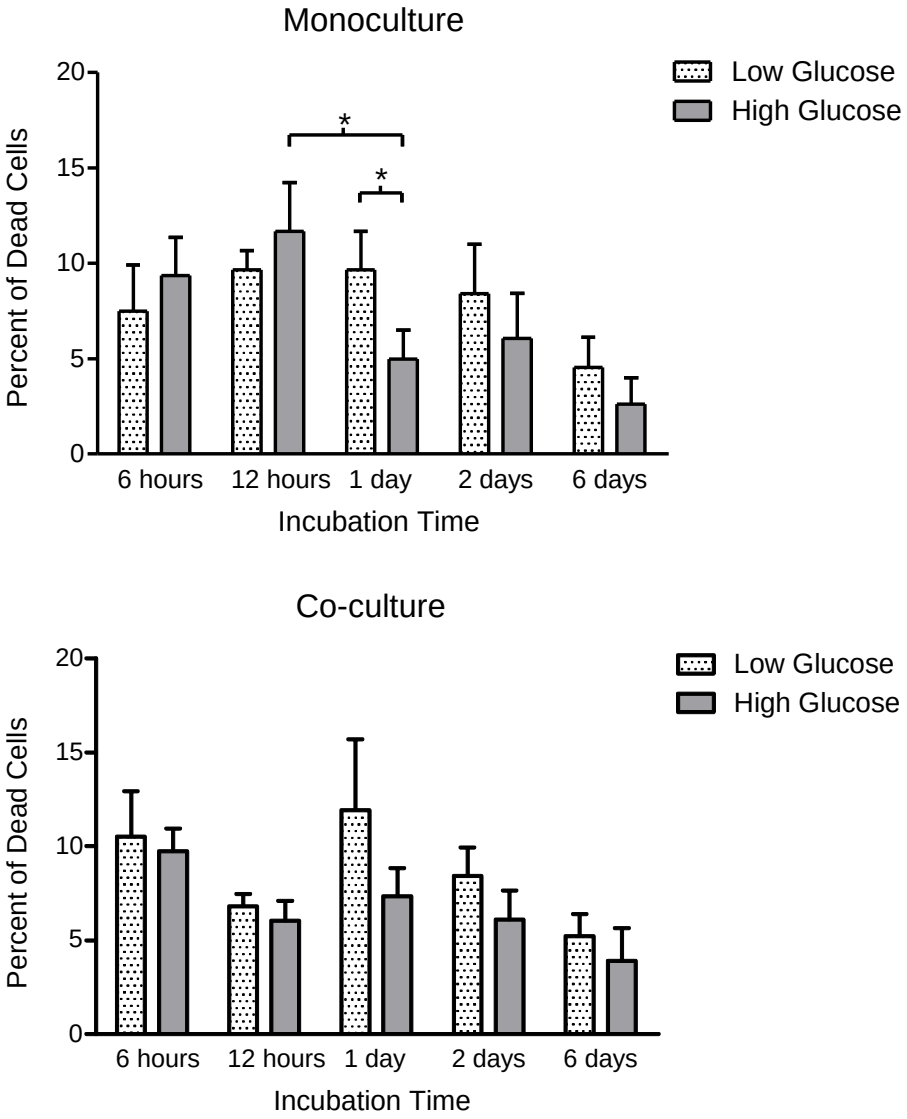

Figure 3.8: High glucose culture media decreases macrophage necrosis. Cells were cultured for 6 hours, 12 hours, 1 day, 2 days or 6 days in a monoculture (top) or in a lens co-culture system (bottom). PI staining was measured by flow cytometry and is reported as the proportion of macrophages staining positively for PI ± the standard error of measurement (SE). * indicates a significant difference ($p < 0.05$). n = 4 for all treatments and controls.

3.2.3 Lens epithelial cell phenotype is unaffected by high glucose media

The co-culture model was also employed to determine the effect of glucose concentration on lens epithelial cell phenotype by examining expression of the cytoskeletal proteins α-SMA and vimentin, and the transmembrane protein E-cadherin. No differences in α-SMA, vimentin or E-cadherin expression were observed between high and low glucose media at any time point ($p > 0.05$), as shown in Table 3.2. Similar to the examination of macrophage integrin expression, no differences in E-cadherin and vimentin expression were observed between the co-culture model and the monoculture model. However, the presence of macrophages induced a small increase in α-SMA expression at 6 days of culture: a similar finding to that of Chapter 2. Expression of all three proteins remained constant over time, except for α-SMA. Please note that a new α-SMA antibody was used in this investigation, and values are therefore not comparable to those presented previously.

Table 3.2: α-SMA, vimentin and E-cadherin expression on lens epithelial cells cultured for 6 hours, 12 hours, 1 day, 2 days or 6 days in media containing high or low glucose concentrations. Protein expression was measured by flow cytometry and is reported as the mean of arbitrary fluorescence units (AFU) ± the standard error of measurement (SE).

Culture Model	Incubation time	Glucose Level	α-SMA	Vimentin	E-cadherin
Monoculture	6 hours	High	4 ± 0.4	38.0 ± 8	13 ± 0.5
		Low	5 ± 0.4	43.7 ± 1	14 ± 1
	12 hours	High	6 ± 2	72 ± 6	18 ± 2
		Low	6 ± 2	84 ± 12	18 ± 2
	1 day	High	4 ± 0.7	61 ± 9	12 ± 0.7
		Low	6 ± 2	54 ± 8	14 ± 0.4
	2 days	High	10 ± 2	79 ± 11	14 ± 0.9
		Low	10 ± 2	64 ± 10	14 ± 2
	6 days	High	5 ± 1	61 ± 10	16 ± 0.8
		Low	10 ± 2	81 ± 17	14 ± 0.8
Co-culture	6 hours	High	5 ± 0.4	41 ± 14	13 ± 3
		Low	4 ± 0.8	46 ± 17	13 ± 3
	12 hours	High	4 ± 2	45 ± 2	13 ± 0.6
		Low	4 ± 1	50 ± 10	12 ± 0.8
	1 day	High	5 ± 1	75 ± 15	12 ± 1
		Low	9 ± 1	54 ± 7	13 ± 0.5
	2 days	High	9 ± 2	78 ± 18	15 ± 2
		Low	9 ± 1	74 ± 15	13 ± 3
	6 days	High	6 ± 2	58 ± 7	16 ± 1
		Low	11 ± 1	77 ± 11	15 ± 1

3.2.4 High glucose media delays lens epithelial cell necrosis but not apoptosis

The effect of high and low glucose media on lens epithelial cell apoptosis was evaluated using a FLICA kit. No difference in the proportion of apoptotic cells was observed between the co-culture model and monoculture model, shown below in Figure 3.9. Similarly, no significant difference in the proportion of apoptotic cells was observed between culture with high glucose media and culture with low glucose media. As well, no significant changes in the proportion of apoptotic cells was observed over time.

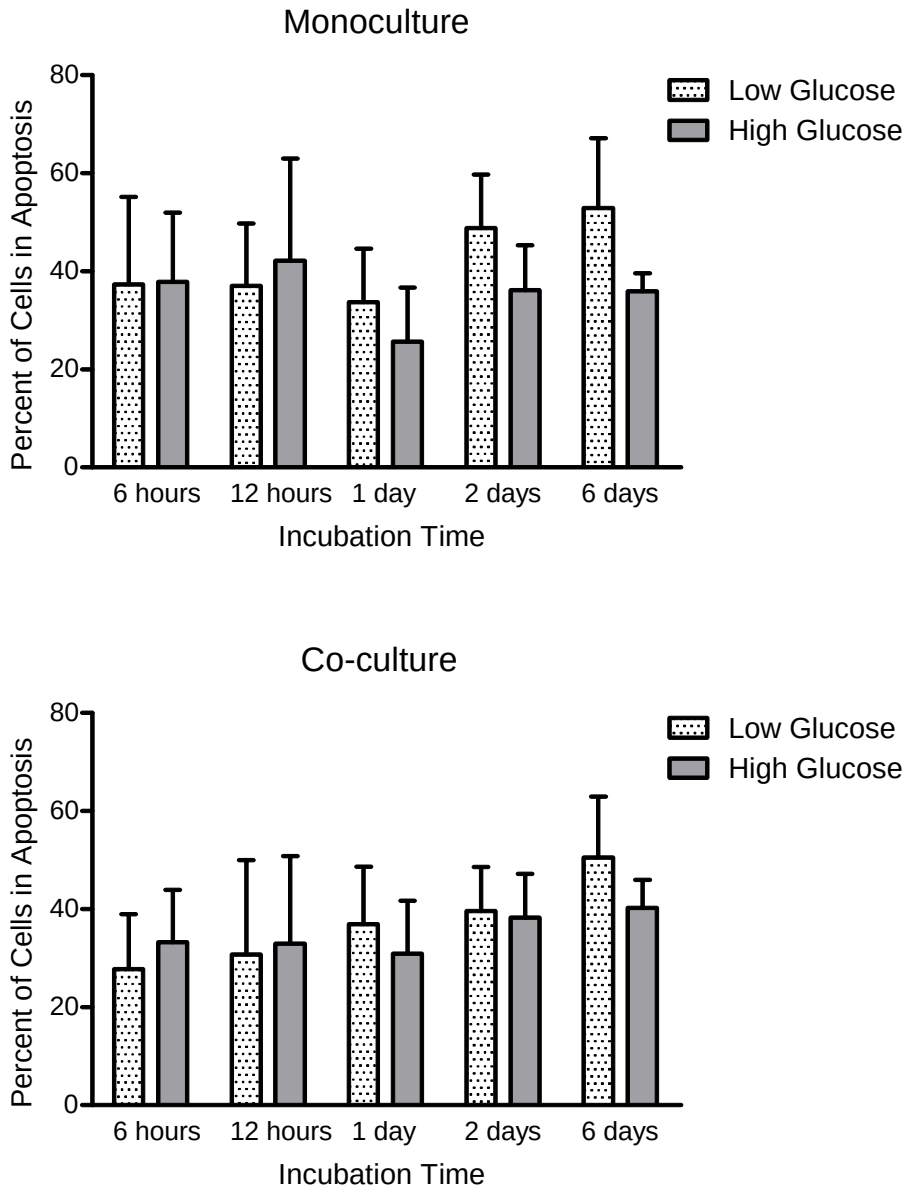

Figure 3.9: The proportion of lens epithelial cells undergoing apoptosis over time is not affected by glucose concentration. Cells were cultured for 6 hours, 12 hours, 1 day, 2 days or 6 days in a monoculture (top) or in a macrophage co-culture system (bottom). Caspase activity was measured by flow cytometry and is reported as the percentage of cells staining positively for caspase and negatively for PI. n = 4 for all treatments and controls.

The effect of high and low glucose media on lens epithelial cell death was evaluated using PI. No significant difference was observed in the proportion of necrotic cells between the co-culture model and monoculture model, shown below in Figure 3.10. Further, no significant difference in the proportion of necrotic cells was observed between culture with high glucose media and low glucose media. However, in low glucose media, the proportion of necrotic cells increased significantly between 6 hours and 1 day of monoculture, from 20% to 55% of cells ($p = 0.005$). In high glucose media, the proportion of necrotic cells remained low between 6 and 12 hours of monoculture (around 23%) before increasing significantly at 1 day of monoculture to 65% ($p = 0.0007$).

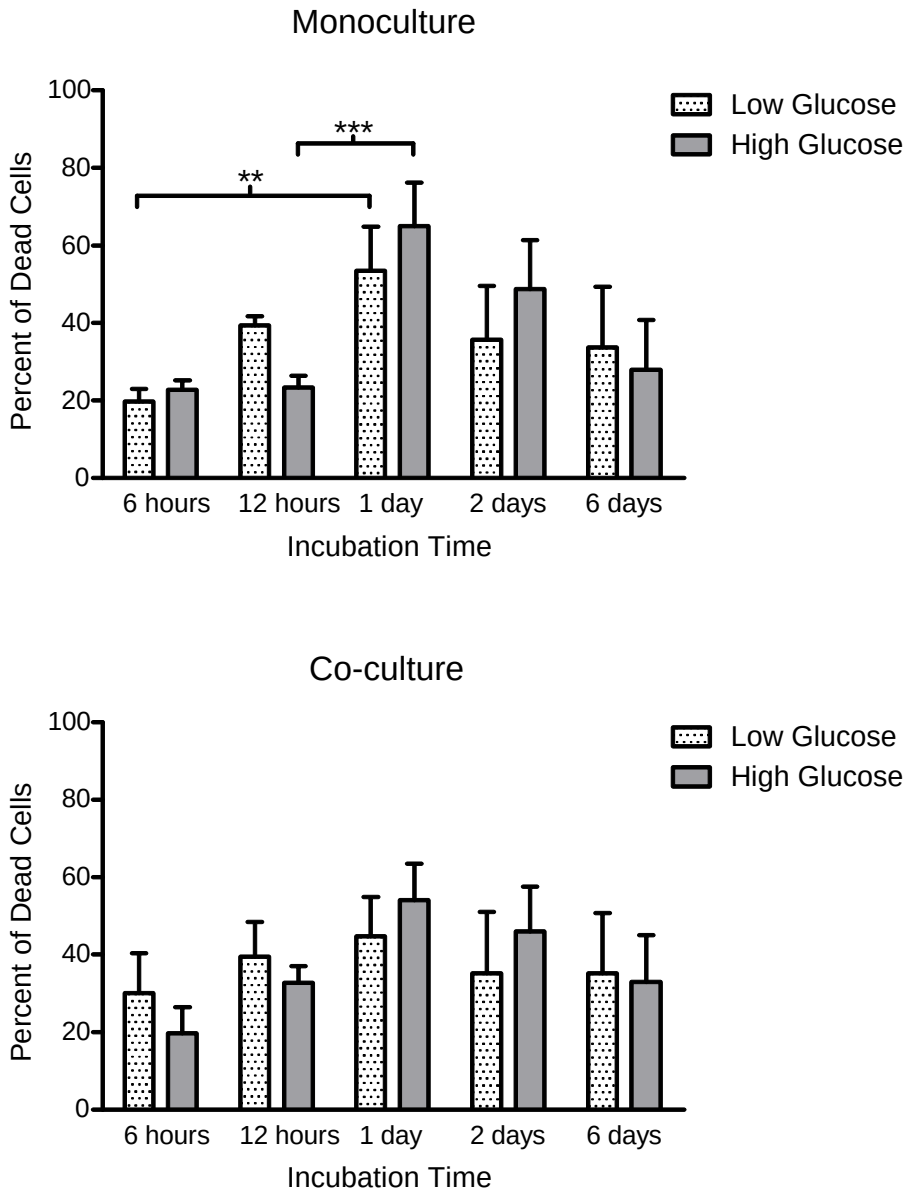

Figure 3.10: High glucose culture media delays necrosis of lens epithelial cells. Cells were cultured for 6 hours, 12 hours, 1 day, 2 days or 6 days in a monoculture (top) or in a macrophage co-culture system (bottom). PI staining was measured by flow cytometry and is reported as the proportion of lens epithelial cells staining positively for PI. ** indicates a significant difference ($p < 0.01$), * indicates ($p < 0.001$). n = 4 for all treatments and controls.**

3.3 Discussion

The novel co-culture model developed in Chapter 2 to examine the relationship between macrophages and lens epithelial cells in the post-operative lens was used to explore interactions in conditions that would mimic the environment of a lens during diabetes. To isolate the effect of elevated glucose levels, co-culture and monoculture of both cell types was performed using the same media formulation in either a high (25 mM) or low (5.5 mM) glucose concentration variant. DMEM was selected due to its extended history of use with both HLE B-3 cells,[211–214] and macrophages,[215,216] a history not shared with RPMI. Further, since RPMI has a base glucose concentration of 11 mM, it falls within the American Diabetes Association's definition of hyperglycemia,[205] and is therefore inappropriate for use in this study. The DMEM media formulation is loosely based on physiological blood concentrations. Although the concentration of glucose in the aqueous humor of a non-diabetic is as much as 50% lower than that of blood,[14] the relative increase in aqueous humor glucose concentration observed during diabetes is consistent to that seen in blood.

Our objective was to examine the cellular response of THP-1 macrophages to high glucose culture media, and the effect of this response on HLE B-3 lens epithelial cell phenotype. Glycoproteins and integrins that enable macrophage adhesion to and infiltration of the endothelium, like CD54 and CD11b, have been thoroughly examined *in vivo* for their contributions to diabetic complications. Although a role for CD11c in diabetic complications and in relation to sugar level has not been reported, its regulation by many of the same pathways as CD11b is well understood.[217,218] Increased CD54 expression has been observed on endothelial cells during hyperglycemia, enabling recruitment of leukocytes out of the circulatory system.[124,125,127,129–131,133,219–221] However, studies examining CD54 and CD11b expression on the membrane of inflammatory cells during hyperglycemia have shown mixed results. Sampson *et al.* reported increases in CD11b, CD54 and

CD11a expression on monocytes as a result of acute hyperglycemia in diabetics and nondiabetics.[208] Cifarelli *ei al.* reported increased CD11b expression but decreased CD54 expression on monocytes obtained from Type-1 diabetic children within one week of their diagnosis compared to 2 months after diagnosis, attributing the difference to better blood-glucose management.[44] Torrecilla *et al.* demonstrated up-regulation of CD54 and CD11a and no change in CD11b expression after induction of hyperglycemia.[222] Although these studies examined monocytes prior to their terminal differentiation into macrophages, and therefore cannot be extrapolated to macrophage response, they illustrate the lack of consensus regarding the regulation of leukocyte adhesion protein expression during hyperglycemia.

In the present study, all three adhesion molecules – CD54, CD11b and CD11c – exhibited a peak in expression at 12 hours of incubation followed by a subsequent significant decline by one day. However, we observed a significant down-regulation of all adhesion integrins at one and two days of incubation in high glucose culture media compared to low glucose culture media. Similar observations were made by Sun *et al.*, who demonstrated that macrophages isolated from long-term diabetic mice displayed significantly down-regulated CD54 expression and secretion of TNF-α and IL-6 but significantly increased NO secretion when stimulated with LPS and IFN-γ compared to control mice.[138] Takahashi *et al.* demonstrated that monocyte-derived dendritic cells in pre-diabetic adult patients showed impaired yield and integrin expression compared to healthy patients.[223] Štulc *et al.* observed a significant increase in expression of CD54, CD11a, CD18 and CD14 on monocytes extracted from patients with diabetes compared to without, but highlighted the absence of a correlation between leukocyte integrin expression and serum glucose concentration.[224] The results presented in the current study may suggest that another factor of the diabetic disease state, and not hyperglycemia, may be responsible for the reported increases in leukocyte integrin expression.

The bacterial pattern recognition receptor CD14 was examined as a measure of non-specific immunological activity.[225] As was the case with macrophage adhesion proteins, previous work examining the expression of CD14 during hyperglycemia and diabetes has returned conflicting results. Patiño *et al.* observed upregulated CD14 expression on circulating monocytes taken from Type-2 diabetics versus healthy subjects.[226] Fogelstrand *et al.* reported higher CD14 expression on monocytes extracted from Type-2 diabetics compared to healthy subjects, with pre-diabetic subjects displaying intermediary CD14 expression.[227] Interestingly, Fogelstrand *et al.* noted stronger correlations between CD14 expression and subject Body Mass Index (BMI) and plasma insulin concentration, and a weak correlation to blood glucose levels.[227] Previously mentioned work by Štulc *et al.* reported upregulation of monocyte CD14 expression in diabetics with a weak correlation to blood glucose concentration.[224] In contrast, Nareika *et al.* reported no difference between U937 mononuclear cells cultured in high glucose for two weeks compared to those cultured in low glucose for two weeks.[228] In the present study, we observed a significant down-regulation of CD14 expression on macrophages cultured in high glucose for one and two days compared to those cultured in low glucose. As the *in vivo* work reporting CD14 upregulation with diabetics noted weak correlations to blood glucose, and the work of Nareika *et. al* directly examining the effect of high glucose levels on macrophage reported no such effect, it seems plausible that aspects of diabetes mellitus other than hyperglycemia are responsible for the observed increases in CD14 expression.

The effects of hyperglycemia on the scavenger receptor CD36 are well established. Early work by Griffin *et al.* demonstrated an upregulation of CD36 expression on macrophages *ex vivo* after 5 days of hyperglycemic culture.[204] However, Sampson *et al.* reported higher CD36 expression on monocytes isolated from Type-2 diabetic patients compared to healthy subjects with no resulting effect of induced hyperglycemia.[229] It was Liang *et al.* who proposed that the increase in CD36 expression on macrophages observed during diabetes might be a result of defective insulin signalling,

or insulinopenia.[158] This hypothesis was corroborated by Yechoor *et al.* using insulin-deficient knockout mice.[230] Chen *et al.* showed that both insulin treatment and treatment with the drug vanadate, which reduces blood glucose by other means than insulin receptor action, reduced expression of CD36 in the small intestine mucosa of rats to baseline levels.[231] In the present study, we observed a significant down-regulation of CD36 expression on macrophages cultured in hyperglycemic conditions. Additionally, we observed a decline in CD36 expression over time on macrophages cultured in isoglycemic conditions. Interestingly, a similar reduction in CD36 expression has been demonstrated as a result of hypertension and insulin resistance.[232,233] It may be that prolonged culture with THP-1 macrophages in high glucose media results in defective insulin signalling, causing down-regulated expression of CD36. Unfortunately, no further explanation of the results reported herein can be offered.

The strong decline in integrin expression observed in the present study could be explained by an increase in macrophage apoptosis, during which translation of live cell functional proteins like integrins is silenced. Intermediate products of the glycation process were reported by Okado *et al.* to induce apoptosis in the U937 macrophages at hyperglycemic concentrations via increases in oxidative stress.[234] However, Turina *et al.* reported that neither hyperglycemia nor hypoglycemia induced significant apoptotic turnover of neutrophils.[235] In the present study, nearly 70% of macrophages displayed a high degree of caspase activity, which is taken to mean they are undergoing apoptosis. However, THP-1 cells have been shown to constitutively express caspase-1 and caspase-3 for use as regulators of cytokine production.[236] Further, in macrophages caspase-1 has been demonstrated to regulate the secretion of important signalling proteins in inflammation, cytoprotection and tissue repair.[237] Therefore, the high caspase activity observed in the present study may partly be explained by processes other than apoptosis. While any increase in caspase activity over time is likely the result of increasing apoptosis, the high baseline value may be the result of caspase activity in other

intracellular processes. Further, the high baseline could be explained by an overly-conservative gating strategy that selects more cells as apoptotic than is the case. Looking at the percentage of secondary necrotic cells indicates that only as many as 5% of cells at 6 days of culture died as a result of apoptosis – far, far fewer than should be with nearly 70% of cells undergoing apoptosis at 2 days of culture. Additional control experiments will be required to determine if the flow cytometry settings can be improved, or if caspase activity is inherently present in differentiated THP-1 macrophages.

In the present study, there was a significant trend of increasing macrophage apoptosis over time in both high and low glucose media. However, the increase in apoptosis was more gradual and occurred at a later time point in high glucose media than in low glucose media. This difference was non-existent by two days of cell culture, due to an eventual increase in apoptosis in high glucose media. Compared to low glucose media, culture in high glucose media caused a significant decrease in the number of necrotic macrophages at one day of culture, where it remained lower through to 6 days of culture. The combination of delayed caspase activity and reduced necrosis over time in high glucose culture media implies that hyperglycemia may delay macrophage cell death. A reduction in the rate of cells beginning apoptosis would explain a reduction in the number of dead cells over time. In the body, it may be that an adverse delay in macrophage cell death enables the pathological inflammatory issues observed during diabetic complications by prolonging the wound-healing response.

No difference was observed in monocultured lens epithelial cell expression of α-SMA, vimentin or E-cadherin were encountered. These results reinforce the current understanding that diabetic cataracts are a result of accumulated oxidative damage due to the osmotic stress of a hyperglycemic aqueous humor,[135,136,202,238] and not the result of phenotypic changes in lens epithelial cells as seen during PCO.[134,239,240] Further, the presence of macrophages had no effect on lens epithelial cell phenotype except for causing an increase in α-SMA expression in both media

conditions. This result confirms the findings of Chapter 2, which utilized low glucose media and determined that the presence of resting macrophages was sufficient for an increase in α-SMA expression. Since macrophages in the present study were observed as undergoing a significant phenotypic shift in hyperglycemic conditions, the lack of observable difference between monocultured and co-cultured lens epithelial cells in high glucose media indicates that the hyperglycemic changes to macrophage phenotype reported here have no effect on lens epithelial cell phenotype. Drawing on the conclusions of Chapter 2, the perceived lack of effect may be the result of either a low level of macrophage activation, or too low a ratio of macrophages to lens epithelial cells in the co-culture system.

The concentration of glucose in culture media had no discernible effect on the rate of lens epithelial cell apoptosis, which increased slightly over time from 40% of cells at 1 day to 50% of cells at 6 days. However, culture with high glucose media did induce a significant increase in lens epithelial cell necrosis at 1 day of culture compared to 12 hours, reaching nearly 65% of cells. Cells cultured in low glucose media displayed a steady increase in necrosis up to 1 day of culture where it remained high. Cells cultured in high glucose, however, showed very little necrosis (less than 20% of cells) until the sharp increase at 1 day. The increase in necrosis without an accompanying increase in apoptosis may imply the effect of a cell death mechanism other than caspase-dependent apoptosis.[241]

The presence of oxidative metabolic by-products of glucose in culture media have been demonstrated to induce lens epithelial cell necrosis both without apoptosis,[242] and with apoptosis.[243] Lens epithelial cells have also been shown to undergo apoptosis in the presence of by-products of lipid metabolism.[244] Since the physiologic glucose concentration of the aqueous humor is approximately half the concentration of the blood and our low glucose media formulation, it may be that HLE B-3 cells cultured in low glucose DMEM are experiencing hyperglycemia, and therefore, elevated apoptosis. As the role of glucose metabolism in lens epithelial cell apoptosis is well

understood, the results of the present study may further support our current understanding of diabetic cataracts as the result of oxidative stress in the lens. Further, Shui *et. al* observed lens epithelial cell phagocytosis, and digestion, of neighbouring necrotic and apoptotic cells,[245] which may explain the high baseline caspase activity herein. However, it seems likely that the gating strategy – which was designed to accurately capture secondary-necrotic cell populations – is overestimating the amount of caspase activity in non-necrotic cells.

3.4 Conclusion

The novel *in vitro* co-culture model designed for biocompatibility testing of intraocular materials was applied to another possible pathological interaction between lens epithelial cells and macrophages: the development of diabetic cataract. Although macrophage phenotype appears heavily affected by hyperglycemic conditions, lens epithelial cells appeared phenotypically stable under monoculture in hyperglycemic conditions, and under macrophage co-culture in hyperglycemic conditions. Macrophage apoptosis appeared delayed under hyperglycemic conditions, consequentially reducing the rate of necrosis and highlighting a possible mechanism for adverse macrophage behaviour in diabetic complications. Lens epithelial cell apoptosis remained unaffected by glucose concentration, although necrosis was increased in hyperglycemic conditions. These findings further the current understanding that diabetic cataracts are not an inflammatory complication of diabetes, but rather a result of the inability of lens epithelial cells to accommodate hyperosmolar conditions in the aqueous humor. Additional work should explore the oxidative stress in THP-1 derived macrophages during hyperglycemic culture and the possible changes in secretory products that may result.

Chapter 4: Conclusions and Recommendations

The role and behaviour of macrophages in the immune privileged environment of the eye, specifically with regard to disease, are not well understood. Evidence for macrophage participation in the development of secondary cataracts provided the motivation for this investigation. The crucial role of macrophage dysfunction during diabetic complications further motivated the exploration of macrophage interaction with cells of the inner eye. A novel *in vitro* model of macrophages and lens epithelial cells in co-culture was developed and used to examine the role of macrophages in two afflictions of the lens epithelium: posterior capsule opacification, and diabetic cataract.

In the present study, macrophage biocompatibility with materials commonly used in cataract surgery influenced lens epithelial cells toward dysfunctional behaviour. Specifically, hydrophilic surfaces activated macrophages and prevented adhesion more than hydrophobic ones. However, macrophage interaction with both materials induced the same degree of inflammatory phenotype disruption in lens epithelial cells. We conclude that macrophage adhesion and activation are inversely related, in agreement with countless studies of macrophage biocompatibility elsewhere in the body. We also conclude that the net inflammatory effect of macrophage interaction is a function of the degree of macrophage activation and number of activated macrophages.

In this thesis, we hypothesized that changes in glucose concentration and the introduction of a secondary cell population would induce changes in primary cell behaviour. The effects of glucose concentration and co-culture on the expression of leukocyte receptors involved in adhesion and activation, as well as cytoskeletal proteins of the lens epithelium, are summarized in Table 4.1.

Table 4.1: Summary table of time trends and co-culture effects on macrophage and lens epithelial cell protein expression in all three media formulations. Data gathered from Chapter 2 and Chapter 3. ↑ indicates increased expression, ↓ indicates decreased expression, = indicates no effect. Proteins not measured with a certain media formulation are left blank. (5.5 mM) refers to a glucose concentration of 5.5 mM.

	Trend over time			Effect of co-culture		
Marker	DMEM (5.5 mM)	RPMI (11 mM)	DMEM (25 mM)	DMEM (5.5 mM)	RPMI (11 mM)	DMEM (25 mM)
CD54	↓	↓	↓	=	=	=
CD45	↓	↓	↓	=	=	=
CD36	↓	↓	↓	=	=	=
CD14	↓	↑	↓	=	=	=
CD11b	↓		↓	=	=	=
CD11c	↓		↓	=	=	=
α-SMA	↑	↑	↑	↑	↑	↑
Fibronectin		↓			=	
Vimentin	↑		↑	=		=
E-cadherin	=	=	=	=	=	=

A significant disruption of macrophage phenotype and behaviour was observed during hyperglycemic conditions. Specifically, a stark decrease in the expression of macrophage cell-surface proteins during hyperglycemia was observed, the effect of which is currently not well understood. In contrast, there was no change in protein expression in lens epithelial cells during hyperglycemia, providing additional evidence to support the hypothesis that diabetic cataract is not a result of phenotypic changes. Additionally, a delay in macrophage apoptosis during hyperglycemia was observed and appears to correspond to reduced rates of macrophage death which may explain the adverse inflammatory reaction observed in diabetes. Results from our *in vitro* model also suggest that lens epithelial cell death as a result of hyperglycemia occurs through a mechanism other than apoptosis, in agreement with previous *in vitro* work from other research groups. We therefore provide

additional evidence to the hypothesis that diabetic cataracts are a product of accumulated oxidative stress during hyperglycemia.

Our model enables a new method of inquiry into macrophage biocompatibility testing with intraocular materials. Specifically, cell-surface proteins involved in leukocyte activation have been quantified for the first time with regards to intraocular materials, providing additional evidence for the influence of macrophages in the development of posterior capsule opacification. Further, the absence of interaction between macrophages and lens epithelial cells during hyperglycemia, and observed direct effect of hyperglycemia on lens epithelial cells, provides additional evidence to the hypothesis that diabetic cataracts are an oxidative complication unlike diabetic retinopathy. The findings presented herein, although far from conclusive, begin to answer the question of what role the macrophage might play in the immune privileged environment of the inner eye.

Future work should focus on the iterative refinement of the *in vitro* model. The movement to more compliant and biocompatible cell-culture substrates should yield improvements in background levels of macrophage activation and lens epithelial cell inflammation. Further, the use of primary (non-immortalized) cell lines or *ex vivo* tissue samples should improve the representation of the *in vivo* environment. To that end, the development of an artificial aqueous humor and its use with the co-culture model would greatly improve the investigation of macrophage and lens epithelial cell interaction in the immune privileged intraocular environment. Given the strong effect of hyperglycemia on macrophage phenotype, future experiments should examine uveal biocompatibility under high glucose conditions. As well, the change in glucose concentration over the time of culture should be elucidated and correlated with macrophage phenotype. Lastly, whether elevated glucose concentration resulted in excessive lactate buildup in the culture media was not examined and may provide a future avenue of investigation.

Appendix A

Supplementary Figures for Chapter 2

The differentiation protocol employed in this thesis was evaluated to determine the optimal length of differentiation to produce large but viable macrophages. As shown in Table A.1, by Day 8 of differentiation the THP-1 macrophages are 2.2x the volume of their monocyte precursor while still nearly 82% viable. An additional day of differentiation, however, results in a viability drop to 78% intact cells and a small decrease in volume despite a higher mean diameter. On this basis, it was decided to end differentiation on Day 8 instead of Day 9 as carried out in work by Daigneault *et al*.

Cell morphology was analyzed using a Moxi Z automated cell counter (Orflo Technologies, Ketchum, Idaho), which measures cell diameter and volume using the Coulter Principle. The Moxi Z also provides a crude live/dead analysis of each sample by comparing the proportion of counted objects in the approximate diameter range of human cells to the proportion of particles below the expected size of human cells. Data for monocytes prior to differentiation, macrophages at 8 days of differentiation and macrophages at 9 days of differentiation are included below.

Table 4.2: Summary of morphological characteristics of THP-1 cells through the differentiation process into macrophages. * indicates a significant difference ($p < 0.0001$) and + indicates a significant difference ($p < 0.001$).

Number of Days into Differentiation	Cell Type	Mean Diameter (μm)	Mean Volume (pL)	Ratio of Cells to Debris
Day 0	Monocyte	13.7401	1.3594	0.914
Day 8	Macrophage	18.2977*	3.2167*	0.8167+
Day 9	Macrophage	19.1673*	3.1717*	0.7767+

Included below are representations of the gating strategy employed in the live/dead analysis of macrophages at each time point in the culture process. Note that each figure is a single sample and may not depict the mean value of all samples for that time point.

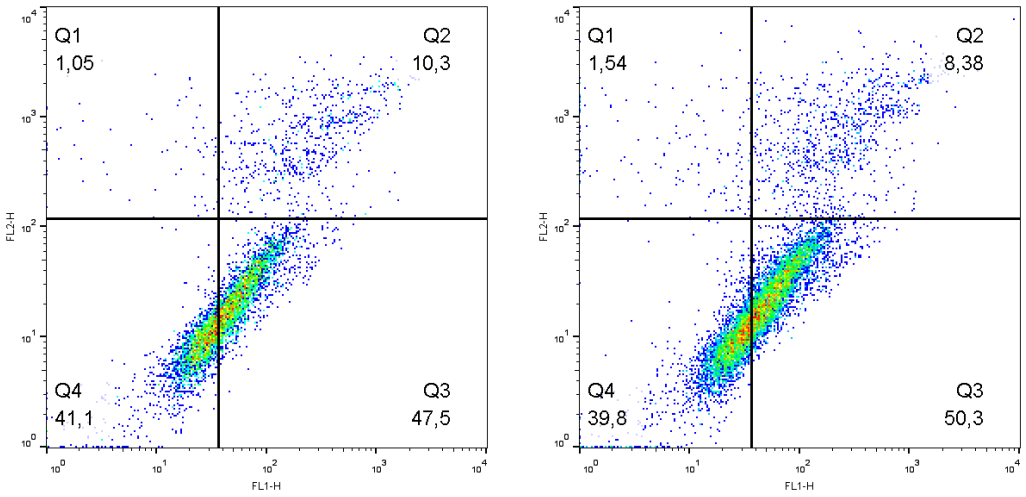

Figure 4.1: Gating strategy for live/dead analysis of macrophages at 6 hours of monoculture. Left: high glucose. Right: low glucose.

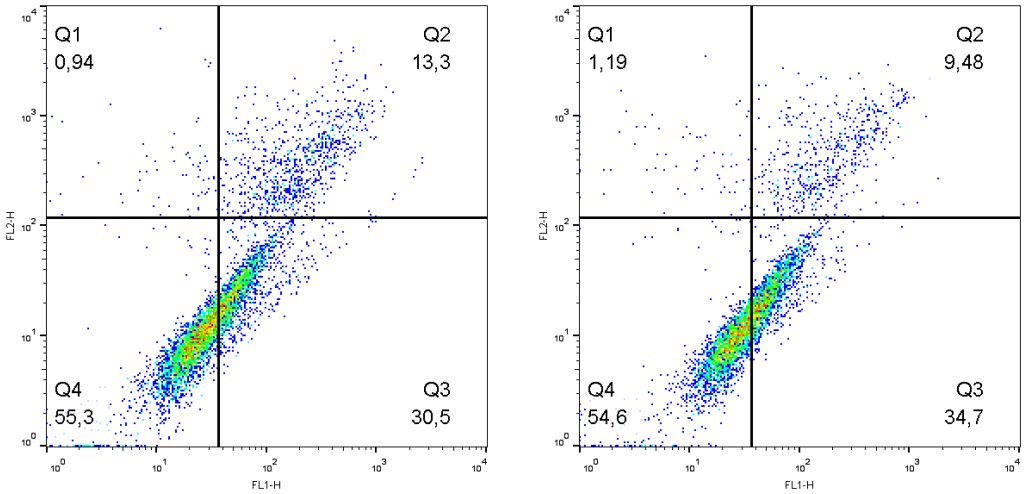

Figure 4.2: Gating strategy for live/dead analysis of macrophages at 12 hours of monoculture. Left: high glucose. Right: low glucose.

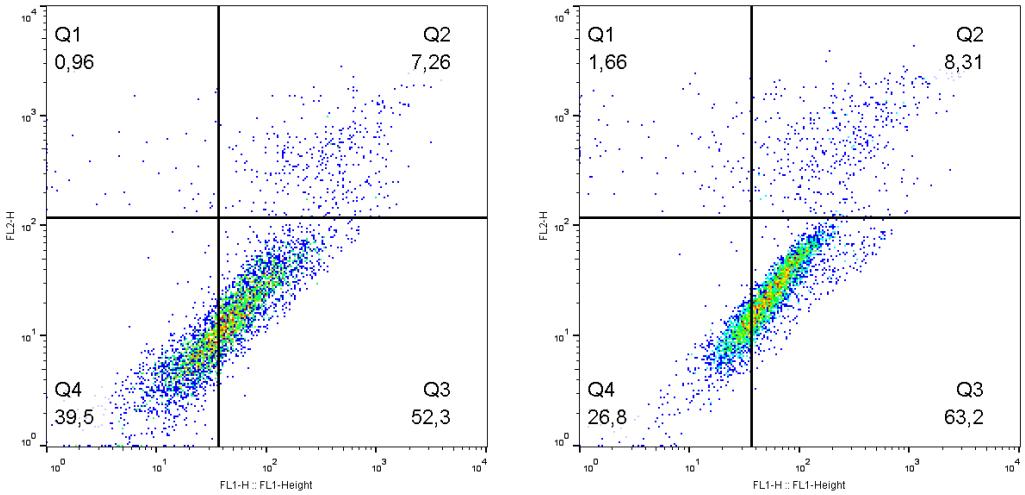

Figure 4.3: Gating strategy for live/dead analysis of macrophages at 1 day of monoculture. Left: high glucose. Right: low glucose.

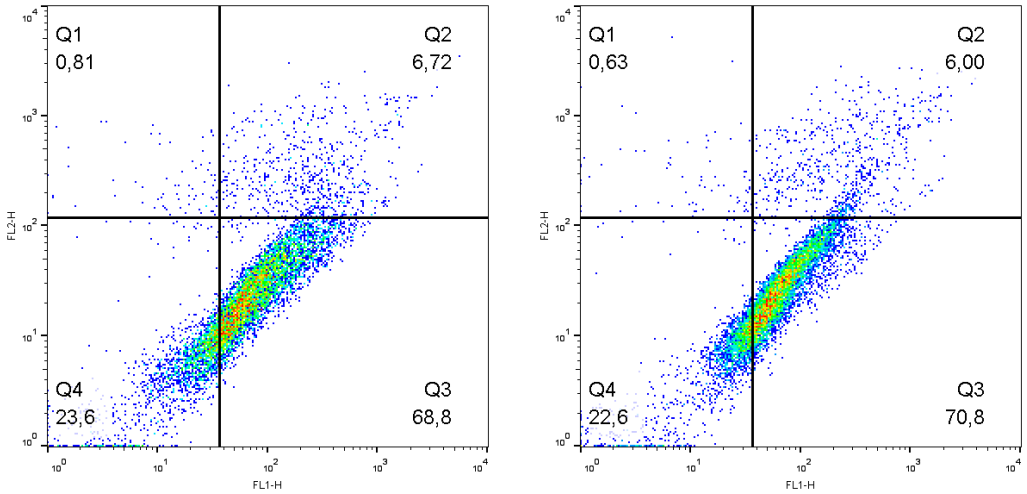

Figure 4.4: Gating strategy for live/dead analysis of macrophages at 2 days of monoculture. Left: high glucose. Right: low glucose.

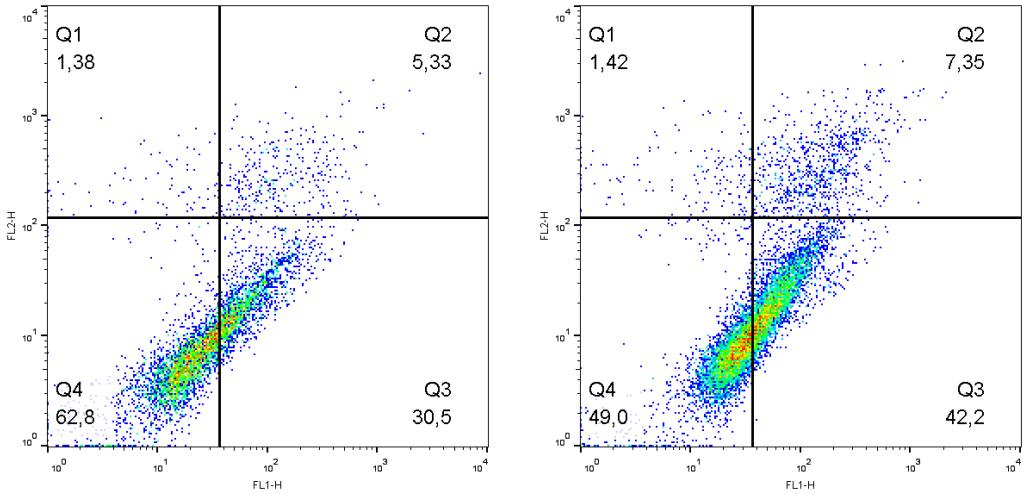

Figure 4.5: Gating strategy for live/dead analysis of macrophages at 6 days of monoculture. Left: high glucose. Right: low glucose.

Appendix B

Supplementary Figures for Chapter 3

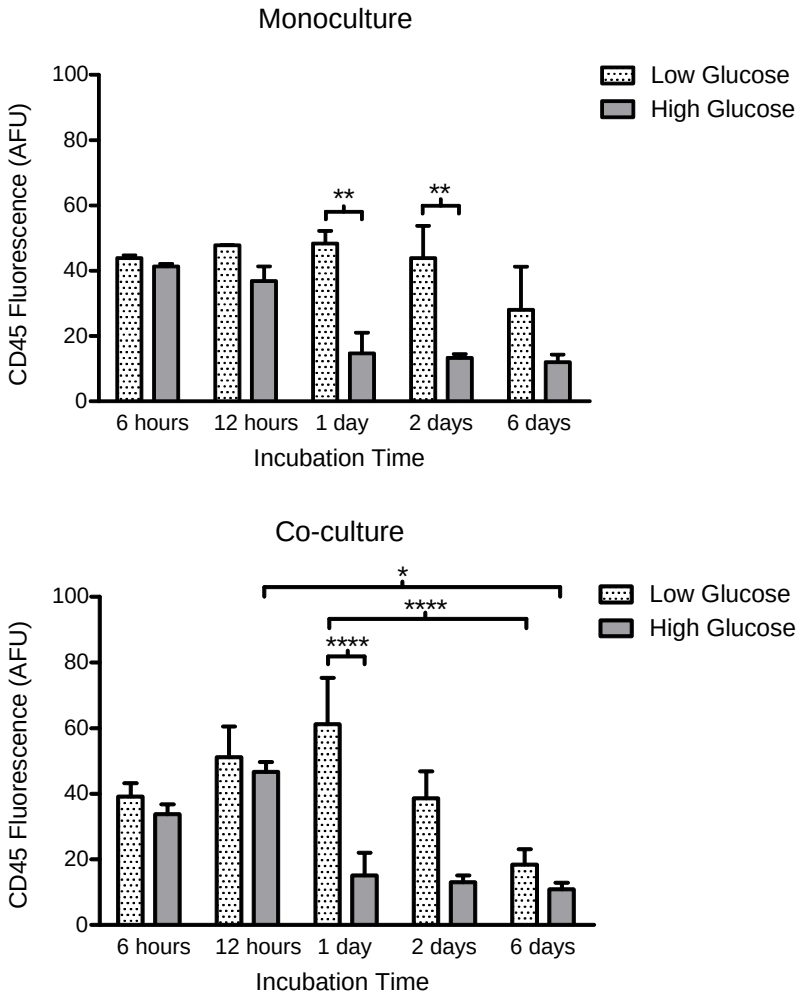

Figure 4.6: High glucose culture media down-regulates expression of CD45 in macrophages. Cells were cultured for 6 hours, 12 hours, 1 day, 2 days or 6 days in a monoculture (top) or in a lens co-culture system (bottom). CD45 expression was measured by flow cytometry and is reported as the mean of arbitrary fluorescence units (AFU). * indicates significant difference ($p < 0.05$); ** significant difference ($p < 0.01$), * significant difference ($p < 0.001$), **** significant difference ($p < 0.0001$). n = 4 for all treatments and controls.**

As shown in Table 4.1, macrophage culture in high glucose media caused a significant down-regulation of the leukocyte common antigen CD45 at 1 day of incubation (monoculture: $p = 0.0019$, co-culture: $p = 0.0001$) and 2 days (monoculture: $p = 0.0096$). In low glucose, CD45 expression peaked at 1 day of co-culture with a significant decline by 6 days of co-culture ($p = 0.0001$) while monoculture produced no discernible time variation. In high glucose, CD45 expression peaked at 12 hours of co-culture with a significant decline by 6 days of co-culture ($p = 0.0155$), while monoculture resulted in a steady but insignificant decline.

Glossary of Terms

Adaptive immune system: the subsystem of the immune system with memory for specific antigens.
Adsorption: the adhesion of a protein or molecule to a surface.
Antibody: small proteins of the adaptive immune system used to identify and attack antigens.
Antigens: any substance that induces an immune response.
Apoptosis: programmed cell death.
AFU: arbitrary fluorescence units.
BAB: blood aqueous barrier.
CD: cluster of differentiation. A naming convention used for various cell-surface proteins in humans.
Cytokine: small secreted proteins that mediate a number of biological processes.
DCF: formally, the fluorescent molecule 2',7'-dichlorofluorescein. Informally, the $DCFH_2$ probe.
ELISA: enzyme-linked immunosorbent assay.
FBGC: foreign body giant cell.
Haptic: the plastic side pieces of an intraocular lens (IOL).
Hydrophilic: water-attracting.
Hydrophobic: water-repelling.
Innate immune system: the non-specific subsystem of the immune system.
Integrin: transmembrane receptor proteins involved in intercellular & extracellular matrix adhesion.
IOL: intraocular lens.
IL: Interleukin. Family of cytokines.
Leukocyte: white blood cells. The cells of the immune system.
Macrophage: the phagocytising cell of the innate immune system. Mediates wound-healing.
Microparticle: small membrane-bound compartments released by activated and dying cells.
Monocyte: precursor cells of the macrophage. Circulate in the blood.
Pathogen: invasive organisms that produce disease. Bacteria, viruses, parasites and fungi.
Pattern recognition receptor: cell-surface proteins that recognise common molecules of pathogens.
PCO: posterior capsule opacification. The re-emergence of cataract following phacoemulsification.
Phacoemulsification: modern cataract extraction surgery.
pHEMA: poly(2-hydroxyethyl methacrylate). A polymer used to produce hydrophilic materials.
PMMA: poly(methyl methacrylate). A polymer used to produce hydrophobic materials.
ROS/RNS: reactive oxygen species, or, reactive nitrogen species.
TCPS: Tissue culture polystyrene. Common basement material used in cell-culture.
TGF-β: Transforming growth factor beta. Cytokine that controls tissue-remodelling and proliferation.

Bibliography

1. Apple, D. J., Escobar-Gomez, M., Zaugg, B., Kleinmann, G. & Borkenstein, A. F. Modern Cataract Surgery: Unfinished Business and Unanswered Questions. *Survey of Ophthalmology* **56,** S3–S53 (2011).

2. Brian, G. & Taylor, H. Round Table Cataract blindness – challenges for the 21st century. *Bulletin of the World Health Organisation* **79,** 249–256 (2001).

3. Foster, A. Cataract--a global perspective: output, outcome and outlay. *Eye* **13,** 449–453 (1999).

4. Khan, A. & Aldahmesh, M. Founder heterozygous P23T CRYGD mutation associated with cerulean (and coralliform) cataract in 2 Saudi families. *Molecular Vision* **15,** 1407–1411 (2009).

5. Ashwin, P. T., Shah, S. & Wolffsohn, J. S. Advances in cataract surgery. *Clinical & Experimental Optometry : Journal of the Australian Optometrical Association* **92,** 333–342 (2009).

6. Martinez, G. & de Iongh, R. U. The lens epithelium in ocular health and disease. *The International Journal of Biochemistry & Cell Biology* **42,** 1945–1963 (2010).

7. Leydolt, C., Kriechbaum, K., Schriefl, S., Pachala, M. & Menapace, R. Posterior capsule opacification and neodymium:YAG rates with 2 single-piece hydrophobic acrylic intraocular lenses: Three-year results. *Journal of Cataract & Refractive Surgery* **39,** 1886–1892 (2013).

8. Lloyd, a W., Faragher, R. G. & Denyer, S. P. Ocular biomaterials and implants. *Biomaterials* **22,** 769–785 (2001).

9. Millar, C. & Kaufman, P. L. in *Duane's Foundations of Clinical Ophthalmology* (eds. Tasman, W. & Jaeger, E.) (Lippincott-Raven, 1995).

10. Krause, U. & Raunio, V. Protein content of normal human aqueous humour in vivo. *Acta Ophthalmologica* **47,** 215–221 (1969).

11. Reiss, G. R., Werness, P. G., Zollman, P. E. & Brubaker, R. F. Ascorbic acid levels in the aqueous humor of nocturnal and diurnal mammals. *Archives of Ophthalmology* **104,** 753–755 (1986).

12. Riley, M., Meyer, R. & Yates, E. Glutathione in the aqueous humor of human and other species. *Investigative Ophthalmology & Visual Science*, **19,** 94–6 (1980).

13. Michelet, F. *et al.* Blood and plasma glutathione measured in healthy subjects by HPLC: relation to sex, aging, biological variables, and life habits. *Clinical Chemistry* **41,** 1509–1517 (1995).

14. Davies, P., Duncan, G. & Pynsent, P. Aqueous humour glucose concentration in cataract patients and its effect on the lens. *Experimental Eye Research* **39,** 605–609 (1984).

15. Wang, S. Y. *et al.* Analysis of metabolites in aqueous solutions by using laser Raman spectroscopy. *Applied Optics* **32,** 925–929 (1993).

16. Bito, L. Z. The physiology and pathophysiology of intraocular fluids. *Experimental Eye Research* **Supplement,** 273–289 (1977).

17. Dickinson, J. C., Durham, D. G. & Hamilton, P. B. Ion exchange chromatography of free amino acids in aqueous fluid and lens of the human eye. *Investigative Ophthalmology* **7,** 551–563 (1968).

18. Allansmith, M. Immunoglobulins in the human eye: location, type, and amount. *Archives of Ophthalmology* **89,** 36–45 (1973).

19. Taylor, A. . Ocular immune privilege. *Eye* **23,** 1885–1889 (2009).

20. Benhar, I., London, A. & Schwartz, M. The privileged immunity of immune privileged organs: the case of the eye. *Frontiers in Immunology* **3,** 1–6 (2012).

21. Wormstone, I. M., Wang, L. & Liu, C. S. C. Posterior capsule opacification. *Experimental Eye Research* **88,** 257–269 (2009).

22. West-Mays, J. & Pino, G. Matrix metalloproteinases as mediators of primary and secondary cataracts. *Expert Review of Ophthalmology* **2,** 931–938 (2007).

23. Parham, P. *The Immune System*. 608 (Garland Science, 2009).

24. Gordon, S. Pattern recognition receptors: Doubling up for the innate immune response. *Cell* **111,** 927–930 (2002).

25. Gorbet, M. B. & Sefton, M. V. Biomaterial-associated thrombosis: roles of coagulation factors, complement, platelets and leukocytes. *Biomaterials* **25,** 5681–5703 (2004).

26. Nicod, L. P. Cytokines. 1. Overview. *Thorax* **48,** 660–667 (1993).

27. Delves, P. J. & Roitt, I. The immune system: first of two parts. *New England Journal of Medicine* **343,** 108-117 (2000).

28. Hanlon, S. D., Smith, C. W., Sauter, M. N. & Burns, A. R. Integrin-dependent neutrophil migration in the injured mouse cornea. *Experimental Eye Research* **120,** 61–70 (2014).

29. Gorbet, M., Luensmann, D., Luck, S. & Jones, L. Response Of Tear Film Neutrophils To Different Stimuli. *Investigative Ophthalmology & Visual Science* **53,** e-abstract 5271 (2012).

30. Mittal, M., Siddiqui, M. R., Tran, K., Reddy, S. P. & Malik, A. B. Reactive oxygen species in inflammation and tissue injury. *Antioxidants & Redox Signaling* **20,** 1126–1167 (2014).

31. Anderson, J. M., Rodriguez, A., Chang, D. T., Body, F. & To, R. Foreign body reaction to biomaterials. *Seminars in Immunology* **20,** 86–100 (2008).

32. Banchereau, J. *et al.* Immunobiology of Dendritic Cells. *Annual Review of Immunology* **18,** 767–811 (2000).

33. Liu, Q., Smith, C. W., Zhang, W., Burns, A. R. & Li, Z. NK Cells Modulate the Inflammatory Response to Corneal Epithelial Abrasion and Thereby Support Wound Healing. *The American Journal of Pathology* **181,** 452–462 (2012).

34. Thiery, J. *et al.* Perforin pores in the endosomal membrane trigger the release of endocytosed granzyme B into the cytosol of target cells. *Nature Immunology* **12,** 770–777 (2011).

35. Kelly, J. M. *et al.* Granzyme M mediates a novel form of perforin-dependent cell death. *The Journal of Biological Chemistry* **279,** 22236–22242 (2004).

36. Delves, P. J. & Roitt, I. M. The immune system. Second of two parts. *The New England Journal of Medicine* **343,** 108–117 (2000).

37. Mosser, D. M. & Edwards, J. P. Exploring the full spectrum of macrophage activation. *Nature Reviews Immunology* **8,** 958–969 (2008).

38. Iovine, N. M. *et al.* Reactive nitrogen species contribute to innate host defense against Campylobacter jejuni. *Infection and Immunity* **76,** 986–993 (2008).

39. Taylor, P. & Martinez-Pomares, L. Macrophage receptors and immune recognition. *Annual Review of Immunology* **23,** 901–944 (2005).

40. Xu, X. H. *et al.* Toll-like receptor-4 is expressed by macrophages in murine and human lipid-rich atherosclerotic plaques and upregulated by oxidized LDL. *Circulation* **104,** 3103–3108 (2001).

41. Greenberg, S. & Grinstein, S. Phagocytosis and innate immunity. *Current Opinion in Immunology* **14,** 136–145 (2002).

42. Peiser, L. & Gordon, S. The function of scavenger receptors expressed by macrophages and their role in the regulation of inflammation. *Microbes and Infection* **3,** 149–159 (2001).

43. Mukhopadhyay, S. & Gordon, S. The role of scavenger receptors in pathogen recognition and innate immunity. *Immunobiology* **209,** 39–49 (2004).

44. Cifarelli, V. *et al.* Increased Expression of Monocyte CD11b (Mac-1) in Overweight Recent-Onset Type 1 Diabetic Children. *The Review of Diabetic Studies* **4,** 112–117 (2007).

45. Lumeng, C. N., DelProposto, J. B., Westcott, D. J. & Saltiel, A. R. Phenotypic switching of adipose tissue macrophages with obesity is generated by spatiotemporal differences in macrophage subtypes. *Diabetes* **57,** 3239–3246 (2008).

46. Williams, M. & Nadler, J. Inflammatory mechanisms of diabetic complications. *Current Diabetes Reports* **7,** 242-248 (2007).

47. Lumeng, C. N., Deyoung, S. M. & Saltiel, A. R. Macrophages block insulin action in adipocytes by altering expression of signaling and glucose transport proteins. *The American Journal of Physiology - Endocrinology and Metabolism* **292,** 166–174 (2007).

48. Oostrom, A. Van & Wijk, J. Van. Increased expression of activation markers on monocytes and neutrophils in type 2 diabetes. *The Netherlands Journal of Medicine* **62,** 320–325 (2004).

49. Zacher, T., Knerr, I. & Rascher, W. Characterization of monocyte-derived dendritic cells in recent-onset diabetes mellitus type 1. *Clinical Immunology* **105,** 17–24 (2002).

50. Olefsky, J. M. & Glass, C. K. Macrophages, Inflammation, and Insulin Resistance. *Annual Review of Physiology* **72,** 219–246 (2010).

51. Roebuck, K. A. & Finnegan, A. Regulation of intercellular adhesion molecule-1 (CD54) gene expression. *Journal of Leukocyte Biology* **66,** 876–888 (1999).

52. Sheikh, N. a & Jones, L. a. CD54 is a surrogate marker of antigen presenting cell activation. *Cancer Immunology, Immunotherapy* **57,** 1381–1390 (2008).

53. Koyama, Y. *et al.* Cross-Linking of Intercellular Adhesion Molecule 1 (CD54) Induces AP-1 Activation and IL-1β Transcription. *The Journal of Immunology* **157,** 5097–5103 (1996).

54. Imanaka, H. *et al.* Ventilator-induced lung injury is associated with neutrophil infiltration, macrophage activation, and TGF-beta 1 mRNA upregulation in rat lungs. *Anesthesia and Analgesia* **92,** 428–436 (2001).

55. Iribarren, P., Correa, S. G., Sodero, N. & Riera, C. M. Activation of macrophages by silicones: phenotype and production of oxidant metabolites. *BMC Immunology* **3,** 6 (2002).

56. Silverstein, R. L. Inflammation, atherosclerosis, and arterial thrombosis: role of the scavenger receptor CD36. *Cleveland Clinic Journal of Medicine* **76 Supplem,** S27–S30 (2009).

57. Febbraio, M. CD36: a class B scavenger receptor involved in angiogenesis, atherosclerosis, inflammation, and lipid metabolism. *Journal of Clinical Investigation* **108,** 785–791 (2001).

58. Kurt-Jones, E. a *et al.* Pattern recognition receptors TLR4 and CD14 mediate response to respiratory syncytial virus. *Nature Immunology* **1,** 398–401 (2000).

59. Lee, E. & Joo, C. Role of Transforming Growth Factor-β in Transdifferentiation and Fibrosis of Lens Epithelial Cells. *Investigative Ophthalmology & Visual Science* **40,** 2025–2032 (1999).

60. Choi, J., Park, S. Y. & Joo, C.-K. Transforming growth factor-beta1 represses E-cadherin production via slug expression in lens epithelial cells. *Investigative Ophthalmology & Visual Science* **48,** 2708–2718 (2007).

61. Saika, S. *et al.* Accumulation of thrombospondin-1 in post-operative capsular fibrosis and its down-regulation in lens cells during lens fiber formation. *Experimental Eye Research* **79,** 147–156 (2004).

62. Saika, S. *et al.* TGFbeta-Smad signalling in postoperative human lens epithelial cells. *The British Journal of Ophthalmology* **86,** 1428–1433 (2002).

63. Gotoh, N. *et al.* An in vitro model of posterior capsular opacity: SPARC and TGF-beta2 minimize epithelial-to-mesenchymal transition in lens epithelium. *Investigative Ophthalmology & Visual Science* **48,** 4679–4687 (2007).

64. Hosler, M. R., Wang-Su, S.-T. & Wagner, B. J. Role of the proteasome in TGF-beta signaling in lens epithelial cells. *Investigative Ophthalmology & Visual Science* **47,** 2045–2052 (2006).

65. Saika, S. *et al.* Latent TGFbeta binding protein-1 and fibrillin-1 in human capsular opacification and in cultured lens epithelial cells. *The British Journal of Ophthalmology* **85,** 1362–1366 (2001).

66. Robertson, J., Nathu, Z. & Najjar, A. Adenoviral gene transfer of bioactive TGFB1 to the rodent eye as a novel model for anterior subcapsular cataract. *Molecular Vision* **13,** 457–469 (2007).

67. Anderson, J. M. & Miller, K. M. Biomaterial biocompatibility and the macrophage. *Biomaterials* **5,** 5–10 (1984).

68. Martinez, F. O., Helming, L. & Gordon, S. Alternative activation of macrophages: an immunologic functional perspective. *Annual Review of Immunology* **27,** 451–483 (2009).

69. Wynn, T. & Barron, L. Macrophages: master regulators of inflammation and fibrosis. *Seminars in Liver Disease* **30,** 245–257 (2010).

70. Wynn, T. Cellular and molecular mechanisms of fibrosis. *The Journal of Pathology* **214,** 199–210 (2008).

71. Lacombe, F., Durrieu, F., Briais, A. & Dumain, P. Flow cytometry CD45 gating for immunophenotyping of acute myeloid leukemia. *Leukemia* **11,** 1878–1886 (1997).

72. Franz, S., Rammelt, S., Scharnweber, D. & Simon, J. C. Immune responses to implants - a review of the implications for the design of immunomodulatory biomaterials. *Biomaterials* **32,** 6692–6709 (2011).

73. Diegelmann, R. F. & Evans, M. C. Wound healing: an overview of acute, fibrotic and delayed healing. *Frontiers in Bioscience : A Journal and Virtual Library* **9,** 283–289 (2004).

74. Nguyen, D. T., Orgill, D. P. & Murphy, G. F. *Biomaterials for Treating Skin Loss*. (Elsevier, 2009).

75. Ratner, B. D. The biocompatibility manifesto: biocompatibility for the twenty-first century. *Journal of Cardiovascular Translational Research* **4,** 523–527 (2011).

76. Zhang, M. & Horbett, T. a. Tetraglyme coatings reduce fibrinogen and von Willebrand factor adsorption and platelet adhesion under both static and flow conditions. *Journal of Biomedical Materials Research Part A* **89,** 791–803 (2009).

77. Wang, Y.-X., Robertson, J. L., Spillman, W. B. & Claus, R. O. Effects of the chemical structure and the surface properties of polymeric biomaterials on their biocompatibility. *Pharmaceutical Research* **21,** 1362–1373 (2004).

78. Kang, C.-K. & Lee, Y.-S. The surface modification of stainless steel and the correlation between the surface properties and protein adsorption. *Journal of Materials Science Materials in Medicine* **18,** 1389–1398 (2007).

79. Anderson, J. M. & Jones, J. a. Phenotypic dichotomies in the foreign body reaction. *Biomaterials* **28,** 5114–5120 (2007).

80. Anderson, J. M. & McNally, A. K. Biocompatibility of implants: lymphocyte/macrophage interactions. *Seminars in Immunopathology* **33,** 221–233 (2011).

81. Pokidysheva, E. N. *et al.* Comparative analysis of human serum albumin adsorption and complement activation for intraocular lenses. *Artificial Organs* **25,** 453–458 (2001).

82. Johnston, R. L., Spalton, D. J., Hussain, a & Marshall, J. In vitro protein adsorption to 2 intraocular lens materials. *Journal of Cataract and Refractive Surgery* **25,** 1109–1115 (1999).

83. Abela-Formanek, C. *et al.* Results of hydrophilic acrylic, hydrophobic acrylic, and silicone intraocular lenses in uveitic eyes with cataract: comparison to a control group. *Journal of Cataract and Refractive Surgery* **28,** 1141–1152 (2002).

84. Roesel, M., Heinz, C., Heimes, B., Koch, J. M. & Heiligenhaus, A. Uveal and capsular biocompatibility of two foldable acrylic intraocular lenses in patients with endogenous uveitis — a prospective randomized study. *Graefe's Archive for Clinical and Experimental Ophthalmology* **246,** 1609–1615 (2008).

85. Huang, X.-D., Yao, K., Zhang, Z., Zhang, Y. & Wang, Y. Uveal and capsular biocompatibility of an intraocular lens with a hydrophilic anterior surface and a hydrophobic posterior surface. *Journal of Cataract & Refractive Surgery* **36,** 290–298 (2010).

86. Saika, S. *et al.* Immunohistochemical evaluation of cellular deposits on posterior chamber intraocular lenses. *Graefe's Archive for Clinical and Experimental Ophthalmology* **236,** 758–765 (1998).

87. Ishikawa, N., Miyamoto, T., Okada, Y. & Saika, S. Cell adhesion on explanted intraocular lenses part 2: experimental study of a surface-modified IOL in rabbits. *Journal of Cataract and Refractive Surgery* **37,** 1339–1342 (2011).

88. Uusitalo, M. & Kivelä, T. Cell types of secondary cataract: an immunohistochemical analysis with antibodies to cytoskeletal elements and macrophages. *Graefe's Archive for Clinical and Experimental Ophthalmology* **235,** 506–511 (1997).

89. Ishikawa, N., Miyamoto, T., Okada, Y. & Saika, S. Cell adhesion on explanted intraocular lenses: part 1: analysis of explanted IOLs. *Journal of Cataract and Refractive Surgery* **37,** 1333–1338 (2011).

90. Lois, N. *et al.* Effect of short-term macrophage depletion in the development of posterior capsule opacification in rodents. *The British Journal of Ophthalmology* **92,** 1528–1533 (2008).

91. Li, Y., Wang, J., Chen, Z. & Tang, X. Effect of hydrophobic acrylic versus hydrophilic acrylic intraocular lens on posterior capsule opacification: meta-analysis. *PloS One* **8,** e77864 (2013).

92. Cheng, J.-W. *et al.* Efficacy of different intraocular lens materials and optic edge designs in preventing posterior capsular opacification: a meta-analysis. *American Journal of Ophthalmology* **143,** 428–436 (2007).

93. Hollick, E., Spalton, D. & Ursell, P. Posterior capsular opacification with hydrogel, polymethylmethacrylate, and silicone intraocular lenses: two-year results of a randomized prospective trial. *American Journal of Ophthalmology* **129,** 577–584 (2000).

94. Medawar, P. B. Immunity to Homologous Grafted Skin. III. The Fate of Skin Homographs Transplanted to the Brain, to Subcutaneous Tissue, and to the Anterior Chamber of the Eye. *British Journal of Experimental Pathology* **29,** 58–69 (1948).

95. Niederkorn, J. Y. & Stein-Streilein, J. History and physiology of immune privilege. *Ocular Immunology and Inflammation* **18,** 19–23 (2010).

96. Van Dooremaal, J. C. Die Entwickelung der in fremden Grund versetzten lebenden Gewebe. *Albrecht von Graefes Archiv Fur Ophthalmologie* **19,** 359–373 (1873).

97. Shechter, R., London, A. & Schwartz, M. Orchestrated leukocyte recruitment to immune-privileged sites: absolute barriers versus educational gates. *Nature Reviews Immunology* **13,** 206–218 (2013).

98. Saika, S. Relationship between posterior capsule opacification and intraocular lens biocompatibility. *Progress in Retinal and Eye Research* **23,** 283–305 (2004).

99. Taylor, a W., Yee, D. G. & Streilein, J. W. Suppression of nitric oxide generated by inflammatory macrophages by calcitonin gene-related peptide in aqueous humor. *Investigative Ophthalmology & Visual Science* **39,** 1372–1378 (1998).

100. Ferguson, T. a & Griffith, T. S. A vision of cell death: Fas ligand and immune privilege 10 years later. *Immunological Reviews* **213,** 228–238 (2006).

101. Chen, J. Regulation of the Proinflammatory Effects of Fas Ligand (CD95L). *Science* **282,** 1714–1717 (1998).

102. Taylor, A. & Yee, D. Neuropeptide Regulation of Immunity: The Immunosuppressive Activity of Alpha-Melanocyte-Stimulating Hormone (αMSH). *Annals of the New York Academy of Sciences* **917,** 239–247 (2000).

103. Namba, K. & Kitaichi, N. Induction of regulatory T cells by the immunomodulating cytokines α-melanocyte-stimulating hormone and transforming growth factor-β2. *Journal of Leukocyte Biology* **72,** 946–952 (2002).

104. Zamiri, P., Masli, S., Streilein, J. W. & Taylor, A. W. Pigment epithelial growth factor suppresses inflammation by modulating macrophage activation. *Investigative Ophthalmology & Visual Science* **47,** 3912–3918 (2006).

105. Cousins, S. W., McCabe, M. M., Danielpour, D. & Streilein, J. W. Identification of transforming growth factor-beta as an immunosuppressive factor in aqueous humor. *Investigative Ophthalmology & Visual Science* **32,** 2201–2211 (1991).

106. Mantel, P.-Y. & Schmidt-Weber, C. B. Transforming growth factor-beta: recent advances on its role in immune tolerance. *Methods in Molecular Biology (Clifton, NJ)* **677,** 303–338 (2011).

107. Moriarty, A. P. *et al.* Studies of the blood-aqueous barrier in diabetes mellitus. *American Journal of Ophthalmology* **117,** 768–771 (1994).

108. Foxman, E. & Zhang, M. Inflammatory mediators in uveitis: differential induction of cytokines and chemokines in Th1-versus Th2-mediated ocular inflammation. *The Journal of Immunology* **168**, 2483–2492 (2002).

109. Dong, N., Xu, B., Wang, B. & Chu, L. Study of 27 aqueous humor cytokines in patients with type 2 diabetes with or without retinopathy. *Molecular Vision* **19,** 1734–46 (2013).

110. Kawai, M. *et al.* Elevated Levels of Monocyte Chemoattractant Protein-1 in the Aqueous Humor after Phacoemulsification. *Investigative Ophthalmology & Visual Science* **53 ,** 7951–7960 (2012).

111. Meacock, W. R., Spalton, D. J. & Stanford, M. R. Role of cytokines in the pathogenesis of posterior capsule opacification. *The British Journal of Ophthalmology* **84,** 332–226 (2000).

112. Funatsu, H. *et al.* Aqueous humor levels of cytokines are related to vitreous levels and progression of diabetic retinopathy in diabetic patients. *Graefe's Archive for Clinical and Experimental Ophthalmology* **243,** 3–8 (2005).

113. Curnow, S. J. & Murray, P. I. Inflammatory mediators of uveitis: cytokines and chemokines. *Current Opinion in Ophthalmology* **17,** 532–537 (2006).

114. Vos, A., Hoekzema, R. & Kijlstra, A. Cytokines and uveitis, a review. *Current Eye Research* **11,** 581–597 (1992).

115. Ferguson, V. M. & Spalton, D. J. Recovery of the blood-aqueous barrier after cataract surgery. *The British Journal of Ophthalmology* **75,** 106–110 (1991).

116. Nishi, O. & Nishi, K. Disruption of the blood-aqueous barrier by residual lens epithelial cells after intraocular lens implantation. *Ophthalmic Surgery* **23,** 325–329 (1992).

117. Deshmane, S. L., Kremlev, S., Amini, S. & Sawaya, B. E. Monocyte chemoattractant protein-1 (MCP-1): an overview. *Journal of Interferon & Cytokine Research* **29,** 313–326 (2009).

118. Zampighi, G. a, Eskandari, S. & Kreman, M. Epithelial organization of the mammalian lens. *Experimental Eye Research* **71,** 415–435 (2000).

119. Brownlee, M. The pathobiology of diabetic complications: a unifying mechanism. *Diabetes* **54,** 1615–1625 (2005).

120. Maruyama, K., Asai, J., Ii, M. & Thorne, T. Decreased macrophage number and activation lead to reduced lymphatic vessel formation and contribute to impaired diabetic wound healing. *The American Journal of Pathology* **170,** 1178–1191 (2007).

121. Khanna, S., Biswas, S., Shang, Y. & Collard, E. Macrophage dysfunction impairs resolution of inflammation in the wounds of diabetic mice. *PLoS One* **5,** (2010).

122. Parathath, S. *et al.* Diabetes Adversely Affects Macrophages During Atherosclerotic Plaque Regression in Mice. *Diabetes* **60,** 1759–1769 (2011).

123. Aronson, D. & Rayfield, E. How hyperglycemia promotes atherosclerosis: molecular mechanisms. *Cardiovascular Diabetology* **10,** 1–10 (2002).

124. Vlassara, H., Fuh, H., Donnelly, T. & Cybulsky, M. Advanced glycation endproducts promote adhesion molecule (VCAM-1, ICAM-1) expression and atheroma formation in normal rabbits. *Molecular Medicine* **1,** (1995).

125. Bansilal, S., Farkouh, M. & Fuster, V. Role of insulin resistance and hyperglycemia in the development of atherosclerosis. *The American Journal of Cardiology* **99,** 6B–14B (2007).

126. Galkina, E. & Ley, K. Leukocyte Recruitment and Vascular Injury in Diabetic Nephropathy. *Journal of the American Society of Nephrology* **17,** 368–377 (2006).

127. Chow, F. & Nikolic-Paterson, D. Intercellular adhesion molecule-1 deficiency is protective against nephropathy in type 2 diabetic db/db mice. *Journal of the American Society of Nephrology* **16,** 1711–1722 (2005).

128. Chow, F., Ozols, E. & Nikolic-Paterson, D. Macrophages in mouse type 2 diabetic nephropathy: correlation with diabetic state and progressive renal injury. *Kidney International* **65,** 116–128 (2004).

129. Sugimoto, H., Shikata, K. & Hirata, K. expression of intercellular adhesion molecule-1 (ICAM-1) in diabetic rat glomeruli: glomerular hyperfiltration is a potential mechanism of ICAM-1 upregulation. *Diabetes* **46,** 2075–2081 (1997).

130. Wang, A. & Hascall, V. Hyaluronan structures synthesized by rat mesangial cells in response to hyperglycemia induce monocyte adhesion. *Journal of Biological Chemistry* **279,** 10279–10285 (2004).

131. Meleth, A., Agrón, E., Chan, C. & Reed, G. Serum inflammatory markers in diabetic retinopathy. *Investigative Ophthalmology & Visual Science* **46,** 4295–4301 (2005).

132. Kojima, H., Kim, J. & Chan, L. Emerging roles of hematopoietic cells in the pathobiology of diabetic complications. *Trends in Endocrinology & Metabolism* **25,** 178–187 (2014).

133. Zorena, K., Raczyńska, D. & Raczyńska, K. Biomarkers in Diabetic Retinopathy and the Therapeutic Implications. *Mediators of Inflammation* **2013,** 1–11 (2013).

134. Pollreisz, A. & Schmidt-Erfurth, U. Diabetic cataract-pathogenesis, epidemiology and treatment. *Journal of Ophthalmology* **2010,** 1–8 (2010).

135. Hashim, Z. & Zarina, S. Osmotic stress induced oxidative damage: Possible mechanism of cataract formation in diabetes. *Journal of Diabetes and Its Complications* **26,** 275–279 (2012).

136. Gul, A., Rahman, M. A., Salim, A. & Simjee, S. U. Advanced glycation end products in senile diabetic and nondiabetic patients with cataract. *Journal of Diabetes and Its Complications* **23,** 343–348 (2009).

137. Ma, H. *et al.* Diabetes-induced alteration of F4/80+ macrophages: A study in mice with streptozotocin-induced diabetes for a long term. *Journal of Molecular Medicine* **86,** 391–400 (2008).

138. Sun, C., Sun, L., Ma, H. & Peng, J. The phenotype and functional alterations of macrophages in mice with hyperglycemia for long term. *Journal of Cellular Physiology* **227,** 1670–1679 (2012).

139. Morris, H. F., Ochi, S. & Winkler, S. Implant survival in patients with type 2 diabetes: placement to 36 months. *Annals of Periodontology* **5,** 157–165 (2000).

140. Javed, F. & Romanos, G. E. Impact of diabetes mellitus and glycemic control on the osseointegration of dental implants: a systematic literature review. *Journal of Periodontology* **80,** 1719–1730 (2009).

141. Salvi, G. E., Carollo-Bittel, B. & Lang, N. P. Effects of diabetes mellitus on periodontal and peri-implant conditions: Update on associations and risks. *Journal of Clinical Periodontology* **35,** 398–409 (2008).

142. Abizaid, A. & Kornowski, R. The influence of diabetes mellitus on acute and late clinical outcomes following coronary stent implantation. *Journal of the American College of Cardiology* **32,** 584–589 (1998).

143. Fong, C. S.-U. *et al.* Three-year incidence and factors associated with posterior capsule opacification after cataract surgery: The Australian Prospective Cataract Surgery and Age-related Macular Degeneration Study. *American Journal of Ophthalmology* **157,** 171–179 (2014).

144. Ebihara, Y., Kato, S., Oshika, T., Yoshizaki, M. & Sugita, G. Posterior capsule opacification after cataract surgery in patients with diabetes mellitus. *Journal of Cataract and Refractive Surgery* **32,** 1184–1187 (2006).

145. Elgohary, M., Hollick, E. & Bender, L. Hydrophobic acrylic and plate-haptic silicone intraocular lens implantation in diabetic patients: pilot randomized clinical trial. *Journal of Cataract & Refractive Surgery* **32,** 1188–1195 (2006).

146. Lee, D., Seo, Y. & Joo, C. Progressive opacification of hydrophilic acrylic intraocular lenses in diabetic patients. *Journal of Cataract & Refractive Surgery* **28,** 1271–1275 (2002).

147. Dadsetan, M., Jones, J. a, Hiltner, A. & Anderson, J. M. Surface chemistry mediates adhesive structure, cytoskeletal organization, and fusion of macrophages. *Journal of Biomedical Materials Research Part A* **71,** 439–448 (2004).

148. Dinnes, D. & Marçal, H. Material surfaces affect the protein expression patterns of human macrophages: a proteomics approach. *Journal of Biomedial Materials Research Part A* **80,** 895–908 (2007).

149. Shen, M. & Horbett, T. a. The effects of surface chemistry and adsorbed proteins on monocyte/macrophage adhesion to chemically modified polystyrene surfaces. *Journal of Biomedical Materials Research* **57,** 336–345 (2001).

150. Kitano, H. Systems biology: a brief overview. *Science (New York, NY)* **295,** 1662–1664 (2002).

151. Melino, M. *et al.* Macrophage secretory products induce an inflammatory phenotype in hepatocytes. *World Journal of Gastroenterology* **18,** 1732–1744 (2012).

152. Chung, S.-H., Jung, S.-A., Cho, Y. J., Lee, J. H. & Kim, E. K. IGF-1 counteracts TGF-beta-mediated enhancement of fibronectin for in vitro human lens epithelial cells. *Yonsei Medical Journal* **48,** 949–954 (2007).

153. Bao, X.-L., Song, H., Chen, Z. & Tang, X. Wnt3a promotes epithelial-mesenchymal transition, migration, and proliferation of lens epithelial cells. *Molecular Vision* **18,** 1983–1990 (2012).

154. Misri, S. *et al.* KCC isoforms in a human lens epithelial cell line (B3) and lens tissue extracts. *Experimental Eye Research* **83,** 1287–1294 (2006).

155. Park, E. K. *et al.* Optimized THP-1 differentiation is required for the detection of responses to weak stimuli. *Inflammation Research* **56,** 45–50 (2007).

156. Daigneault, M., Preston, J. a, Marriott, H. M., Whyte, M. K. B. & Dockrell, D. H. The identification of markers of macrophage differentiation in PMA-stimulated THP-1 cells and monocyte-derived macrophages. *PloS One* **5,** e8668 (2010).

157. Cammarata, P. R., Braun, B., Dimitrijevich, S. D. & Pack, J. Characterization and functional expression of the natriuretic peptide system in human lens epithelial cells. *Molecular Vision* **16,** 630–638 (2010).

158. Liang, C. & Han, S. Increased CD36 protein as a response to defective insulin signaling in macrophages. *The Journal of Clinical Investigation* **113,** 764–773 (2004).

159. Auwerx, J., Staels, B., Van Vaeck, F. & Ceuppens, J. L. Changes in IgG Fc receptor expression induced by phorbol 12-myristate 13-acetate treatment of THP-1 monocytic leukemia cells. *Leukemia Research* **16,** 317–327 (1992).

160. Auwerx, J. The human leukemia cell line, THP-1: a multifacetted model for the study of monocyte-macrophage differentiation. *Experientia* **47,** 22–31 (1991).

161. Irwin, E. F. *et al.* Modulus-dependent macrophage adhesion and behavior. *Journal of Biomaterials Science Polymer Edition* **19,** 1363–1382 (2008).

162. Ziegelaar, B. & Fitton, J. The modulation of cellular responses to poly (2-hydroxyethyl methacrylate) hydrogel surfaces: phosphorylation decreases macrophage collagenase production in vitro. *Journal of Biomaterials Science, Polymer Edition* **9,** 849–862 (1998).

163. Fitzpatrick, L. E., Chan, J. W. Y. & Sefton, M. V. On the mechanism of poly(methacrylic acid -co- methyl methacrylate)-induced angiogenesis: gene expression analysis of dTHP-1 cells. *Biomaterials* **32,** 8957–8967 (2011).

164. Schutte, R. J., Parisi-Amon, A. & Reichert, W. M. Cytokine profiling using monocytes/macrophages cultured on common biomaterials with a range of surface chemistries. *Journal of Biomedical Materials Research Part A* **88,** 128–139 (2009).

165. Lee, H. & Stachelek, S. Correlating macrophage morphology and cytokine production resulting from biomaterial contact. *Journal of Biomedical Materials Research Part A* **101,** 203–212 (2013).

166. Wang-Su, S.-T. Proteome Analysis of Lens Epithelia, Fibers, and the HLE B-3 Cell Line. *Investigative Ophthalmology & Visual Science* **44,** 4829–4836 (2003).

167. Morarescu, D., West-Mays, J. a & Sheardown, H. D. Effect of delivery of MMP inhibitors from PDMS as a model IOL material on PCO markers. *Biomaterials* **31,** 2399–2407 (2010).

168. Yan, Q., Perdue, N. & Sage, E. H. Differential responses of human lens epithelial cells to intraocular lenses in vitro: hydrophobic acrylic versus PMMA or silicone discs. *Graefe's Archive for Clinical and Experimental Ophthalmology* **243,** 1253–1262 (2005).

169. Kao, E. C. Y., McCanna, D. J. & Jones, L. W. Utilization of in vitro methods to determine the biocompatibility of intraocular lens materials. *Toxicology in Vitro* **25,** 1906–1911 (2011).

170. Bernatchez, S. F., Atkinson, M. R. & Parks, P. J. Expression of intercellular adhesion molecule-1 on macrophages in vitro as a marker of activation. *Biomaterials* **18,** 1371–8 (1997).

171. Stern, M., Savill, J. & Haslett, C. Human monocyte-derived macrophage phagocytosis of senescent eosinophils undergoing apoptosis. Mediation by alpha v beta

3/CD36/thrombospondin recognition mechanism and lack of phlogistic response. *The American Journal of Pathology* **149,** 911–921 (1996).

172. Fadok, V. a, Warner, M. L., Bratton, D. L. & Henson, P. M. CD36 is required for phagocytosis of apoptotic cells by human macrophages that use either a phosphatidylserine receptor or the vitronectin receptor (alpha v beta 3). *Journal of Immunology* **161,** 6250–6257 (1998).

173. Ren, Y., Silverstein, R., Allen, J. & Savill, J. CD36 gene transfer confers capacity for phagocytosis of cells undergoing apoptosis. *The Journal of Experimental Medicine* **181,** 1857–1862 (1995).

174. Draude, G. & Lorenz, R. L. TGF-beta1 downregulates CD36 and scavenger receptor A but upregulates LOX-1 in human macrophages. *American Journal of Physiology Heart and Circulatory Physiology* **278,** H1042–H1048 (2000).

175. Devitt, a *et al.* Human CD14 mediates recognition and phagocytosis of apoptotic cells. *Nature* **392,** 505–509 (1998).

176. Martin, T. & Mongovin, S. The CD14 differentiation antigen mediates the development of endotoxin responsiveness during differentiation of mononuclear phagocytes. *Journal of Leukocyte Biology* **56,** (1994).

177. Ziegler-Heitbrock, H. W. & Ulevitch, R. J. CD14: cell surface receptor and differentiation marker. *Immunology Today* **14,** 121–125 (1993).

178. Bosshart, H. & Heinzelmann, M. Spontaneous decrease of CD14 cell surface expression in human peripheral blood monocytes ex vivo. *Journal of Immunological Methods* **368,** 80–83 (2011).

179. Kindlund, B., Henning, P., Lindholm, C. & Lerner, U. H. From monocytes to osteoclasts: Through down-regulation of CD14 and CD16. *Bone* **50,** S87 (2012).

180. Penninger, J. M., Irie-Sasaki, J., Sasaki, T. & Oliveira-dos-Santos, a J. CD45: new jobs for an old acquaintance. *Nature Immunology* **2,** 389–396 (2001).

181. Gomes, A., Fernandes, E. & Lima, J. L. F. C. Fluorescence probes used for detection of reactive oxygen species. *Journal of Biochemical and Biophysical Methods* **65,** 45–80 (2005).

182. Curtin, J. F., Donovan, M. & Cotter, T. G. Regulation and measurement of oxidative stress in apoptosis. *Journal of Immunological Methods* **265,** 49–72 (2002).

183. Brubacher, J. L. & Bols, N. C. Chemically de-acetylated 2',7'-dichlorodihydrofluorescein diacetate as a probe of respiratory burst activity in mononuclear phagocytes. *Journal of Immunological Methods* **251,** 81–91 (2001).

184. Robinson, J. P. *et al.* Measurement of intracellular fluorescence of human monocytes relative to oxidative metabolism. *Journal of Leukocyte Biology* **43,** 304–310 (1988).

185. Labow, R. S., Meek, E., Matheson, L. a & Santerre, J. P. Human macrophage-mediated biodegradation of polyurethanes: assessment of candidate enzyme activities. *Biomaterials* **23,** 3969–3975 (2002).

186. Matheson, L. a, Santerre, J. P. & Labow, R. S. Changes in macrophage function and morphology due to biomedical polyurethane surfaces undergoing biodegradation. *Journal of Cellular Physiology* **199,** 8–19 (2004).

187. Rice, J. Quantitative assessment of the response of primary derived human osteoblasts and macrophages to a range of nanotopography surfaces in a single culture model in vitro. *Biomaterials* **24,** 4799–4818 (2003).

188. Cerri, C., Chimenti, D. & Conti, I. Monocyte/macrophage-derived microparticles up-regulate inflammatory mediator synthesis by human airway epithelial cells. *The Journal of Immunology* **177,** 1975–1980 (2006).

189. Gauley, J. & Pisetsky, D. S. The release of microparticles by RAW 264.7 macrophage cells stimulated with TLR ligands. *Journal of Leukocyte Biology* **87,** 1115–1123 (2010).

190. Ravalico, G., Baccara, F., Lovisato, A. & Tognetto, D. Postoperative Cellular Reaction on Various Intraocular Lens Materials. *Ophthalmology* **104,** 1084–1091 (1997).

191. Yao, H.-W., Xie, Q.-M., Chen, J.-Q., Deng, Y.-M. & Tang, H.-F. TGF-beta1 induces alveolar epithelial to mesenchymal transition in vitro. *Life Sciences* **76,** 29–37 (2004).

192. Hao, W. *et al.* Ω-3 Fatty Acids Suppress Inflammatory Cytokine Production By Macrophages and Hepatocytes. *Journal of Pediatric Surgery* **45,** 2412–2418 (2010).

193. Ceppo, F. *et al.* Implication of the Tpl2 kinase in inflammatory changes and insulin resistance induced by the interaction between adipocytes and macrophages. *Endocrinology* 1–15 (2014). doi:10.1210/en.2013-1815

194. Ren, W. & Wu, B. Polyethylene and methyl methacrylate particle-stimulated inflammatory tissue macrophages up-regulate bone resorption in a murine neonatal calvaria in vitro. *Journal of Orthopaedic Research* **20,** 1031–1037 (2002).

195. Duffield, J. S. *et al.* Activated macrophages direct apoptosis and suppress mitosis of mesangial cells. *Journal of Immunology* **164,** 2110–2119 (2000).

196. Glim, J. E., Niessen, F. B., Everts, V., van Egmond, M. & Beelen, R. H. J. Platelet derived growth factor-CC secreted by M2 macrophages induces alpha-smooth muscle actin expression by dermal and gingival fibroblasts. *Immunobiology* **218,** 924–929 (2013).

197. Hinz, B., Celetta, G., Tomasek, J. J., Gabbiani, G. & Chaponnier, C. Alpha-smooth muscle actin expression upregulates fibroblast contractile activity. *Molecular Biology of the Cell* **12,** 2730–2741 (2001).

198. Känel, R. Von, Mills, P. & Dimsdale, J. Short-term hyperglycemia induces lymphopenia and lymphocyte subset redistribution. *Life Sciences* **69,** 255–262 (2001).

199. Kwoun, M., Ling, P. & Lydon, E. Immunologic effects of acute hyperglycemia in nondiabetic rats. *Journal of Parenteral and Enteral Nutrition* **21,** 91–95 (1997).

200. Reaven, G. M. Role of Insulin Resistance in Human Disease. *Diabetes* **37,** 1595–1607 (1988).

201. Diederen, R. M. H., Starnes, C. a, Berkowitz, B. a & Winkler, B. S. Reexamining the hyperglycemic pseudohypoxia hypothesis of diabetic oculopathy. *Investigative Ophthalmology & Visual Science* **47,** 2726–2731 (2006).

202. Kyselova, Z., Stefek, M. & Bauer, V. Pharmacological prevention of diabetic cataract. *Journal of Diabetes and Its Complications* **18,** 129–140 (2004).

203. Tuttle, K. R. Linking metabolism and immunology: diabetic nephropathy is an inflammatory disease. *Journal of the American Society of Nephrology* **16,** 1537–1538 (2005).

204. Griffin, E., Re, A., Hamel, N., Fu, C. & Bush, H. A link between diabetes and atherosclerosis: glucose regulates expression of CD36 at the level of translation. *Nature Medicine* **7,** (2001).

205. American Diabetes Association. Diagnosis and classification of diabetes mellitus. *Diabetes Care* **33 Suppl 1,** S62–S69 (2010).

206. Lamharzi, N., Renard, C. & Kramer, F. Hyperlipidemia in Concert With Hyperglycemia Stimulates the Proliferation of Macrophages in Atherosclerotic Lesions Potential Role of Glucose-Oxidized LDL. *Diabetes* 3217–3225 (2004).

207. Conti, G., Scarpini, E. & Baron, P. Macrophage infiltration and death in the nerve during the early phases of experimental diabetic neuropathy: a process concomitant with endoneurial induction of IL-1β. *Journal of the Neurological Sciences* **195,** 35–40 (2002).

208. Sampson, M., Davies, I. & Brown, J. Monocyte and neutrophil adhesion molecule expression during acute hyperglycemia and after antioxidant treatment in type 2 diabetes and control patients. *Arteriorsclerosis, Thrombosis, and Vascular Biology* **22,** 1187–1193 (2002).

209. Piga, R., Naito, Y., Kokura, S., Handa, O. & Yoshikawa, T. glucose exposure induces monocyte-endothelial cells adhesion and transmigration by increasing VCAM-1 and MCP-1 expression in human aortic endothelial cells. *Atherosclerosis* **193,** 328–334 (2007).

210. Hinz, B. The myofibroblast: paradigm for a mechanically active cell. *Journal of Biomechanics* **43,** 146–155 (2010).

211. Meissner, A. & Noack, T. Proliferation of human lens epithelial cells (HLE-B3) is inhibited by blocking of voltage-gated calcium channels. *European Journal of Physiology* **457,** 47–59 (2008).

212. Awasthi, N., Wang-Su, S. T. & Wagner, B. J. Downregulation of MMP-2 and -9 by proteasome inhibition: a possible mechanism to decrease LEC migration and prevent posterior capsular opacification. *Investigative Ophthalmology & Visual Science* **49,** 1998–2003 (2008).

213. Moschos, M. M. *et al.* Expression of the insulin-like growth factor 1 (IGF-1) and type I IGF receptor mRNAs in human HLE-B3 lens epithelial cells. *In Vivo* **25,** 179–84 (2011).

214. Jin, X.-H. *et al.* Inhibition of nuclear factor-kappa B activation attenuates hydrogen peroxide-induced cytotoxicity in human lens epithelial cells. *The British Journal of Ophthalmology* **91,** 369–371 (2007).

215. Jr, J. H., Taintor, R., Vavrin, Z. & Rachlin, E. Nitric oxide: a cytotoxic activated macrophage effector molecule. *Biochemical and Biophysical Research Communications* **157,** 87–94 (1988).

216. Pabst, M. & Johnston, R. Increased production of superoxide anion by macrophages exposed in vitro to muramyl dipeptide or lipopolysaccharide. *The Journal of Experimental Medicine* **151,** 101–114 (1980).

217. Li, R. *et al.* A peptide derived from the intercellular adhesion molecule-2 regulates the avidity of the leukocyte integrins CD11b/CD18 and CD11c/CD18. *The Journal of Cell Biology* **129,** 1143–1153 (1995).

218. Noti, J. D. & Reinemann, B. C. The leukocyte integrin gene CD11c is transcriptionally regulated during monocyte differentiation. *Molecular Immunology* **32,** 361–369 (1995).

219. Okada, S., Shikata, K., Matsuda, M. & Ogawa, D. Intercellular adhesion molecule-1–deficient mice are resistant against renal injury after induction of diabetes. *Diabetes* **52,** (2003).

220. Verma, S., Weisel, R. & Badiwala, M. Hyperglycemia potentiates the proatherogenic effects of C-reactive protein: reversal with rosiglitazone. *Journal of Molecular and Celular Cardiology* **35,** 417–419 (2003).

221. Morigi, M. & Angioletti, S. Leukocyte-endothelial interaction is augmented by high glucose concentrations and hyperglycemia in a NF-kB-dependent fashion. *Journal of Clinical Investigation* **101,** 1905–1918 (1998).

222. Torrecilla, E. Time-dependent changes in the expression of lymphocyte and monocyte cell adhesion molecules after meals of different composition. *British Journal of Nutrition* **104,** 1650–1654 (2010).

223. Takahashi, K., Honeyman, M. C. & Harrison, L. C. Impaired yield, phenotype, and function of monocyte-derived dendritic cells in humans at risk for insulin-dependent diabetes. *Journal of Immunology* **161,** 2629–2635 (1998).

224. Štulc, T. & Svobodová, H. Rosiglitazone Influences the Expression of Leukocyte Adhesion Molecules and CD14 Receptor in Type 2 Diabetes Mellitus Patients. *Physiology Research* **63,** 293–298 (2014).

225. Landmann, R., Müller, B. & Zimmerli, W. CD14, new aspects of ligand and signal diversity. *Microbes and Infection / Institut Pasteur* **2,** 295–304 (2000).

226. Patiño, R., Ibarra, J. & Rodriguez, A. Circulating monocytes in patients with diabetes mellitus, arterial disease, and increased CD14 expression. *The American Journal of Cardiology* **85,** 1288–1291 (2000).

227. Fogelstrand, L., Hulthe, J. & Hulten, L. Monocytic expression of CD14 and CD18, circulating adhesion molecules and inflammatory markers in women with diabetes mellitus and impaired glucose tolerance. *Diabetologia* **47,** 1948–1952 (2004).

228. Nareika, A., Im, Y. & Game, B. High glucose enhances lipopolysaccharide-stimulated CD14 expression in U937 mononuclear cells by increasing nuclear factor κB and AP-1 activities. *Journal of Endocrinology* **196,** 45–55 (2008).

229. Sampson, M., Davies, I., Braschi, S., Ivory, K. & Hughes, D. Increased expression of a scavenger receptor (CD36) in monocytes from subjects with Type 2 diabetes. *Atherosclerosis* **167,** 129–134 (2003).

230. Yechoor, V. K. *et al.* Distinct pathways of insulin-regulated versus diabetes-regulated gene expression: an in vivo analysis in MIRKO mice. *Proceedings of the National Academy of Sciences of the United States of America* **101,** 16525–16530 (2004).

231. Chen, M., Yang, Y. & Loux, T. The role of hyperglycemia in FAT/CD36 expression and function. *Pediatric Surgery International* **22,** 647–654 (2006).

232. Pravenec, M., Landa, V., Zidek, V. & Musilova, A. Transgenic rescue of defective Cd36 ameliorates insulin resistance in spontaneously hypertensive rats. *Nature Genetics* **27,** 13–15 (2001).

233. Aitman, T. J. *et al.* Identification of Cd36 (Fat) as an insulin-resistance gene causing defective fatty acid and glucose metabolism in hypertensive rats. *Nature Genetics* **21,** 76–83 (1999).

234. Okado, A., Kawasaki, Y. & Hasuike, Y. Induction of apoptotic cell death by methylglyoxal and 3-deoxyglucosone in macrophage-derived cell lines. *Biochemical and Biophysical Research Communications* **224,** 219–224 (1996).

235. Turina, M., Mulhall, A., Gardner, S., Jr, H. P. & Miller, F. Mannitol upregulates monocyte HLA-DR, monocyte and neutrophil CD11b, and inhibits neutrophil apoptosis. *Inflammation* **31,** 74–83 (2008).

236. Akita, K. *et al.* Involvement of Caspase-1 and Caspase-3 in the Production and Processing of Mature Human Interleukin 18 in Monocytic THP.1 Cells. *Journal of Biological Chemistry* **272,** 595–603 (1997).

237. Keller, M., Rüegg, A., Werner, S. & Beer, H.-D. Active caspase-1 is a regulator of unconventional protein secretion. *Cell* **132,** 818–31 (2008).

238. Malone, J., Lowitt, S. & Cook, W. Nonosmotic diabetic cataracts. *Pediatric Research* **27,** 0–3 (1990).

239. Esteves, J., Pizzol, M. & Sccoco, C. Cataract and type 1 diabetes mellitus. *Diabetes Research and Clinical Practice* **82,** 324–328 (2008).

240. Patel, J. I., Hykin, P. G. & Cree, I. a. Diabetic cataract removal: postoperative progression of maculopathy--growth factor and clinical analysis. *The British Journal of Ophthalmology* **90,** 697–701 (2006).

241. Lockshin, R. A. & Zakeri, Z. Caspase-independent cell death? *Oncogene* **23,** 2766–73 (2004).

242. Long, A. C., Colitz, C. M. H. & Bomser, J. A. Apoptotic and necrotic mechanisms of stress-induced human lens epithelial cell death. *Experimental Biology and Medicine* **229,** 1072–80 (2004).

243. Yao, H. *et al.* Parthenolide protects human lens epithelial cells from oxidative stress-induced apoptosis via inhibition of activation of caspase-3 and caspase-9. *Cell Research* **17,** 565–71 (2007).

244. Choudhary, S. *et al.* Cellular lipid peroxidation end-products induce apoptosis in human lens epithelial cells. *Free Radical Biology and Medicine* **32,** 360–369 (2002).

245. Shui, Y. B. *et al.* Morphological observation on cell death and phagocytosis induced by ultraviolet irradiation in a cultured human lens epithelial cell line. *Experimental Eye Research* **71,** 609–18 (2000).